CATHEPSIN-MEDIATED FIBRIN(OGEN)OLYSIS IN ENGINEERED MICROVASCULAR NETWORKS AND CHRONIC COAGULATION IN SICKLE CELL DISEASE

A Dissertation

Presented to

The Academic Faculty

by

Simone Andrea Douglas

In Partial Fulfillment

of the Requirements for the Degree

Doctor of Philosophy in the

School of Wallace H. Coulter Department of Biomedical Engineering

Georgia Institute of Technology and Emory University

August 2020

CATHEPSIN-MEDIATED FIBRIN(OGEN)OLYSIS IN ENGINEERED MICROVASCULAR NETWORKS AND CHRONIC COAGULATION IN SICKLE CELL DISEASE

Approved by:

Dr. Manu O. Platt, Advisor
Department of Biomedical Engineering
Georgia Institute of Technology

Dr. Clint Joiner
Department of Pediatrics, Division of Hematology/Oncology
Emory University School of Medicine

Dr. Rodney Averett
School of Mechanical Engineering
University of Georgia

Dr. Roger Kamm
Department of Mechanical Engineering & Department of Biological Engineering
Massachusetts Institute of Technology

Dr. Edward Botchwey
Department of Biomedical Engineering
Georgia Institute of Technology

Dr. Johnna Temenoff
Department of Biomedical Engineering
Georgia Institute of Technology

Date Approved: April 24, 2020

For Mom and Dad

And to the people of Jamaica

“Out of Many, One People”

One Love.

ACKNOWLEDGEMENTS

I would like to start by acknowledging my PhD Advisor, Dr. Manu Platt. I owe a lot of my growth as a person and scientist over the past five years to him. Dr. Platt has challenged me, pushing me out of my comfort zone and encouraging me to grow far beyond what I thought I was capable of. Through Dr. Platt's encouragement I was lucky to have many opportunities and experiences in graduate school- international travel, earning travel and poster presentation awards, mentoring Project ENGAGES scholars and REU students, serving as a lead volunteer for BME graduate recruitment, mentoring ESTEEMED scholars in the summer bridge program, and attending events to support the Sickle Cell Foundation of Georgia. As Dr. Platt always reminds his students, "luck is when preparation meets opportunity". He has more than prepared me and other students to take advantage of opportunities to help us grow, making sure we leave with the Platt Lab trademark so we can thrive wherever we land. Former lab mates jokingly call me "mini Manu" because of my chosen career path and mannerisms. Honestly, I could not think of anyone better to be compared to.

To my committee members, Dr. Rodney Averett, Dr. Ed Botchwey, Dr. Clint Joiner, Dr. Roger Kamm, and Dr. Johnna Temenoff, thank you for the scientific discussions and feedback. My dissertation was interdisciplinary which required assembling an equally interdisciplinary team. They challenged my work which drove my dissertation forward; helping me go beyond the comfort of my initial hypotheses and ideas to develop my work. Even in our final committee update when we were talking about post-doctoral positions/advisors, they encouraged me to "go to the best" to get top training to

help advance my career. I thank them for their time invested in me and helping me become a better scientist.

I owe a great deal of gratitude to my Platt Lab family; we have a great lab culture and environment, which I believe is an extension of Dr. Platt's contagious personality. My Platt Lab family has always been there for every step of my PhD journey- troubleshooting zymos, triple checking calculations, editing papers, listening to practice presentations, and celebrating achievements/milestones. I would especially like to thank my older lab siblings, Dr. Meghan Ferrall-Fairbanks, Dr. Chris Rivera, Dr. Akia Parks, and Dr. Andrew Shockey who helped me as I transitioned into the Platt Lab family. They answered all my questions and taught me most of my wet lab skills. When I started, there was a 3-4 year gap between all of us. They were all so far in their research projects, but they still took the time to train me, help me get through my classes, and prepare for my qualifying exam. The truth is, I wanted to be like them and felt the desire to catch up. Staying in the lab late with them, gave my work momentum. Even after they graduated, they still checked in on me as I was finishing final experiments and writing my dissertation, always giving me advice and providing endless words of encouragement.

I would also like to acknowledge some of the lab's research scientists and postdocs: Dr. Chris Kieslich, Dr. Adeola Michael, and Dr. Hannah Song. I was fortunate enough to have them around the lab over the past five years. From offering advice about mentoring students in the lab to troubleshooting experimental protocols, they have been a constant and reliable source of extra guidance.

A couple years went by before we finally got a new graduate student in lab, Victor Omojola, who has done a good job taking over for Andrew as the lab's baker. I admire his

tenacity, and have enjoyed watching him progress with his project, growing as a scientist since he gave his first lab meeting presentation. Danielle Miller, Pallavi Misra, and Sophia Upshaw are our newest lab members; a triple threat with new ideas and projects that I know will propel the next Platt Lab generation forward. Although it has been a short time, it has been a pleasure working with them in lab and I appreciated the new energy they brought to the lab. We also had the pleasure of having a student in the PKU program, Jiabei Yang; she brought a new skillset to the lab and I cannot wait to see what she does when she starts looking at cathepsins in her work.

I would be remiss if I did not acknowledge the "core four" Platt Lab members: Dr. Catera Wilder, Dr. Phil Keegan, Dr. Ivana Parker, and Dr. Keon Young Park all of whom I was fortunate enough to meet at least once while I was in the Platt Lab. They paved the way troubleshooting some of the assays and techniques I used. I found some of the notes in lab notebooks/protocol folder helpful in times of doubt. Most especially, I appreciate them checking in on me and always responding to my emails when I reached out for help.

The group of high school and undergraduate students I have had the pleasure of mentoring over the past few years, known as "Simone's Science Squad," include: Tatiyanna Singleton, Surafel Argaw, Sarah Lamothe, Niara Botchwey, Jacob Klamm, Elizabeth Martin, Kevin Baez, Omar Ahmed, Amrit Bhatia, Teresa Ozga, and Giancarlo Riccobono. My work with these students has helped me develop my teaching and mentorship skills. Having students work with me in lab was another contributing factor that helped drive my project forward, as they got just as good as me with lab techniques and would ask questions that led to more experiments. It has been great watching their scientific skillset grow in lab, and see them become just as invested as I was in the work. I

am very proud of their accomplishments and look forward to seeing what they do in their future careers.

Dr. Kristina (Tina) Haase, from MIT, was the best collaborator to work with over the past couple years. During my research exchange, she took time to prepare for my arrival by ordering chemicals/reagents and finding equipment in other labs for us to borrow. She was a fantastic host when I arrived; integrating me into the lab and making me feel welcomed. There was true exchange of knowledge as Tina took the time to teach me about the microvascular network protocols and confocal staining, while I introduced her to the world of proteases and zymography. I not only think of her as a collaborator, but also as a mentor as she has helped me improve my scientific skills and has offered me feedback on my writing.

I would like to acknowledge the technicians and veterinarians at IBB and EBB Physiology Research Laboratories for assisting with our animals, especially during times when we were unable to come in. Also, I appreciate Hannah, Adeola, Victor and Jiabei for helping with the animal work, especially to Hannah, who taught me all the animal techniques I know and used in animal studies. It was great working with a team that worked well together to do these animal studies, and I will miss our “mouse parties”.

To Lakeita Servance, Laura Paige, Dr. Kim Paige, Ashley James, and Dr. Kyla Ross who provided personal, social, and academic support especially when the days got tough. I appreciate everything they did for me over the past five years- lending an ear when I needed to vent, printing posters for me last minute, handling reimbursements, and providing professional development advice. It takes a village to train a graduate student, and all of them are very much a part of mine.

Most especially I would like to acknowledge the late Dr. Robert Nerem. To be mentored by my mentor's mentor was a blessing. One of our last conversations was about my defense; he was looking forward to watching "the finale" and said it would be special. Having had Dr. Nerem's support from early on in graduate school was pivotal and helped me overcome self-doubt about going into academia. I hope I can continue to make "Grandpa Bob" proud and leave a legacy as great as his.

As I worked on my dissertation, I could not help but reflect on the teachers I had earlier in my education. I want to acknowledge the foundation they provided for me and how many encouraged me to pursue a STEM field. I do not think I would be on this path if several teachers were not standing at the "forks in the road" to guide me. My 9th grade Biology teacher encouraged me to join the pre-med program, providing me the opportunity to take extra science classes to foster my interests. My 10th grade Chemistry teacher agreed to start an after school science research class so I and a couple other students could prepare for the science fair. I also want to acknowledge my other teachers who helped turn me into a well-rounded student: my English teachers who worked hard to turn me into a stronger writer, my Student Government advisor for providing a space for me to learn leadership skills, and my Band Director who motivated me to use music as a creative outlet.

I would also like to acknowledge some important professors who have challenged and inspired me during my time at the University of Miami and even after I graduated. My undergraduate research advisor Dr. Noelle Ziebarth- I appreciate that she took a chance on me as a sophomore and allowed me to join her research group. That was my first lab experience and working with her helped me realize that I wanted to pursue a career in academia. To my graduate student research mentor Dr. Janice Dias, for being one of the

first black women scientists in my life to inspire me. She gave me the opportunity to work on my own project, and the space to make mistakes with feedback to help me be better in the future. To my FGAMP program director, Dr. Michael Gaines who gave me a second chance to become a FGAMP scholar; he helped me meet the required curriculum, get admitted to an REU program, and still graduate on time, with an offer for a PhD program.

To the many friends who have been by my side over the years from before graduate school until now. I want to acknowledge my St. Mary Magdalene family, especially Youth Group. As I grew up, and even after I left for college, your thoughts, prayers, and continued words of encouragement have always surrounded me. I grew up with my Youth Group family; all of us went in different directions facing new challenges, but I always knew no matter how tough times got, we always had each other's backs. To the lovely ladies of UV6-307 at the University Miami, I appreciate the late-night calls/texts and listening to me vent about grad school, but who always offer constant words of support. Last, I want to acknowledge my Georgia Tech friends- a group of scientists that are equally crazy as me for wanting to go to graduate school. I thank you for providing a safe space to commiserate but also celebrate, especially the BME Black Girl Magic Group- the "Wine Downs" inspired and revitalized me over the past couple years.

I want to acknowledge my wonderful family. My mom, who is the most loving and caring person I know. Her words of support and encouragement have been uplifting my whole life. Despite not understanding science, she would always edit my abstracts or fellowship applications. My mom was the first person to give me a lesson in representation through an American Girl Doll by the name of Addy. It was this story that not only framed my NSF essay, but a lot of what I stand for today and aim to fight for as a future professor.

She refused to buy me a doll that did not “look like me”, and over 20 years later I thank her for that. My dad and I both think like engineers. He is one of the smartest and most intuitive people I know. I draw inspiration from him when I face challenging technical problems. My dad taught me that having the right tools makes work easier, and more often than not he has been right. I thank him for teaching me that lesson from a young age, it has saved me a lot of headaches over the past couple years. To my best friend and one of my favorite people on the planet, my younger brother, Johann. He is a man of few words, but always sent me funny videos and pictures to make the heavy moments lighter and make overwhelming days more manageable.

Finally, I would like to acknowledge my loving and incredibly patient fiancé, Arman. Words cannot express how much his unwavering support and unconditional love has meant to me over the past several years. I appreciate that he gave me the time and space to reach my goal of completing my PhD. He has been so patient and understanding, especially when I was late for date night or had to bring him into the lab so I could finish work. He is always texting to check in on me and offer words of love, support, and encouragement. Even though he did not always get the science I would ramble on about, I appreciated that he listened and would be just as happy as I was when I got “good” data. I am lucky to have found an incredible man to share this journey with, and look forward to the adventures we will face together.

I will do my best to continue to make my village proud.

TABLE OF CONTENTS

LIST OF TABLES

LIST OF FIGURES

LIST OF SYMBOLS AND ABBREVIATIONS

Ang	angiopoietins
Bio-bot	biological machine
catK	cathepsin K
catL	cathepsin L
catS	cathepsin S
CysC	cystatin C
DTT	dithiothreitol
EC	endothelial cell
ECM	extracellular matrix
EDTA	ethylenediaminetetraacetic acid
EPC	endothelial progenitor cells
ETP	endogenous thrombin potential
FDP	fibrin degradation product
FGF	fibroblast growth factor
FpA	fibrinopeptide A
FpB	fibrinopeptide B
Hb	hemoglobin
ICAM	intracellular adhesion molecule
IF	immunofluorescence
IL-1β/8/17	Interleukin- 1β/8/17
MMP	matrix metalloproteinase
MVN	microvascular network
PBMC	peripheral blood mononuclear cells
PMN	polymorphonuclear neutrophils
RBC	red blood cell

SCA	sickle cell anemia
SCD	sickle cell disease
SDS-PAGE	sodium dodecyl sulfate-polyacrylamide electrophoresis
TAT	thrombin-antithrombin complexes
TF	tissue factor
TGF-β	transforming growth factor-beta
TIMPs	tissue inhibitors of metalloproteinases
VCAM	vascular adhesion molecule

SUMMARY

Cysteine cathepsins are powerful proteases involved in tissue destructive disease progression, including angiogenesis and pathogenic vascular remodeling, and some of their functions and mechanisms in biological processes have yet to be discovered. Their potential role in polymerizing and degrading fibrin, an essential blood clotting protein and commonly used biomaterial scaffold for tissue repair, have not been characterized well. I hypothesize that cysteine cathepsins have unique fibrin(ogen)olytic properties which can facilitate fibrin matrix remodeling. The objective of this research is to study cathepsin-mediated fibrin(ogen)olysis in the context of fibrin-based microvascular network destabilization and novel blood clotting mechanisms.

Overall, this dissertation has uncovered fibrin as a novel substrate for cysteine cathepsins. A unique property was identified where cathepsin L adsorbed to fibrin, which served as a bioactive reservoir to sustain cathepsin activity for extended periods of time. This knowledge can be expanded to have an impact in two areas: tissue engineering and clinical applications. It will (1) help us understand the role of cathepsin-mediated fibrin degradation *in vitro* and how cathepsins remodel matrix of microvascular networks and (2) improve our understanding of cathepsin involvement in coagulation in sickle cell anemia (SCA).

This work is innovative because, within the field of regenerative medicine, cysteine cathepsins have not fully been considered as mediators in remodeling and destabilizing the extracellular matrix (ECM) of fibrin-based constructs. While several factors (growth factors and biomechanical cues) have been perturbed in studies, researchers typically focus on matrix metalloproteinases (MMPs) proteolytic activity. When constructing tissue-

engineered constructs, protease expression and activity can be perturbed by factors including matrix composition, cell-cell contact, and shear stress. This work provides insight into upregulated proteases in microvascular networks, which can help improve designs to prevent microvessel regression.

Researchers need to better understand how chronic coagulation activation leads to the pathophysiology of SCA. Studies using anticoagulants and antiplatelet therapeutics have not helped prevent or treat hypercoagulation and vaso-occlusive conditions in people with SCA. This work has identified upregulated plasma cathepsin levels that could perturb the coagulation cascade. Identifying this mechanism can provide insight into the role cathepsins could play in coagulation, with further implications to uncover novel blood clotting mechanisms and abnormal fibrinolysis in cardiovascular diseases that have not been identified in the field.

CHAPTER 1 INTRODUCTION AND SPECIFIC AIMS

Cysteine cathepsins are powerful proteases first discovered in lysosomes involved in non-specific protein turnover or degradation, and are secreted by various cell types in tissue destructive diseases such as cancer/tumor metastasis, atherosclerosis, arthritis, and tendinopathy [1-8]. These enzymes degrade extracellular matrix (ECM) proteins and are some of the most powerful collagenases and elastases [7, 9]. Cysteine cathepsins have substrate redundancy [2], however few studies have identified their proteolytic potential on fibrin(ogen) [10-12], an essential blood clotting protein and commonly used biomaterial scaffold for tissue repair. To identify the putative role of cathepsins in cleaving fibrinogen and degrading fibrin, fibrin-based constructs were used as a biological mimicking test bed and sickle cell disease (SCD) for a pathological condition.

In tissue engineering, fibrin-based tissue constructs are favored due to controllable gelation time and network geometry. This makes fibrin a promising scaffold for multicellular engineered living systems such as vascular tissue engineered constructs and vascularized organ-on-a-chip systems [13-17]. Proteolytic activity is needed for matrix remodeling during vasculogenesis [18-20]. Matrix metalloproteinases (MMPs) are commonly studied in these processes [21-23], but other proteases like cysteine cathepsins could facilitate remodeling, seeing as they have been implicated in angiogenesis [24-28]. Cathepsins are secreted by several cell types, including ECs and fibroblasts [28, 29], which are both used to develop microvascular networks. Through biomechanical and biochemical inhibition strategies, the role of cathepsins were characterized in matrix remodeling during microvascular network development. This was a unique model to study fibrin matrix as a bioactive reservoir for cathepsins using an *in vitro* platform.

Sickle cell anemia (SCA) is red blood cell disorder, where people are in a state of chronic coagulation activation, also known as hypercoagulation. Etiology of SCA-mediated hypercoagulation is not well understood, but can contribute to the canonical problem, sickle pain crisis [30-34]. There is a need to understand mechanisms underlying the hypercoagulable state in SCA to develop effective anticoagulant therapies, specific to the SCA population. Thrombin is the canonical protease in the coagulation cascade that cleaves fibrinopeptide A and B from fibrinogen, promoting fibrin polymerization and coagulation [35-37]. It has been reported that people with SCA have increased plasma concentrations of fibrinopeptide A (FpA) [38, 39], a biomarker of clotting activation, however, researchers suggest it is not solely due to thrombin activity [39]. Our lab has shown that cathepsins are upregulated in sickle cell disease (SCD) [28, 40, 41]. Based on computational docking algorithms, cathepsin K has putative binding and cleavage sites on fibrinogen within the central E-domain where FpA is found and cleavage occurs [42]. Also, SCA activates peripheral blood mononuclear cells to induce and upregulate cathepsin K activity in endothelial cells [40]. Combining these observations, it is suggested that elevated circulating FpA plasma levels in SCA is due to cysteine cathepsin cleavage of fibrinogen, contributing to chronic coagulation activation.

1.1 Research Objectives and Specific Aims

The **objective of this dissertation** is to study cathepsin-mediated fibrin(ogen)olysis to better understand enzymology of cathepsins on a novel substrate. It is important to understand how cathepsins remodel fibrin, as there are implications for cathepsins in fibrin-based microvascular network matrix remodeling and aberrant blood clotting mechanisms. Researchers have not fully considered fibrin polymerization and

degradation by proteases other than thrombin and plasmin, respectively, the canonical proteases involved in the coagulation cascade and fibrinolysis. Cathepsins are not normally associated with the coagulation cascade, however, they are implicated in homeostasis to facilitate tissue remodeling, acting on various matrix proteins including collagen and elastin. The goal is to investigate novel hydrolysis and regulatory mechanisms between cathepsins and fibrin(ogen). The ***central hypothesis*** of this dissertation is that cysteine cathepsins have unique fibrin(ogen)olytic properties that contribute to fibrin-based microvascular network matrix remodeling and aberrant blood clotting in SCD. This work could lead to design strategies to improve longevity of fibrin-based tissue engineered microvessels, as well as help improve treatment options to reduce chronic coagulation activation in SCD.

Aim 1: Determine fibrinolytic activity of cathepsins K, L, and S. *Hypothesis: Cathepsins hydrolyze fibrin and degrade the α, β, or γ fibrin polypeptide chains.* Fibrin gels were formed and used to assess fibrinolytic activity of cathepsins (cat) K, L, and S. Fibrin gels were polymerized, then incubated with increasing amounts of recombinant cat K, L, or S, or plasmin as a control, for 24 hours. Samples were run on SDS-PAGE and multiplex cathepsin zymography to assess fibrin cleavage into smaller molecular weight products and amounts of active cathepsins, respectively. These studies demonstrate that cat K, L, and S were fibrinolytic, and specifically degraded the α and β fibrin polypeptide chains, in cleavage patterns that differ from plasmin. Incubating fibrin gels with increasing amounts of catL correlated with increased amount of active catL in the supernatant at higher molecular sizes (37-75 kDa) than the size at which catL normally produces a signal (20 kDa). The larger molecular weight appearance of active catL observed in the

zymography was most likely catL bound to fibrin and fibrin degradation products, which was unique for catL among the others, suggesting that fibrin can serve as a substrate to prolong active catL. Chapter 3 discusses these findings.

Aim 2: Determine the role of cathepsin activity in microvascular network matrix remodeling. *Hypothesis: Cysteine cathepsin, secreted by ECs and fibroblasts, hydrolyze fibrin and other matrix proteins facilitating microvascular network matrix remodeling.* ECs and fibroblasts were cultured in a fibrin gel within a PDMS platform. Microvascular networks formed via a vasculogenesis-like process over ~7days, then half of the devices were exposed to continuous flow, inducing a low shear stress for 48hrs. Endothelial or stromal cells were examined to identify which cell type produced more cathepsins, and if fibrin could sustain active cathepsins *in vitro,* by culturing ECs and fibroblasts on fibrin gels. Microvascular networks exposed to luminal flow have a significantly lower amount of active cathepsins compared to networks grown under static conditions. There was more catL present in networks developed under flow, which was accompanied by an increased amount of cystatin C. ECs and fibroblasts separately cultured on fibrin had increased amounts of active cathepsins in supernatants and homogenates, however, there was more catL present in fibroblasts compared to ECs. Active cathepsins were significantly increased in statically cultured microvascular networks which regress over time, as evidenced by thinning of microvessels by day 10. Taken together, this suggests that fibrin in the microvascular networks matrix may stabilize cathepsin activity in the system. This work demonstrates the need to consider novel cathepsin inhibition strategies to control

proteolysis and meet design criteria for fibrin-based engineered tissues. Chapter 4 discusses these findings.

Aim 3: Determine fibrinogenolytic activity of cysteine cathepsins in promoting chronic coagulation activation due to sickle cell disease (SCD). *Hypothesis: Cathepsin K can release fibrinopeptides A (FpA) by cleaving the Gly-Pro-Arg (GPR) sequence on fibrinogen, which contributes to hypercoagulation in sickle cell disease.* The amounts of active cathepsins and FpA in plasma were quantified in Townes' humanized sickle cell mouse model: wildtype (AA), sickle cell trait (AS), and sickle cell anemia (SS) genotypes. To determine if cysteine cathepsins, and specifically cathepsin K (catK), were causal agents of increased FpA, mice were injected daily with E-64, cathepsin inhibitor, from 1 month to 3 months of age. Plasma was collected from untreated and E-64 treated mice. Samples were run on multiplex cathepsin zymography to assess amount of active cathepsins in plasma, and ELISA was used to quantify concentrations of FpA in plasma. Untreated 1-month SS mice had increased amounts of active cathepsins compared to 1-month AA and AS mice, and 3-month SS mice had more active cathepsins compared to 1-month SS mice. Preliminary data showed plasma from male untreated SS mice may contain higher amounts of circulating FpA compared to AA and AS mice. E-64 treatment reduced amounts of active cathepsins in plasma accompanied by a reduction in plasma FpA in SS male mice. These data support that SCA mediates increased levels of active catK in the plasma that cleaves FpA from circulating fibrinogen, promoting the hypercoagulable state. Inhibiting catK with E-64 treatment not only reduced the active cathepsins, but also reduced circulating FpA in this humanized sickle cell mouse model, implicating SCA-induced cathepsin-mediated fibrinogenolysis. This data can be applied to help us

understand chronic coagulation activation in SCA, and sex differences in disease complications. Chapter 5 discusses these findings.

1.2 Significance of Results

This dissertation is innovative because it focuses on the role cathepsins play in polymerization and degradation of fibrin, and will provide a foundation for understanding cathepsin-mediated fibrin(ogen)olysis. This work is giving more consideration to a novel class of proteases involved in fibrin(ogen)olysis, as there have been limited studies on cathepsin-mediated fibrin polymerization and degradation. The concept that the same protease can not only degrade, but also polymerize the same protein is interesting, especially considering that cathepsins are involved in tissue remodeling for homeostasis as well as destructive disease states. This knowledge can be used to develop cathepsin inhibition strategies for improving microvascular network design to improve network longevity and implement anticoagulant therapies for the SCA population.

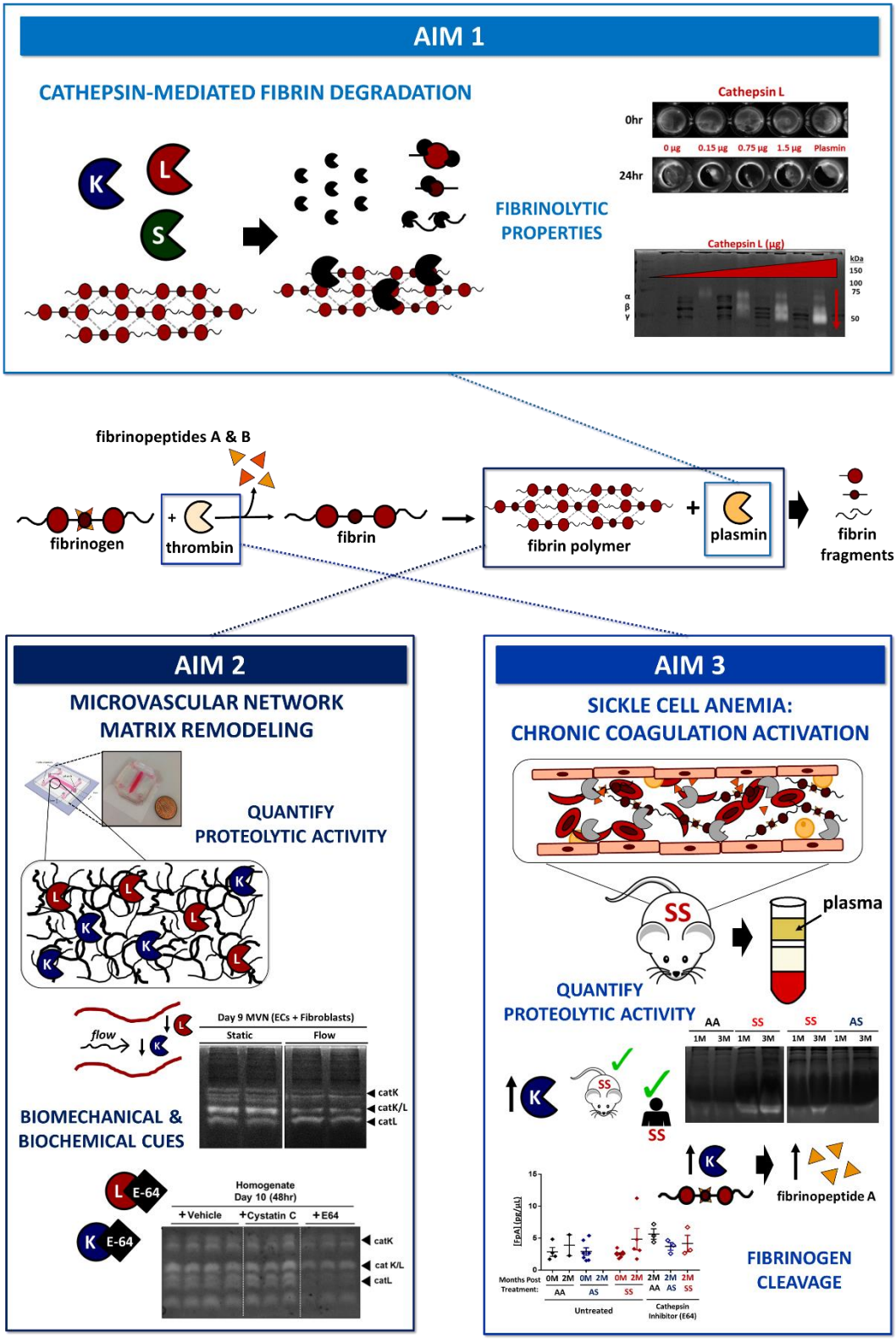

Figure 1-1: Overview of Specific Aims

CHAPTER 2 LITERATURE REVIEW

2.1 Cysteine Cathepsins

Proteolysis, the irreversible hydrolysis of peptide bonds, is a mechanism used by cells to regulate cell function and fate. Proteases are needed to maintain homeostasis processes; endogenous inhibitors, pH, and inactive zymogen activation help control and regulate them [43]. Proteases are destructive, and when improperly regulated, this can lead to alterations in cell function, apoptosis, and tissue degradation [44]. Proteases are defined by their active site hydrolysis mechanism (amino acid sequences found in the catalytic triad). There are five major types of proteases: aspartic, cysteine, metallo, serine, and threonine [45].

2.1.1 An Overview of Cathepsins

Within the past few decades, researchers have identified that cathepsins play key roles in the regulation of cellular processes, protein turnover, and progression of diseases [2, 3, 46, 47]. Cysteine cathepsins are members of the C1 family of papain-like peptidases [2]; currently, 11 human cysteine cathepsins have been identified (B, C, F, H, K, L, V, O, S, W, X/Z). Our studies will focus on cathepsins K, L, and S, which share more than 60% sequence identity [1-3, 48, 49] yet have unique cellular functions, catalytic efficiencies, and target substrate redundancy [2, 50].

Various cell types, including those found in vasculature or used in developing engineered microvessels, produce cathepsins- specifically, this includes endothelial cells, fibroblasts, and macrophages [6, 51-53]. Cathepsins are implicated in extracellular matrix (ECM) degradation in tissue destructive diseases including arthritis, atherosclerosis,

osteoporosis, and tumor metastasis [4-7, 51, 52]. These enzymes degrade ECM proteins and are some of the most powerful collagenases and elastases [7, 9, 54, 55].

2.1.2 Regulation of Cysteine Cathepsins

Cysteine cathepsins were first discovered in lysosomes; they are proteolytically optimal in acidic and reducing environments, a property that prevents unnecessary proteolysis if they escape from the lysosome [1, 2, 47]. Due to their high potency, cathepsins are highly regulated. In the endoplasmic reticulum, cathepsins are translated as an inactive zymogen or propeptide. The propeptide sequence serves as a signaling molecule to traffic cathepsins to the Golgi [45]. Cathepsins are trafficked through the ER to the Golgi through a prepropeptide sequence, which serves as a signaling molecule. During transport, the pre-region is cleaved, and, in the Golgi, the pro-cathepsin is post-translationally modified via glycosylation to prevent autodigestion or self-activation [2, 7]. After, the cathepsin is targeted to endolysosomal or lysosomal compartments where it is activated or secreted into the extracellular space [45]. While in the pro-cathepsin form, the propeptide sequence blocks the active site. Upon cleavage of the propeptide, the enzyme will be in its mature, active form where it can bind to and cleave substrate This propeptide is critical to prevent cathepsins from being continuously catalytically active when it is not needed for degrading substrate. Cathepsins are optimally active at acidic pH; under these conditions, cathepsins can self-cleave their own propeptide or other proteases can cleave the propeptide [1, 2, 56].

Cells can endogenously produce inhibitors for cathepsins to regulate cathepsin activity. Cystatin C is a competitive inhibitor that binds reversible and tightly to active sites of cathepsins to prevent substrate degradation [57]. Cathepsins and cystatin C, are found

within the same space extracellularly, where they can interact through activation, inhibition, or enhancement of proteolytic functions [1, 7, 49, 57]. Dysregulation of inhibitor levels can contribute to ECM degradation, dysfunction, and disease progression [3, 19, 43, 44].

2.2 Proteases and Fibrin(ogen)

2.2.1 Fibrin(ogen) Structure

Fibrinogen has an important role in hemostasis, a process to prevent or stop bleeding. It forms a clot to prevent blood loss and serves as a substrate to facilitate tissue repair where it helps maintain blood vessel tone, angiogenesis, cell migration, and proliferation of cells including fibroblasts and smooth muscle cells [36]. Fibrinogen is a 340kDa hexameric protein, composed of three pairs of symmetrical polypeptide chains, Aα, Bβ, and γ, and held together by numerous disulfide bonds. Fibrinogen has a central E region where the N-terminus meets with a coiled-coiled region to the side D domain and Aα protuberances (further extension of the Aα chain) that coil back to the central E domain (Fig 2-1A) [58, 59]. The domains contain binding sites to facilitate different processes including fibrinogen conversion into fibrin, fibrin cross linking, and platelet adhesion [37]. The coagulation cascade is initiated after vascular injury and EC damage; an amplification cascade where various serine proteases cleave factors to produce activated factors, that ends in thrombin activation, which cleaves fibrinogen [35].

2.2.2 Fibrin Formation During the Coagulation Cascade

Hemostasis and the clotting cascade are defined by a series of proteolytic reactions, dominated by serine proteases [60], resulting in cleavage of fibrinogen. Fibrinogen is

hydrolyzed by thrombin, which releases fibrinopeptides A (FpA) and B (FpB) from the N-terminal part of the Aα and Bβ chains of fibrinogen resulting in a fibrin monomer [61, 62]. Specifically, FpA is cleaved at the AαArg16-Gly17 peptide and FpB is cleaved at the AαArg16-Gly17 peptide. After FpA cleavage, the α chains have new N-terminal sequences (Gly-Pro-Arg) called knobs "A" [62]. When the fibrin molecules interact, the knob "A" forms a complementary interaction with hole "A", found on the γ-nodules within the side D domain; this is called an "A-a" interaction (Fig 2-1A) [63].

Fibrin polymerization begins when two fibrin molecules interact and the "A-a" interactions hold the two fibrin monomers together resulting in a fibrin dimer. An additional fibrin monomer is added to the fibrin dimer where the D domain of the new monomer interacts with the D domain and E domain of the fibrin dimer resulting in fibrin oligomers [61]. These monomers are added longitudinally and the process continues to form two-stranded protofibrils, which are then cross-linked by activated factor XIII (Fig 2-1B) [35-37, 59].

After FpB cleavage, the β chains have new N-terminal sequences (Gly-His-Arg-Pro) called knobs "B" which binds to hole "b" located on the β-nodule [62]. Once fibrin protofibrils reach a certain length, they aggregate laterally through interactions of knob "B" and hole "b", and the C-terminal part of the γ chains (Fig 2-1A) [64]. The lateral assembly results in a fibrin fiber which acts like a meshwork where other factors, like platelets, albumin, and red blood cells, are incorporated to grow and strengthen the fibrin clot that can withstand pressure in the blood vessel and prevent blood loss (Fig 2-1B) [65].

2.2.3 Fibrinolysis by Plasmin

Homeostasis is also maintained through clot resolution, which is defined as degradation and clearance of blood clots, to avoid occlusion of blood vessels. Fibrinolysis or fibrin degradation helps regulate coagulation and aids with wound healing [65]. Plasmin is the canonical enzyme that degrades fibrin and is controlled by the plasminogen activator (PA) system [35, 58]. Plasminogen, the inactive zymogen of plasmin, is cleaved by tissue-type and urokinase PA (tPA and uPA) to form plasmin [66]. Plasmin hydrolyzes fibrin in the coiled-coiled region between the E and D domain [58] releasing fragment E from the central part of fibrin and two D fragments from the side regions [62]. Fibrinogen and its cleavage products have binding sites that facilitate tissue repair including vasoconstriction, angiogenesis, cell migration, and proliferation of various cells including fibroblasts, smooth muscle cells, and lymphocytes suggesting fibrinogen involvement in local immune response [36].

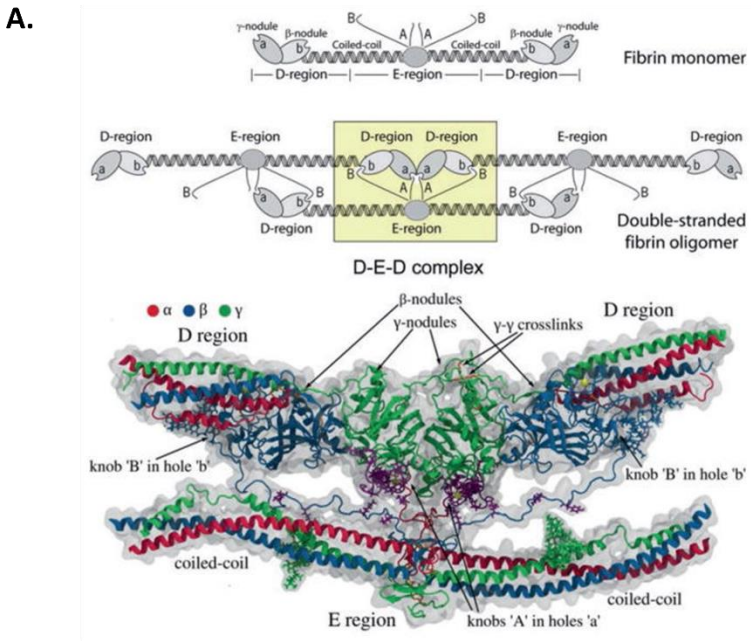

Image from Weisel et al. *Subcellular Biochemistry* 2017

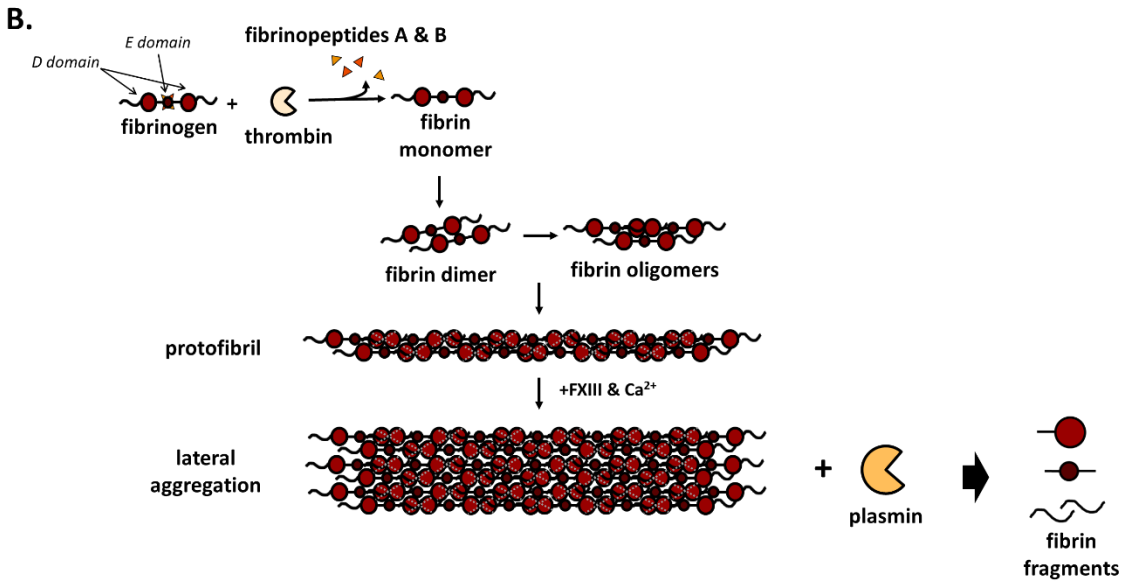

Figure 2-1: Schematic of fibrin formation and degradation.
(A) Top- Schematic of complimentary knob-hole interactions during fibrin polymerization. Bottom- Atomic resolution of knob-hole interactions. **(B)** Steps of fibrin polymerization, including longitudinal and lateral aggregation of fibrin and fibrin degradation by the canonical protease plasmin.

2.2.4 Fibrinolysis by Non-Plasmin Proteases

Although plasmin is the canonical enzyme for fibrin degradation, other proteases have been identified that hydrolyze fibrin at different sites generating different cleavage products. Cysteine cathepsins are members of the papain-like cysteine protease family [46], a large group of proteases with structure similar to papain. Papain can cleave mammalian fibrinogens and cause fibrin gelation [67-69]. Papain and cysteine cathepsins have similar structures, suggesting cathepsin fibrinolytic potential. An alternative fibrinolytic system was identified in peripheral blood leukocytes, where elastases and cathepsin G (serine proteases) are localized in leukocyte granules, which generate fibrin cleavage fragments that are distinct from the canonical plasmin system [70]. Other studies have shown that plasminogen activator-deficient transgenic mice have an alternative fibrinolytic pathway that does not use plasmin to clear thrombi [71, 72]. This led to studying a non-plasmin fibrinolytic pathway that uses integrin Mac-1 on monocytes which binds and internalizes fibrin [11]. Later, cathepsin D (aspartyl protease) was identified as the lysosomal fibrinolytic enzymes responsible for monocyte-mediated fibrinolysis [10]. These studies challenge that fibrinolysis could be perturbed by non-plasmin proteases via novel pathways and mechanisms.

2.3 Vasculogenesis

Vasculogenesis is *de novo* formation of microvessels seen in embryogenesis, tumor growth, and following extensive vascular damage [73, 74]. This is different from angiogenesis where microvessels are formed from pre-existing vessels, usually in response to injury. Microvessel formation is a complex and coordinated process that includes ECM

remodeling, endothelial cell (EC) migration, cytokine secretion, lumen formation, and mural cell (i.e. pericyte) recruitment [22, 73, 74].

In embryogenesis, precursor cells called angioblasts differentiate into ECs which form the inner most lining of vessels, called the tunica intima layer. ECs proliferate to form a neo-capillary network organized into a vascular tree with branches [75]. During postnatal vasculogenesis bone marrow-derived endothelial progenitor cells migrate to the site of damage and differentiate into mature ECs forming a neo-vascular network [73, 76].

2.3.1 Cell matrix and protease interactions in angiogenesis

Angiogenesis includes proteolytic remodeling of ECM during EC migration, invasion into perivascular tissue, and tubulogenesis (lumen formation). Dynamic regulation of enzymatic activity is critical to facilitating this process. During the beginning of angiogenesis, the basement membrane, which lies below the EC layer and interstitial connective tissue matrix, is degraded, and proteases are required to break down the ECM. [77]. Three groups of endopeptidases regulate angiogenesis: matrix metalloproteinases (MMPs), serine proteases, and cysteine cathepsins. Their activities are controlled by activation cascades and inhibitors, tissue inhibitors of metalloproteinases (TIMPs), serpins (serine inhibitors), and cystatins (cathepsin inhibitors) [20].

Similar to cathepsins, soluble MMPs are secreted as inactive pro-enzymes that become activated in the cellular environment [21]. MMP-1, -2, and -9, degrade ECM and basement membrane to aid in vascular remodeling, cell migration, and sprout formation [77]. Additionally, MMPs can release ECM-bound angiogenic growth factors (i.e.: VEGF and bFGF) in pericytes from vessels undergoing angiogenesis [20, 78]. Conversely, MMP-7, -9, and -12 can generate an endogenous inhibitor for angiogenesis by converting

plasminogen into angiostatin [21, 77]. TIMPs are endogenous inhibitors of MMPs and function by binding to activated MMPs, and proteolytic activity is regulated based on the ratio of TIMPs bound to MMPs [19]. Some TIMPs can play a role in angiogenesis independent of MMP inhibition, such as TIMP-3 which can bind to VEGF receptor blocking VEGF which reduces angiogenesis [20].

Serine proteases are a broad class of proteases involved in various functions, some of which might have indirect involvement in angiogenesis. However, more attention has been placed on the plasminogen activators, urokinase activators (uPA) and tissue-type plasminogen activators (tPA), and plasmin. uPA and plasmin are involved in cell migration and invasion by degrading ECM and regulating intracellular signaling upon binding to PARs (plasminogen activator receptor) [20, 79]. Both uPA and tPA can cleave plasminogen into activated plasmin, and are inhibited by plasminogen activator inhibitors [20]. Further, the pro-angiogenic effects of VEGF are mediated by a single chain variant of uPA. After uPA is endocytosed via uPAR and transported to the nucleus where uPA binds to a transcription factor (HHEX/PRH) that is a repressor of VEGF1 and VEGF2 gene promoters, thus inducing expression of VEGF receptors which helps regulate EC proliferation [80]. ECM proteins and MMPs can be activated by plasmin which aids remodeling during angiogenesis. Studies have shown plasminogen is involved in angiogenesis; aminocaproic acid, a plasmin inhibitor reduced formation of capillary structures in ECs treated with bFGF, and aortic ring assays using plasminogen deficient mice had reduced sprouting of capillaries [81, 82].

Mechanisms of cathepsins in angiogenesis have not been completely understood, but some studies have shown potential roles they could play in the process. CatK and catL

are secreted outside cells and localize around cell membranes, which can help contribute to endothelial progenitor cells (EPC) recruitment to the angiogenic area [20]. CatL deficient mice had impaired blood flow restoration in ischemic limbs, and when their bone marrow cells were transplanted in mice neovascularization was reduced [83], suggesting that catL could be implicated in EPC-induced neovascularization. Inhibition of catS impairs mouse EC invasion in assays using Matrigel^{TM} and type I collagen. Further, despite normal VEGF and bFGF levels, during wound repair, catS deficient mice had impaired microvessel development as indicated by less number of microvessels forming, suggesting catS plays a role in angiogenesis [24]. Another study identified pro-angiogenic properties of catL. MDA-MD-231 (breast cancer cell line) were intradermally added to nude mice, then treated with catL inhibitor, and it was demonstrated that catL is implicated in angiogenesis including stimulating EC sprouting, promoting migration, invasion, and tube formation, and increasing EC proliferation [84].

Cathepsins, MMPs, and serine proteases are part of a complex proteolytic network that facilitate *de novo* vessel formation. By understanding the role of cathepsins in angiogenesis, researchers will be able to better control angiogenesis and vasculogenesis for wound healing and other regenerative medicine applications in tissue engineering.

2.3.2 Vascularization in Regenerative Engineering

According to the US Government Information on Organ Donation and Transplantation, as of July 2019 there are over 113,000 people on the national transplant waiting list. Every 10 minutes another person is added to the list. This list continues to grow, and the gap between donors and transplants widens. Regenerative medicine could help address the issue of organ transplant shortages [85, 86]. The goal of tissue engineering

is to regenerate tissue and organs to replace, maintain, and improve damaged tissue and organs [87]. A main hurdle to translate tissue engineering to the clinic is vascularization [88-91]- a way to diffuse oxygen, nutrients, and remove waste (similar to how our vasculature works) in these constructs.

Vascular networks supply cells with nutrients to maintain viability, thus, cells need to be within 100-200μm of a capillary for diffusion of oxygen, nutrients, and waste [91-93]. Diffusion of oxygen into tissue is a major limitation, and because of this, developing larger constructs is challenging [94]. Vascularization of thinner (hundreds of microns in size) constructs and avascular tissue have been more successful. This is likely because vascularization takes time (days to weeks) and cells in the middle of larger tissue constructs die during this time without proper diffusion [95]. To decrease vascularization time of constructs, one strategy is to add a network to the tissue or organ before implantation, this is termed pre-vascularization. Pre-vascularization approaches will allow the engineered networks to integrate with the patient's vasculature and perfusion of the tissue construct will be faster [90, 91]; this is advantageous to ensure proper diffusion of oxygen and nutrients, and removal of waste [90, 91, 96]. Pre-vascularization techniques include scaffolds, cell-based, rotating and perfusion bioreactors, microfluidic devices, and modular assembly [13, 93, 97-99].

2.3.3 A Microfluidic Device for Vascularization

Generating vascular constructs in 3D engineered tissue constructs in microfluidic devices provide an optimal, reproducible platform for developing vasculature allowing spatial and temporal control over the microenvironment including applying flow, addition of growth factors, and perturbing biomaterial mechanical properties [100]. Continuous

perfusion of culture media is advantageous, as it provides nutrients and oxygen, and waste removal in order to sustain long term culture. To recapitulate 3D microvessels both microphysical function and 3D microstructure must be replicated; including formation of lumen where cells are aligned luminal to basal axis, which induces hollowing or tubulogenesis [100, 101].

Microfluidic devices are advantageous for developing vasculature *in vitro*, allowing for control over the microenvironment with the ability to easily manipulate three major factors that induce vasculogenesis: 1) biomechanical (i.e.: interstitial flow, shear stress, gel stiffness), 2) extracellular signaling molecules (paracrine signaling), and 3) cell type/cell-cell interactions (i.e.: co-culture with EC and mural cells to improve vessel stability or cell-cell contact of ECs via cadherins and tight junctions to form lumen) [89, 100, 102]. To control network morphology, including vessel diameter, number of branches, and branch length, engineered microvessel design approaches have focused on manipulating proangiogenic factors, such as VEGF or FGF, or scaffold/hydrogel parameters, such as collagen and fibrin(ogen) concentration [91-94, 103]. Additionally, applying interstitial flow helped direct vasculogenesis during microvessel formation, particularly in the formation of branching vessels [92, 94, 103].

Microvascular networks are formed *in* vitro in a microfluidic device, made using polydimethylsiloxane (PDMS) and soft lithography, with separate channels for human umbilical vein endothelial cells (HUVECs) and normal human lung fibroblasts (fibroblasts) encapsulated in fibrin gel (Fig 2-2A). Various combinations of parameters including cell type, hydrogel density, and addition of growth factors altered the number of branches, average branch length, percent vascularized area, and average vessel diameter.

It was determined that using combining HUVECs and fibroblasts (stromal cells), was needed for microvascular networks to remain stable beyond 4 days. Also, networks made with HUVECs and fibroblasts had increased area of vascularization and perfusable segments compared to networks only made using HUVECs. Addition of growth factors, VEGF and sphingosine-1-phosphate (S1P), to ECs and fibroblasts added stimulatory signals, changing morphology where there was increased branching compared to EC only, EC and fibroblasts, and ECs and growth factors. There was a dose dependent relationship between microvessel stability and the fibroblast seeding density. Last, fibrin gel density was manipulated by increasing the fibrinogen concentration; as fibrinogen concentration increased, the number of branches increased, branch length and vessel diameter decreased, and percent vascularized area did not change. A table qualitatively demonstrates the effect of altering growth factors, fibroblast seeding density, and fibrin concentration is in Figure 2-2C [15].

Another iteration of the microfluidic device is made with three channels for a gel scaffold, allowing for multiple matrix compositions to be tested simultaneously (Fig 2-2D). Various combinations of collagen only, fibrin only, and collagen and fibrin were tested, as well (Fig 2-2E); in the fibrin gel only conditions the fibrin did not retract, meaning the fibrin gel was not detached from the walls of the microfluidic channel during microvascular network development. Thus, fibrin was selected as the matrix for the development of microvessels over a 2-week period, where microvessels became patent by day 7 which lasted until day 14 [14].

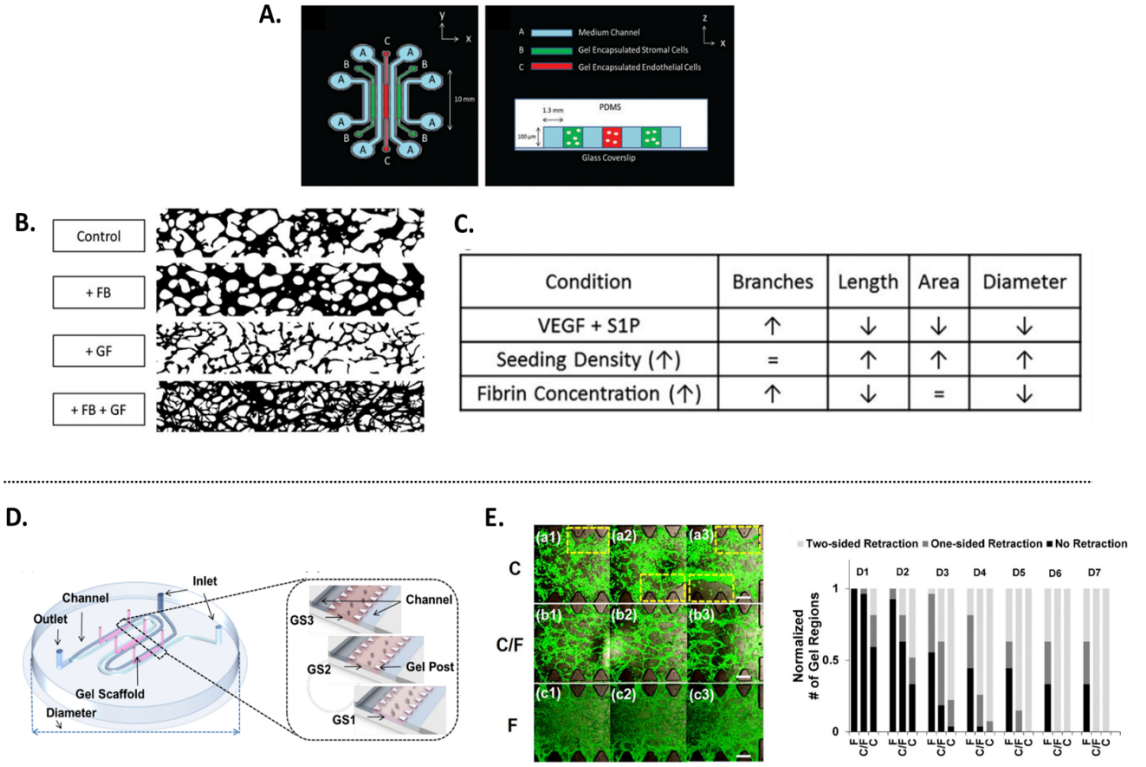

Figure 2-2: Design approaches using a microfluidic device for developing microvascular networks. (A) Schematic of microfluidic device; separate channels for human umbilical vein endothelial cells (ECs) encapsulated in fibrin gel and normal human lung fibroblasts (fibroblasts) encapsulated in fibrin gel. **(B)** Microvasculature networks made with ECs only compared to ECs and fibroblasts without or without growth factors (VEGF and S1P) to demonstrate differences in number of vessel branches, branch length, vessel diameter, and vessel area. **(C)** Table of microvascular network conditions including growth factors, fibroblast seeding density, and fibrin concentration, and whether there was increase, decrease, or no change in vessel branching, length, area, and diameter. **(D)** Schematic of microfluidic device; GS1, GS2, and GS3 are three sections for gel scaffolds to assess multiple matrix compositions in an experiment. **(E)** Microvascular networks made in different types of matrix: collagen only, collagen and fibrin, and fibrin only. Gel retraction was observed in collagen only and collagen and fibrin gel.

Top Figure adapted from Whisler et al. *Tissue Engineering: Part C* 2014
Bottom Figure adapted from Park et al. *Cellular and Molecular Bioengineering* 2014

2.4 Sickle Cell Anemia

Sickle cell anemia (SCA) is the most commonly inherited blood disorder in the United States affecting 100,000 Americans [34]. According to the Center for Disease Control and Prevention (CDC), 1 in 365 African American babies are born with the disease and 1 in 13 African American babies are born with sickle trait. Globally, there is an increase in the burden of SCA where 300,000 children are affected each year, and it is estimated that by 2050 more than 400,000 children under the age of 5 will be born with SCA [104]. SCA is a lifelong and serious condition, where people are under long-term treatment and pain/symptom management, and the healthcare costs for SCA is approximately $1.1 billion USD, annually [105].

Sickle cell disease (SCD) is the umbrella term for a group of inherited blood disorders that affect β-globin, a subunit on hemoglobin, a protein in red blood cells that aids in the transport of oxygen [106]. There are different types of hemoglobin; adult "normal" hemoglobin is defined as HbA and sickle mutated hemoglobin is defined as HbS. Sickle cell anemia (SCA) is inherited autosomal recessively, where both copies of the gene have the same sickle mutated hemoglobin; this is denoted as homozygous sickle (HbSS or SS) [34]. Another variation includes individuals who are heterozygous for HbS, but do not have SCA, which is termed sickle trait (HbAS) [107].

2.4.1 Molecular Level

SCA is a multifactorial disease caused by a single point mutation in the nucleotide on the sixth position of β-globin, a subunit of hemoglobin, where glutamic acid, a hydrophilic molecule, is substituted for valine, a hydrophobic molecule [106]. Under oxygenated conditions, hemoglobin is soluble because valine is not exposed to the red

blood cell (RBC) cytoplasm. Under deoxygenated conditions, some of the HbS polymerizes due to valine being exposed to the aqueous environment, resulting in rigid fibers that contort the RBC membrane, giving RBCs their characteristic “sickle” shape [34, 106, 108]. As the hemoglobin binds oxygen, the fibers “melt,” and the RBCs return to their normal circular shape. Repetitive sickling and unsickling damages the RBC membrane, and when the RBC membrane is damaged, this results in irreversibly sickled RBCs and, and reduces the RBCs lifespan from ~120 days to 9 to 10 days [106].

2.4.2 Sickle Pain Crisis and Other Complications

Vasculopathy occurs due to RBC membrane rupture, hemolysis, which releases byproducts causing increased inflammatory cytokines [109], mononuclear cells [40], and monocyte adhesion to the endothelium [110]. These proinflammatory conditions lead to vascular remodeling characterized by intimal thickening and lumen narrowing in larger cerebral vessels [111]. This includes infiltration of monocytes into sub-endothelial lining, elastic lamina degradation, and proliferation of smooth muscle which enhances lumen narrowing and lesion progression [110, 112]. Other complications include strokes, acute chest syndrome, hemolytic anemia, venous thrombosis, vaso-occlusive crisis (VOC) which is blockage of small vessels, and ischemic organ damage [34, 106].

Acute pain, referred to as sickle pain crisis, is a common, frequent, unpredictable complication of SCA leading to recurrent hospitalization [34, 106]. Normally, RBCs are deformable and can easily pass through microcirculation. However, sickled RBCs are rigid and sickled reticulocytes (immature RBCs) are more adherent under SCA conditions [32, 113]. Collectively, these properties result in RBCs getting stuck in post-capillary venules causing blockage of blood flow which can lead to complete vessel occlusion causing

ischemic injury to the organ and sudden sharp pain [114, 115]. Even though SCA is a hematological disorder, blocked blood flow deprives organs of blood and oxygen [106].

2.4.3 Chronic Coagulation Activation

People with SCA are said to be in a hypercoagulable state where they experience chronic coagulation activation, which is mediated by factors involved in the intrinsic and extrinsic coagulation pathways. The state of chronic coagulation activation is multifactorial; almost every part of the coagulation system is altered in SCA [31, 116]. Evidence of hypercoagulation in SCA includes increased platelet and tissue factor activation, depletion of natural anticoagulant proteins, protein C and protein S, and abnormal fibrinolytic activation [33]. Clinical and animal model studies are characterized by coagulation, chronic hemolysis, and inflammation which suggests that chronic coagulation activation could contribute to pathogenesis of SCA [117]. Although it is known that chronic coagulation activation is prevalent in SCA, researchers need to understand mechanisms of chronic coagulation activation and how it contributes to the hypercoagulable state in SCA pathophysiology and subsequent complications [30, 33]. This leaves a gap in knowledge for defining the role of hypercoagulability in SCA, including understanding its pathogenesis.

Thrombin generation is an indicator of a balanced effect of all coagulation cascade components [118]. Thrombin generation assays are used to measure thrombin generation rate and potential to generate thrombin *ex vivo* in plasma and whole blood [119-122]. An increase in thrombin generation is indicated by an increase in concentration of markers including, fibrinopeptide A, α-thrombin-antithrombin (αTAT) complexes, and D-dimers [30, 32, 123].

Studies from *ex vivo* thrombin generation assays have some inconsistent results when measuring parameters such as time to peak thrombin generation, thrombin peak height, and endogenous thrombin potential (ETP). There was a report of higher peaks [124] for thrombin generation time, while others have identified shorter peaks [119, 125, 126] in people with SCD compared to controls. Discrepancies in thrombin peak height (measurement of highest thrombin concentration) have also been identified between disease state and control; with some reports of higher peaks [124, 126] versus lower peaks [119]. ETP is the amount of thrombin generated *in vitro* after coagulation activation [127]. Decreased ETP has been reported in people with SCD at healthy state compared to healthy controls [125, 128], but another group has reported increased ETP [124]. The same studies also had inconsistent results when reporting time to peak thrombin generation and ETP when comparing values during steady state versus crisis state in people with SCD.

Although researchers acknowledge limitations with studies using thrombin generation assays, the inconsistencies leave a gap in knowledge. It has been suggested that sample preparation, timing of blood collection, and analytic conditions (i.e.: types and concentration of factors used to trigger *ex vivo* clotting need to be standardized) [33]. Correlating thrombotic complication from assays to disease state has proven challenging. Herein, lies an opportunity to look at other abnormal circulating biomarkers in plasma, such as cysteine cathepsins.

2.4.4 Using Anticoagulants in Patients with SCD

Anticoagulant and antiplatelet therapies have not significantly helped prevent or treat VOC and thrombotic complications in SCA [129]. Although anticoagulants initially showed promise, hemorrhage and bleeding risks have limited studies [130]. Direct oral

anticoagulants, including rivaroxaban and dabigatran, have been given to people with SCD that had venous thromboembolisms (VTE), but there was no difference in recurrence or minor bleeding incidences compared to people treated with warfarin (blood thinner/anticoagulant) [131]. Sevuparin, derived from heparin, inhibits the conversion of prothrombin to thrombin, reduces anticoagulant activity and inhibits human SS RBCs from adhering to ECs *in vitro.* An "adoptive" mouse model was used where human SS RBCs were infused into mice; sevuparin prevented vaso-occlusion and normalized blood flow [132]. Findings like these made sevuparin a leading therapeutic agent, leading to one of the largest VOC studies to date. However, in 2019 sevuparin failed during phase II clinical trials, because there were no meaningful clinical benefits or improvements in patients and was not effective for improving resolution time of VOC [133].

Anticoagulant therapeutics have been used as a treatment option to reduce or prevent thrombotic complications in SCA, however they have risks for bleeding complications and hemorrhaging. This motivates the need to develop new therapies for novel anti-coagulant targets. I hypothesize that cysteine cathepsins can perturb the coagulation cascade and promote coagulation activation, but are not essential clotting factors such as thrombin or plasmin. This introduces the idea of targeting proteases, like cathepsins, rather than clotting factors to prevent coagulation.

2.4.5 SCD Mouse Models for Chronic Coagulation Activation Studies

Mouse models are useful for studying pathophysiology and underlying etiology of SCD by targeting specific parts of the coagulation cascade to understand the roles specific coagulation factors. Figure 2-3 is a simplified overview of the coagulation cascade that can be used for reference. Researchers have sought to understand the interplay between SCA

and coagulation. Techniques range from treating mice with inhibitors for specific coagulation cascade factors to generating new mouse models by cross breeding mice from sickle transgenic backgrounds and hemostasis models or using gene editing approaches.

To test the relationship between sickle cell pathology and hemostasis activation, studies have been done by cross breeding plasminogen or fibrinogen deficient mice with sickle cell disease transgenic (SAD) mice. The SAD mouse model has three combined mutations of human α-globin and human β-globin: $\beta^{6Glu\text{-}Val}$ (Hb S), $\beta b^{23Val\text{-}Ile}$ (Hb Antilles), and $b^{121Glu\text{-}Gln}$ (Hb D-Punjab). SAD mice resembles human SCA pathophysiology including *in vivo* erythrocyte sickling under deoxygenated conditions, vaso-occlusion, age-dependent splenomegaly, vascular congestion with thrombi in lung, kidney, and liver [134]. SAD mice with fibrinogen deficiency had higher incidences of mortality and poorer survival profiles, likely due to bleeding related events leading to death, and hypoxic conditions [135]. Typically, fibrinogen deficient mice do not experience significant bleeding under normoxic conditions, suggesting that SCA conditions in double transgenic mice aggravated bleeding and mortality related outcomes. By contrast, SAD mice with plasminogen deficiency had similar deleterious effects to SAD and control mice, and did not worsen mortality [135]. In other words, SCA conditions in plasminogen deficient cross bred mice do not exacerbate conditions. Overall, this study concludes fibrinogen has beneficial effects to maintain vascular integrity, aid in tissue repair, and support hemostasis under SCA conditions [135].

Tissue factor (TF), a high affinity receptor and co-factor for factor VII that initiates blood coagulation, was elevated in leukocytes from Berkeley SS mice [136]. Berkley SS mice express human sickle hemoglobin and are generated from deletions of murine α and

β globins (α-/-, β-/-) with a transgene containing human α, β^s, $^A\gamma$, $^G\gamma$, and β globins. These mice have similarities to human SCA pathophysiology including erythrocyte sickling and intravascular hemolysis [137]. Treating Berkeley SS mice with anti-tissue factor antibody reduced coagulation activation, inflammation, and EC injury, but the antibody did not reduce RBC hemolysis rate or improve the anemic state. Berkeley SS mice with EC-specific deletion of the TF gene had decreased levels of interlukin-6, a proinflammatory cytokine, but there was no effect on coagulation activation, as indicated by similar elevated α-thrombin-antithrombin (αTAT) complexes compared to control Berkeley SS mice [136]. Follow up work assessed how factor X, a serine protease that cleaves prothrombin to active thrombin, and thrombin contributed to coagulation activation and vascular inflammation in SCA. To test this, Berkeley SS mice were given rivaroxaban (factor X inhibitor) or dabigatran (thrombin inhibitor). Additionally, protease active receptor (PAR) -1 and -2, thrombin receptors, deficient mice were transplanted with bone marrow from Berkeley SS mice. Overall, inhibiting factor X and thrombin reduced thrombotic complications and vascular inflammation in SCA, suggesting that factor X and thrombin contribute to vascular inflammation, and PAR-2 is a potential target for inhibition [138].

Thrombin has been another target in mouse model studies. Treating Berkeley SS mice with prothrombin (factor II) antisense oligonucleotide "gapmer" reduced circulating prothrombin, the precursor to thrombin, correlated with reduced early mortality. Genetic mutation was also used; hematopoietic stem cells from Berkeley SS mice were transplanted into prothrombin deficient mice. Genetically modified mice had reduced inflammation, reduced EC dysfunction, and improvement in end organ damage associated with SCD.

Together, these studies demonstrate prothrombin contributes to SCA-induced end organ damage, suggesting another therapeutic target [139].

Fibrinogen binds with leukocytes through the $\alpha_M\beta_2$ integrin receptor, which triggers leukocyte functions including phagocytosis and production of inflammatory cytokines [140]. To see if fibrinogen-mediated inflammation contributes to SCD pathophysiology, hematopoietic stem cells from Berkeley SS mice were transplanted into mice with a mutant form of fibrinogen, that does not bind to the $\alpha_M\beta_2$ integrin receptor on leukocytes [141]. The genetically modified SCD mice had a reduction in reactive oxygen species, circulating white blood cells, and inflammatory cytokines/chemokines. Although there was no improvement in heart, liver, and lung function, there was improvement in kidney function in the mice. Thus, fibrinogen-leukocyte signaling is activated in SCA and potential therapeutic target [141].

These SCA mouse models demonstrate how targeting factors in the coagulation cascade including tissue factor, prothrombin/thrombin, factor X, and fibrinogen can help researchers understand the interactions between SCA and coagulation. The coagulation cascade includes serine proteases, however, I hypothesize that under SCA conditions when other proteases, like cysteine cathepsins are upregulated [40, 41], they can be involved in chronic coagulation activation, as well. Sickle cell mouse models with targeted cathepsin inhibition could be used to study how cathepsins mediate pathophysiology in SCA.

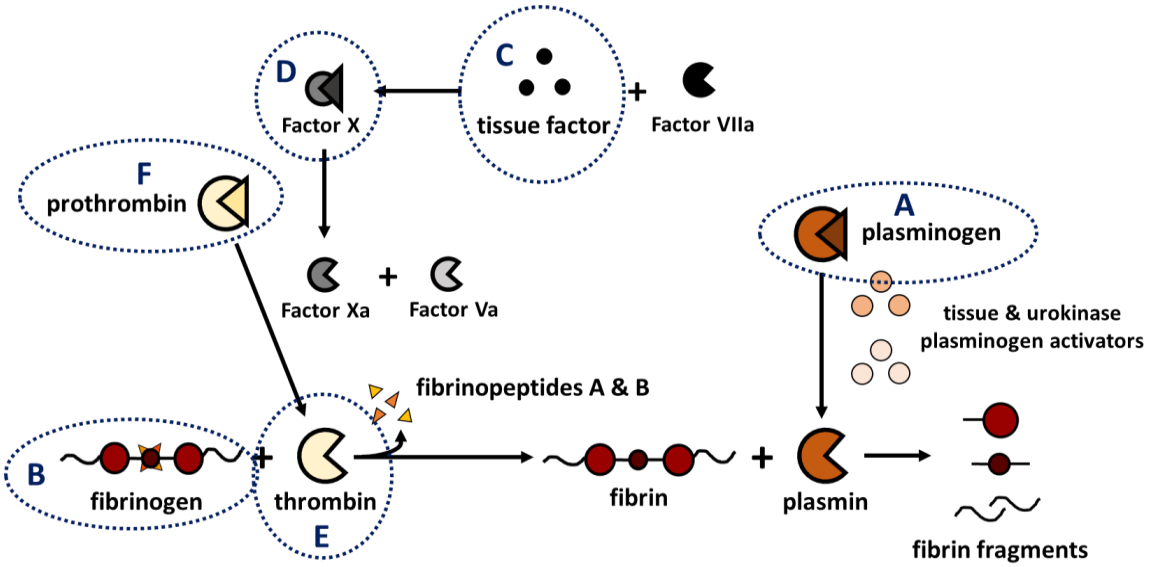

Figure 2-3: Schematic to illustrate aspects of coagulation cascade targeted in mouse studies to understand the roles of specific coagulation factors.
Mouse models have been used to study pathophysiology and underlying etiology of SCD by targeting specific parts of the coagulation cascade to understand the roles specific coagulation factors: **(A)** plasminogen deficient mice, **(B)** fibrinogen deficient mice, bone marrow transplant from Berkeley SS mice into mice with a mutant form of fibrinogen, **(C)** anti-tissue factor antibody, endothelial cell-specific deletion of tissue factor gene, **(D)** treatment with rivaroxaban (factor X inhibitor), **(E)** treatment with dabigatran (thrombin inhibitor), bone marrow transplant from Berkeley SS mice into mice with protease active receptor (PAR) -1 and -2 (thrombin receptors) deficient , and **(F)** prothrombin antisense oligonucleotide "gapmer" to reduce circulating prothrombin.

CHAPTER 3 HUMAN CATHEPSINS K, L, AND S: RELATED PROTEASES, BUT UNIQUE FIBRINOLYTIC ACTIVITY

This chapter was adapted from Douglas, S.A. et al. (2018) "Human cathepsins K, L, and S: related proteases, but unique fibrinolytic activity." Biochimica et Biophysica Acta 1862(9)1925-1932. doi: 10.1016/j.bbagen.2018.06.015.

3.1 Introduction

Hemostasis and the clotting cascade have been defined by a series of proteolytic reactions usually dominated by serine proteases [35, 36, 61], eventually resulting in cleavage of fibrinogen which self-assembles into a fibrin meshwork that catches red blood cells to form a clot and prevent excess blood loss. Fibrin forms from the self-assembly of cleaved fibrinogen, a hexameric protein with quaternary structure of three pairs of symmetrical polypeptide chains (α, β, and γ) held together by multiple disulfide bonds [35, 58]. Once a fibrin clot is formed, it can be resolved through the fibrinolytic action of plasmin, a serine protease, that itself is activated from the zymogen plasminogen by tissue plasminogen activator or urokinase plasminogen activator [142]. The action of plasmin on fibrin is well defined, but the action of other protease families on fibrin are still to be determined.

Cysteine cathepsins are powerful proteases known to be secreted by various cell types in tissue destructive diseases, including cancer [5], atherosclerosis [4, 6, 143]. These enzymes are known to degrade extracellular matrix (ECM) proteins and are some of the most powerful collagenases and elastases [7, 9]. The substrate redundancy of cysteine cathepsins has been documented [2], however few studies have identified cathepsin-mediated fibrin degradation. Cysteine cathepsins are members of the papain-like cysteine protease family [46]. Papain cleaves mammalian fibrinogens and cause gelation [67-69]. Papain polymerizes fibrin that is insoluble in 5M urea, 1M sodium bromide, or 0.1 M

monochloroacetic acid forming intermolecular cross-links, similar to how fibrin cross-links with factor XIII and Ca^{2+} [67]. Other studies demonstrated that cathepsin D, an aspartyl protease, has dose-dependent (100 nM – 10 μM) fibrinolytic activity, and can lyse fibrin, albumin-enriched and albumin/red cell-enriched fibrin clots [10].

Beyond fibrin's physiological and pathophysiological, native roles, fibrin is becoming more popular as a building tool for biomaterials and regenerative medicine applications with promise demonstrated for vascularized tissue engineered constructs [15], biological machines [144], micro and nanoscaffold applications [145], and vascularized organ-on-chip systems [13]. Fibrin-based constructs are favored materials to engineers, designing matrices, because of controlled gelation time, defined network architecture, and well characterized mechanical properties [16, 17, 37]. Degradation kinetics are required to control structural and biochemical properties in these fibrin-based constructs. Proper design and tuning fibrin degradation due to proteolytic cleavage is needed for optimal cellular signaling and matrix interactions [16, 17]. The aim of this work is to determine proteolytic susceptibility of fibrin by cysteine proteases. Our studies show that non-plasmin fibrinolytic proteases, cathepsins K, L, and S, have emerged as an alternative mechanism for fibrin destabilization in long term tissue cultivation.

Our lab has used molecular docking and bioinformatics sequence specificity analysis (PACMANS), to predict potential binding and cleavage sites of cathepsins K, L and S on fibrin [42]. It was determined that catK, L, and S are capable of binding to the α, β, and γ chains on fibrinogen at overlapping and different sites. Specifically, catK, L, and S have preferential binding sites in both the E (central) domain, an area prone to cleavage, which is also the known location of where thrombin cleaves, to initiate fibrin formation and where plasmin cleaves to break down and degrade the fibrin clot. The evidence of cleavage site redundancy in our model is representative of redundancy of cathepsins on other substrates, and this could be indicative of the conserved active sites of cathepsins. Understanding cathepsin-mediated fibrin(ogen) olysis has implications in fibrin-based

tissue engineered constructs as researchers understand environmental cues that influence network remodeling.

3.2 Materials and Methods

3.2.1 Fibrin Gel Formation

Fibrin gels were formed in a 96 well plate. Human fibrinogen (FIB 3 Plasminogen, von Willebrand Factor and Fibronectin Depleted; Enzyme Research Laboratories) was co-incubated with human alpha thrombin (Enzyme Research Laboratories) in 50mM Tris-HCl/100mM NaCl, at a concentration of 2.5 mg/mL and 1 NIH U/mL in a final volume of 100 µl, respectively, for 2 hours at 37^{o}C. Fibrin gels were carefully washed with Tris-HCl to remove unpolymerized fibrinogen and thrombin. Before enzymes were added, plates were imaged using the ImageQuant LAS 4000 (GE Healthcare).

3.2.2 Fibrin Gel Degradation

Increasing amounts (0, 0.15, 0.375, 0.75, or 1.5 µg) of recombinant human cathepsins K, L, S (Enzo) in 50 µl assay buffer (0.1M sodium phosphate buffer, pH 6.0, 1mM EDTA) with 2mM dithiothreitol (DTT) for 24 hours at 37^{o}C. Fibrin gels were alternatively incubated with plasmin (5µg/µL; Enzyme Research Laboratories) or Tris-HCl/NaCl. Plates were imaged after degradation. The samples were centrifuged at 8000 rpm and the soluble fraction as collected and saved. The insoluble fraction was prepared in 50mM Tris-HCl/100mM NaCl with 25% β-mercaptoethanol (OmniPur) and sonicated. insoluble fraction and soluble fraction samples were prepped for reduced SDS-PAGE and multiplex gelatin zymography.

3.2.3 Fibrin Fragment Degradation

Fibrin gels were formed using the protocol described above. Gels were incubated with plasmin (5µg/µL) for 24 hours and the soluble fraction, containing released fibrin fragments, was collected. Recombinant human cathepsins K, L, and S (1.5µg) in assay buffer (0.1M sodium phosphate buffer, pH 6.0, 1mM EDTA) with 2mM dithiothreitol (DTT) was added to fibrin fragments for 24 hours at 37ºC. Samples were prepared for reduced SDS-PAGE and multiplex gelatin zymography.

3.2.4 SDS-PAGE

Samples were prepared with reduced loading dye (5X - 0.05% bromophenol blue, 10% SDS, 1.5 M Tris, 50% glycerol, 25% beta-mercaptoethanol) and run on 10% SDS-PAGE gels. Gels were stained with Coomassie stain (10% acetic acid, 25% isopropanol, 4.5% Coomassie blue), followed by destaining (10% isopropanol and 10% acetic acid) and imaged with an ImageQuant LAS 4000 (GE Healthcare), and densitometry performed with ImageJ (NIH) to quantify fibrin polypeptide chains.

3.2.5 Multiplex Cathepsin Zymography

Samples were resolved in multiplex cathepsin zymography using methods previously described [146]. Briefly, samples were prepared using a non-reducing loading buffer (5×-0.05% bromophenol blue, 10% sodium dodecyl sulfate (SDS), 1.5 M Tris, 50% glycerol. A 12.5% SDS-PAGE gel was used and embedded with 5 mg/ml gelatin substrate. Both gels were run at 200 V at 4 °C. Proteases were renatured in 65mM Tris buffer pH 7.4 with 20% glycerol for 3 washes, 10 min each, then incubated in and pH 4 (acetate buffer, 1mM EDTA with 2mM DTT, freshly added) or pH 6 (phosphate buffer, 1mM EDTA with 2mM DTT, freshly added) activity assay buffer. After overnight incubation, gels were

stained with Coomassie Blue (4.5% Coomassie blue; Sigma-Aldrich, 10% acetic acid, and 10% isopropanol) then destained (10% acetic acid and 10% isopropanol).

3.2.6 Statistical Analysis

Statistical significance was determined using a two-way ANOVA between normalized no enzyme control and recombinant enzyme control, respectively, using GraphPad. All experiments were replicated at least three times and a p value of <0.05 was considered statistically significant.

3.3 Results

3.3.1 Cathepsin L degrades fibrin gels, releasing degraded fibrin products into the supernatant.

To test if human cathepsin L (catL) has fibrinolytic activity, polymerized fibrin gels were incubated with increasing amounts of catL, or plasmin as a positive control, in 96-well plates for 24 hours. Fibrin gels were imaged before and after degradation; areas of grey are intact fibrin and areas of black indicate regions where fibrin gel was degraded (Fig 3-1A). Empty wells are all black. The mean value of grey areas was measured to quantify percent intact fibrin gel. As catL amount incubated with the gels increased, there was a loss of fibrin gel by 3%, 26%, and 48% for 0.15, 0.75, and 1.5 µg, respectively, with a significant decrease at 1.5µg of catL compared to the no enzyme control ($n=4$, $*p<0.005$) (Fig 3-1A). Next, it was determined if the fibrin molecule itself was degraded into fragments using reducing SDS-PAGE. After incubation, the supernatant was collected, containing solubilized fragments released from the fibrin gel (referred to as the soluble fraction), and the remaining fibrin gel (referred to as the insoluble fraction) was solubilized by breaking disulfide bonds between the fibrin α, β, and γ chains with 25% beta-mercaptoethanol in Tris-HCl. Proteins were then resolved by reducing SDS-PAGE and stained with Coomassie blue to determine proteolysis of the α, β, and γ chains in both

supernatant (soluble) and fibrin gel (insoluble) fractions. For the soluble fraction α, β, and γ chains were only identified in supernatant of gels incubated with 0.15μg catL, the lowest amount, suggested by hydrolysis of α band in other lanes. There was a significant loss of the α chain in the insoluble gel fraction as the amount of catL increased (n=3-5, *p<0.005; #p<0.0001) (Fig 3-1B), which corroborates the gel degradation images from Figure 3-1A.

Multiplex cathepsin zymography was used to identify active catL remaining in the soluble fractions, after incubations, which are visualized as cleared, white bands (Fig. 3-1C). To determine if there was a correlation with the degraded fibrin in the insoluble fraction, visualized as Coomassie stained dark bands (Fig. 3-1D). It should be noted that catL was not expected to provide a zymography signal in the insoluble fraction due to gel dissolution with β-mercaptoethanol, which also breaks cathepsin disulfide bridges and diminishes activity. Soluble fractions contained active catL bands at the expected molecular size of 20 kDa, with increasing intensity as the incubated amount of active catL increased. With as little as 0.15 μg, the active catL band was visible at 100 kDa and 37 kDa, but as the amount of catL incubated with the fibrin gels increased, active catL appeared at other molecular weights: between 100 and 75 kDa, and between 75 and 50 kDa (n=3–5, **p < .05; %p < .01; #p < .0001). The associations between fibrin and catL were even able to withstand the ionic detergent, SDS, denaturation as they migrated through the polyacrylamide gel. The cascading pattern of higher molecular weight active catL bands corresponded to the loss of α and β chains of fibrin protein. Active catL bands were quantified by densitometry and displayed in the graph for the 75, 50, 37, and 20 kDa.

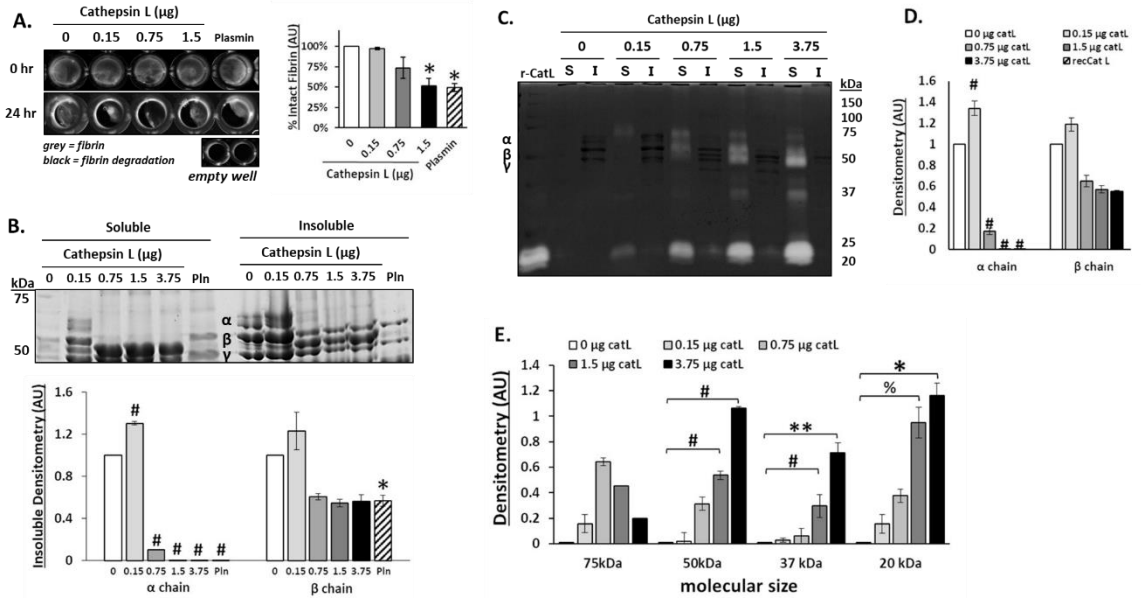

Figure 3-1: Cathepsin L degrades fibrin gels, releasing fibrin degradation products into the supernatant. Fibrin gels (100 µl) were polymerized in 96 well plates then incubated with increasing amounts of cathepsin L (catL) in 50 µl assay buffer for 24hrs. **(A)** Fibrin gels were imaged in 96 well plates before (0 h) and after (24 h) incubation, where grey color indicates intact fibrin and black indicates areas of degraded fibrin gel, as shown by the black levels in the empty wells. Area of grey intensity were quantified to determine intact fibrin percentage. The fibrin gel was degraded by 3%, 26%, and 48% for 0.15, 0.75, and 1.5 µg, respectively, with a significant decrease at 1.5µg of catL compared to the no enzyme control. **(B)** After degradation, the fibrin fragments released into the supernatant (denoted to as the soluble fraction) were collected and the remaining fibrin gel (insoluble fraction), was collected and solubilized with β-mercaptoethanol to prepare it for SDS-PAGE. Coomassie stained protein bands of α (63.5 kDa), β (56 kDa), and γ (47 kDa) chains of fibrin were visible in the insoluble fraction. Densitometry of bands are quantified in the graph. As the amount of catL increased, there was a significant loss of the α chain from the insoluble gel fraction. **(C)** Cathepsin zymography was used to assess the amount of active catL. Active catL bands were identified in the soluble fraction at multiple molecular sizes. Unbound active catL appears at 20 kDa and the higher molecular weight (75 to 37kDa) bands of active catL appear in a cascading pattern that corresponds to the degraded α and β fibrin fragments. Bands are quantified in the graph at the right by densitometry for the insoluble α and β chains of fibrin, and 75 kDa, 50 kDa, 37 kDa, and 20 kDa bands. (n=3-5, **p<0.05; %p<0.01; *p<0.005; # p<0.0001)

3.3.2 Cathepsin K degrades α and β fibrin polypeptide chains, and fibrin degradation products.

Cathepsin K (catK) was also investigated to determine if it could degrade fibrin. Fibrin gels were prepared as described above, incubated with increasing amounts of catK for 24 hours, and both supernatant and fibrin gel were assayed, as was done for catL. There was a significant decrease in fibrin gel with 1.5µg of catK compared to no enzyme controls (n=5, ^$p<0.001$) (Fig 3-2A). CatK degraded the α and β fibrin chains with as little as 0.15µg, as shown in the SDS-PAGE of the insoluble fibrin gel (n=5, *$p<0.005$; #$p<0.0001$) (Fig 3-2B). As the amount of catK was increased, little to no solubilized fibrin was detected in the supernatant, suggesting that even the released fibrin was subject to further degradation by catK. From zymography, no active catK was detected in the soluble or insoluble fractions as indicated by no cleared white bands (n=5) (Fig 3-2C).

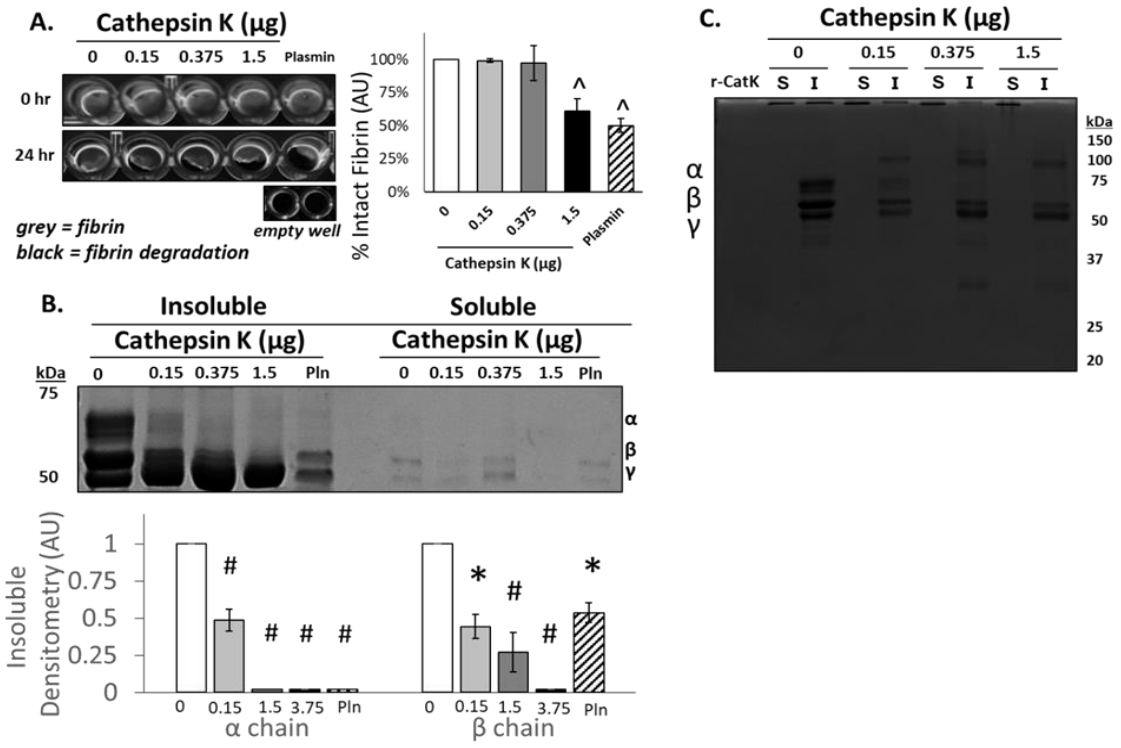

Figure 3-2: Cathepsin K degrades α and β fibrin polypeptide chains. Increasing amounts of cathepsin K (catK) were incubated with fibrin gels for 24 hours in 96-well plates. **(A)** Fibrin gels were imaged before and after incubation, with grey indicating intact fibrin. As the amount of catK increased, more fibrin degradation was observed with a significant decrease in fibrin with 1.5µg of catK. **(B)** Loss of fibrin α, β, and γ bands in the insoluble gel was determined using SDS-PAGE; densitometry below is for the α and β chain of remaining fibrin gel (insoluble). In the soluble fraction, little to no fibrin fragments were detected. **(C)** The zymogram showed no active catK remained in either the fibrin gel or in the supernatant with the released fibrin fragments. (n=5, *$p<0.005$; ^ $p<0.001$, # $p<0.0001$)

3.3.3 Cathepsin S degrades α, β, and γ fibrin polypeptide chains, and fibrin degradation products.

There was complete dissolution of the fibrin gel when incubated with either 0.75 or 1.5 µg of catS after 24 hours (n=5, *p<0.05; #p<0.0001) (Fig 3-3A). SDS-PAGE confirmed that 0.15 µg of catS significantly hydrolyzed the α chain of fibrin, and both the α and β chains were completely degraded with 0.75µg of catS (n=5, *p<0.05; #p<0.0001) (Fig 3-3B). Released fragments were not detected in the soluble fraction, except for after incubation with 0.75 µg catS, suggesting near complete degradation of released fragments. Zymography was used to quantify active catS. Active catS was detected only at 25kDa, the expected size for free catS, and not associated with any higher molecular weight fibrin fragments (n=5, #p<0.0001) (Fig 3-3C). As with catK, large macromolecules, unable to migrate through the gel, were also observed in the soluble fraction at the top of the gels (open arrow). The intensity of these large fragments is inversely related to the amount of catS during the incubation period, and smaller fragments were detectable in the supernatant (50 to 37kDa) at the highest amount of catS, when no large protein is present, suggesting its degradation.

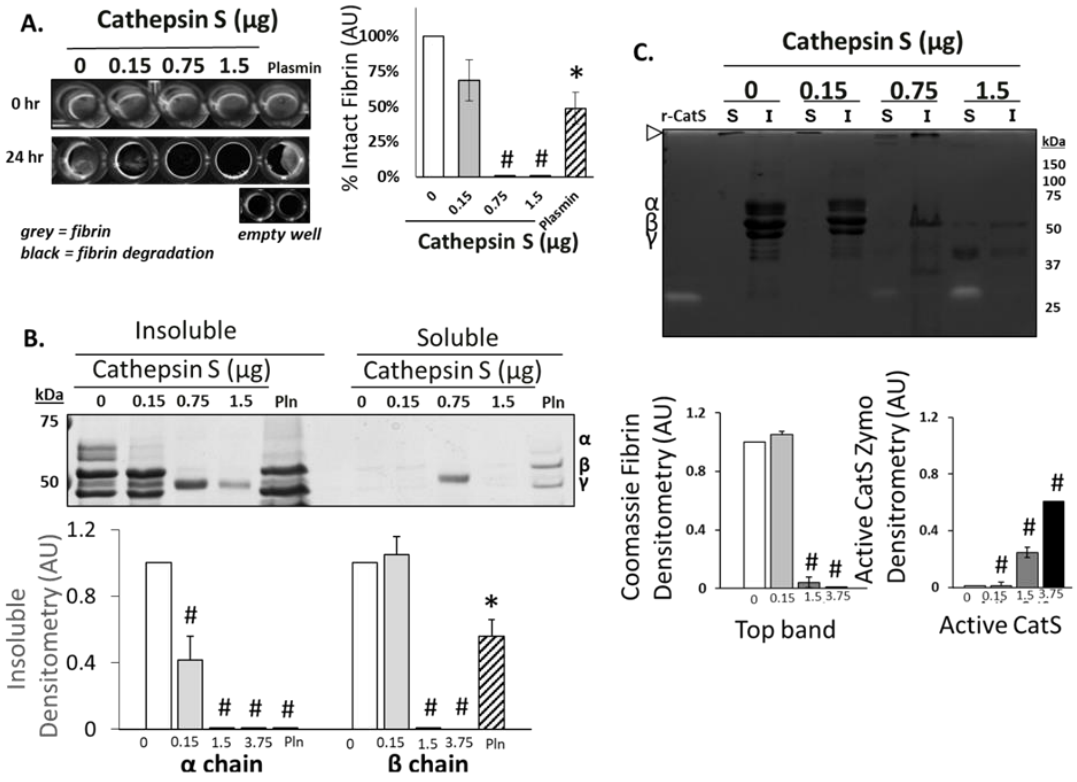

Figure 3-3: Cathepsin S degrades the α, β, and γ fibrin polypeptide chains, and fibrin fragments. Fibrin gels were formed and incubated with increasing amounts of cathepsin S (catS) for 24 hours. **(A)** 96-well plates were imaged pre- and post cathepsin incubation. As the catS amount increased, more fibrin degradation was observed and was quantified as shown with complete degradation of fibrin with 0.75 and 1.5µg of catL. **(B)** SDS-PAGE used to image loss of fibrin α, β, and γ polypeptides due to catS hydrolysis fibrin degradation; densitometry below is for the α and β chain of remaining fibrin gel (insoluble) normalized to the no enzyme control. Increased catS amounts correlated with loss of the α and β fibrin chains in the fibrin gel (insoluble fraction) and little to no detection of fibrin fragments (soluble fraction). Densitometry is shown below for the α and β fibrin gel. **(C)** Zymography was used to quantify active catS. Unbound catS was detected in the soluble fraction with increasing intensity correlated to increasing catS amount. Large macromolecules that are unable to migrate through the gel were also observed in the soluble fraction (open arrow at top of gel image). (n=5, *p<0.05; #p<0.0001).

3.3.4 Time course of fibrin gel degradation by cathepsins K, L, and S.

Incubation of fibrin gels with either catK or catS led to minimal detection of released fibrin fragments from the supernatant, contrary to catL. It was hypothesized that cleaved fibrin fragments were initially released but not detected because they were completely degraded by the cathepsins over time. To test this hypothesis, fibrin gels were incubated with 1.5μg of catK, L, S, or plasmin for a time course of 4, 8, or 24 hours. A statistically significant loss of fibrin gels was observed after 24 hours for catK, catL, and catS (n=5, %$p<0.01$, #$p<0.0001$) (Fig 3-4A). CatS, however, seemed to degrade the fibrin faster, reaching statistical significance after only 4 hours. After incubation with catK, the α chain of fibrin was not detected by as early as 4 hours from the fibrin gel fraction (Fig 3-4B). Of the fibrin fragments released into the soluble fraction, α and β fibrin polypeptides were detected after both 4 hrs and 8 hrs ($p<0.05$), but then there was a loss of the α chain by 24 hrs, suggesting catK released the fragments and then degraded the fragments in the supernatant (Fig 3-4B- left). For catL, there was a steady loss of the α chain of fibrin from 4hrs to 8 and 24hrs in the supernatant and fibrin gel (Fig 3-4B- center). CatS completely degraded the α and β chains of fibrin in the supernatant and fibrin gel after only 4hrs (Fig 3-4B- right), with complete loss of all signal by 24 hrs, coinciding with the complete degradation of the fibrin gels previously observed (Fig 3-4A).

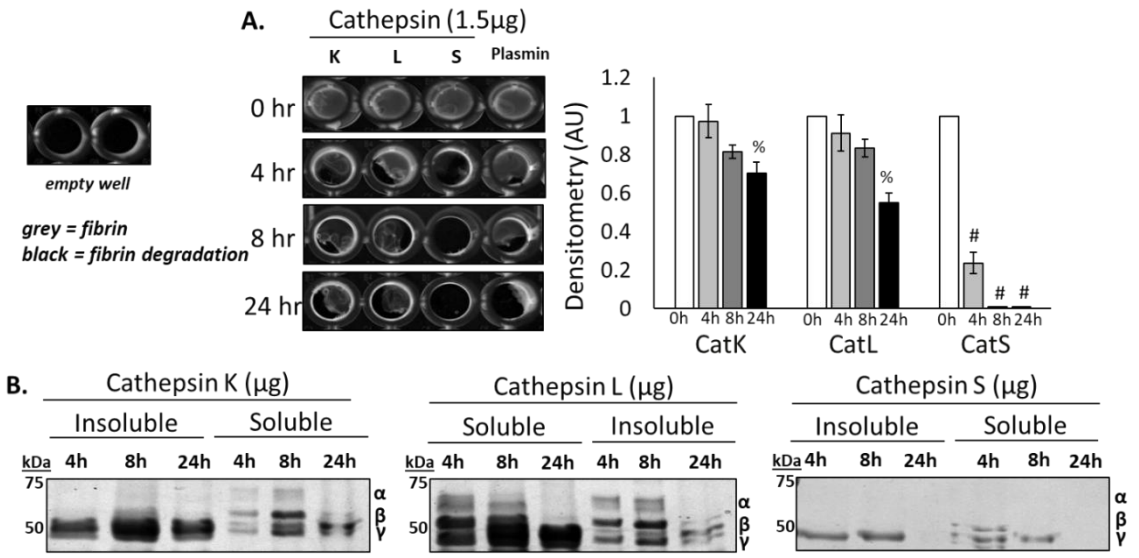

Figure 3-4: Cathepsin L degrades fibrin gels, releasing fibrin degradation products into the supernatant. Fibrin gels (100 µl) were polymerized in 96 well plates then incubated with increasing amounts of cathepsin L (catL) in 50 µl assay buffer for 24hrs. **(A)** Fibrin gels were imaged in 96 well plates before (0 h) and after (24 h) incubation, where grey color indicates intact fibrin and black indicates areas of degraded fibrin gel, as shown by the black levels in the empty wells. Area of grey intensity were quantified to determine intact fibrin percentage. The fibrin gel was degraded by 3%, 26%, and 48% for 0.15, 0.75, and 1.5 µg, respectively, with a significant decrease at 1.5µg of catL compared to the no enzyme control. **(B)** After degradation, the fibrin fragments released into the supernatant (denoted to as the soluble fraction) were collected and the remaining fibrin gel (insoluble fraction), was collected and solubilized with β-mercaptoethanol to prepare it for SDS-PAGE. Coomassie stained protein bands of α (63.5 kDa), β (56 kDa), and γ (47 kDa) chains of fibrin are visible in the insoluble fraction. Densitometry of bands are quantified in the graph. As the amount of catL increased, there was a significant loss of the α chain from the insoluble gel fraction. **(C)** Cathepsin zymography was used to assess the amount of active catL. Active catL bands were identified in the soluble fraction at multiple molecular sizes. Unbound active catL appears at 20 kDa and the higher molecular weight (75 to 37kDa) bands of active catL appear in a cascading pattern that corresponds to the degraded α and β fibrin fragments. Bands are quantified in the graph at the right by densitometry for the insoluble α and β chains of fibrin, and 75 kDa, 50 kDa, 37 kDa, and 20 kDa bands. (n=3-5, **p<0.05; %p<0.01; *p<0.005; # p<0.0001).

3.3.5 Cathepsins L and S remain active over longer periods in the presence of fibrin.

Mature cathepsins can lose their proteolytic activity in vitro over short periods of time (within a few hours), but the presence of specific macromolecular substrates, such as collagen and elastin, can stabilize and extend cathepsin activity [50, 147]. To test if fibrin was one such substrate, cathepsin zymography was used to determine the amounts of active cathepsins K, L, and S that were present after increasing incubation times with fibrin gels. No active catK was detected in the released fibrin fragments at any of the time periods (n=4) (Fig. 3-5A). However, active catL was observed at all time points tested (Fig. 3-5B). As the incubation period extended from 4 to 24 hours, there was a significant cascading loss of active catL signal at higher molecular weight bands (100, 75, 50, and 37kDa) progressively, with the 50kDa band remaining relatively constant, as quantified in the densitometry (n=4, #$p<0.0001$). CatS was different from both catK and catL, in that active catS was detected only at 25 kDa, unbound catS, its expected size, and the signal was diminishing from 4 to 24hrs concomitant with loss of Coomassie stained fibrin fragment signal (n=4) (Fig. 3-5C).

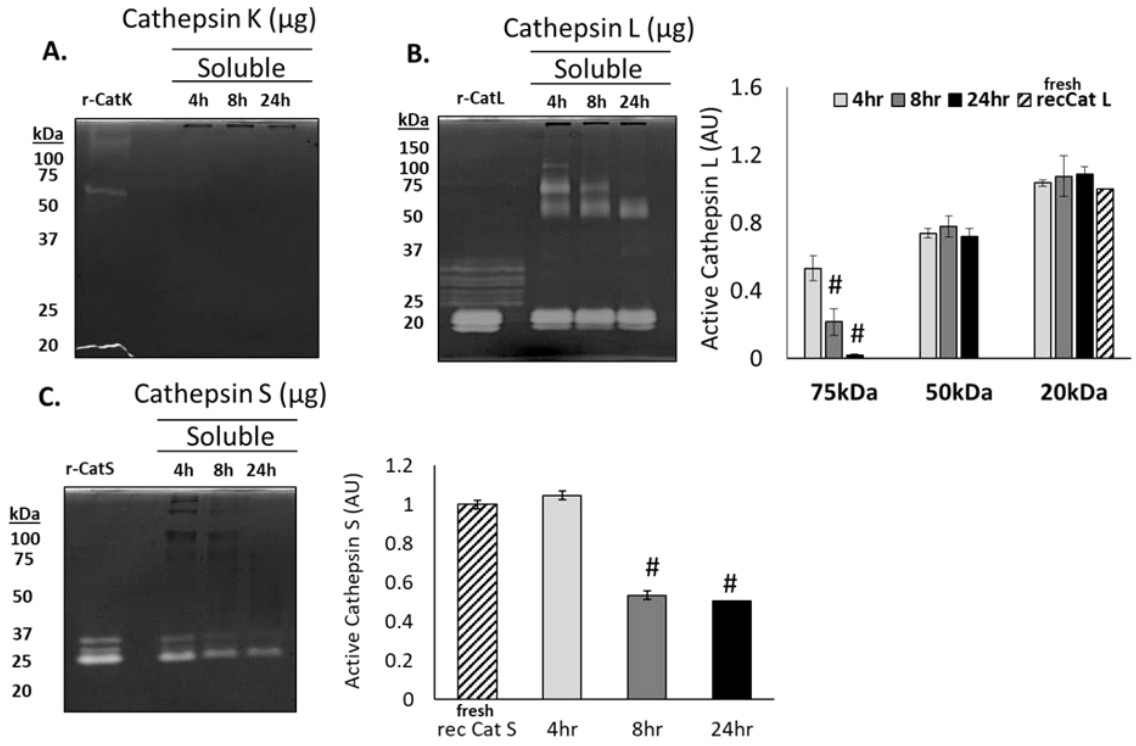

Figure 3-5: Cathepsins L and S remain active over longer periods of time in the presence of fibrin. Zymography was used to determine the ability for fibrin to extend the activity time of cathepsins K, L, and S. **(A)** No active catK was detected in the supernatant after 4, 8, or 24 hours. **(B)** Bands of active catL appear with a cascading loss of higher molecular weight bands (100, 75, 50, and 37kDa) between 4 and 24 hours. **(C)** Active catS was only detected at 25kDa, its expected molecular weight, with the amount of active catS decreasing over 24 hours. (n=4, #p<0.0001)

3.3.6 Cathepsins K, L, and S degrade plasmin-generated fibrin fragments.

To specifically demonstrate if cathepsins are capable of successively proteolyzing released fibrin fragments from the bulk fibrin gel into undetectable fragments, catK, L, and S were incubated with fibrin fragments. To generate these fragments, polymerized fibrin gels were first incubated with plasmin for 24 hours, and the soluble fraction was collected, then separately incubated with 1.5μg of either catK, catL, or catS for an additional 24hrs. All samples were resolved in SDS-PAGE, alongside aliquots of the plasmin-generated fragments sample that was not subject to cathepsin proteolysis as a control (n=4). Compared to control, there was a loss of the 55kDa fibrin fragment after incubation with catK and catL (Fig 3-6A). CatS also completely degraded the 55kDa fibrin fragment in addition to the 50kDa and 45kDa fibrin fragments (Fig 3-6A). Cathepsins K, L, and S successively processed the plasmin-generated fibrin fragments into lower molecular weight fragments (25 kDa to 37kDa), supporting our hypothesis that cathepsins cleave fragments from fibrin gel, but can also successively proteolyze released fibrin fragments generated by plasmin.

Zymography was used to assess the amount of active cathepsins present after incubation with plasmin-generated fibrin fragments (Fig 3-6B). Zymograms were incubated at pH4 for optimal catL activity and pH6 for optimal catK activity [148]. In contrast to catK co-incubation with fibrin gels (Fig 3-2C), when catK was co-incubated with fibrin fragments (Fig 3-6B), active catK was detected at 75kDa, a size where active catK has been detected when bound to ECM [149], different from its usual expected electrophoretic migration distance of 37 kDa. Active catL and catS were observed at their expected molecular sizes, 20kDa and 25kDa, respectively. When catL was co-incubated with fibrin (Fig 3-1C) or fibrin fragments (Fig 3-5B), active catL was detected at higher molecular weights, ~50kDa and 37kDa. This demonstrates catL can successively cleave fibrin fragments and remain bound to fibrin fragments during successive proteolytic cleavage.

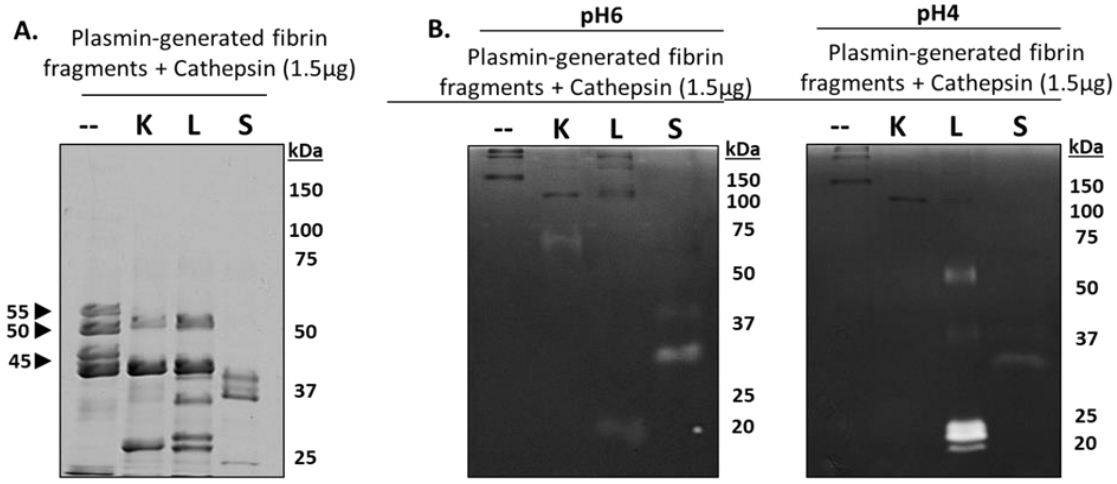

Figure 3-6: Cathepsins K, L, and S degrade plasmin-generated fibrin fragments. To identify if cathepsins K, L, or S could successively degrade the released fibrin fragments into smaller molecular weight fibrin fragments, fibrin gels were first incubated with plasmin for 24 hours, then the fibrin fragments released into the supernatant were collected then incubated with catK, L, or S for 24 hours. **(A)** Compared to the no enzyme control, catK, L, and S successively degraded the fibrin fragments into lower molecular weight fragments. CatS completely degraded the 55kDa, 50kDa, and 45kDa fragments while catK and L only degraded the 55kDa fibrin fragments. **(B)** From zymography, active catL was at its expected molecular size (20kDa), as well as the higher molecular weights (~50kDa and faintly at 37kDa), corresponding to the results from the dosing and time course fibrin degradation experiments. Active catK is observed at 75kDa. Unbound active catS was observed at 25kDa in the zymograms incubated at pH 6. Active catL appears in the zymograms incubated at pH 4.

3.4 Discussion and Conclusions

Taken together, these results demonstrate that human cysteine cathepsins K, L, and S are fibrinolytic proteases. This has not been demonstrated for the human cathepsins previously, although parasitic orthologues have indicated they had fibrinolytic potential [12, 150]. From these data, catK, L, and S can hydrolyze the α and β chains of fibrin as indicated by the loss of these chains in SDS-PAGE after incubation with the proteases of interest. Further, it was demonstrated that although cat K, L, and S share 60% sequence homology; cleavage patterns after fibrinolysis are unique to each cathepsin (Fig 3-7), plus their rates of fibrinolysis differed, which was shown by the degradation and loss of the fibrin gels with increasing amounts of enzyme and when they were incubated for different periods of time. CatS was the most fibrinolytic, followed by catK and L, yet catK and L differed in a number of ways. CatL was bound to multiple cleavage fragments of fibrin, and this mechanism of association, still to be determined, was sufficient to retain its binding even in the presence of SDS, a strong ionic detergent. CatK, however, did not show this property and the amount of active catK was not detected by zymography after the incubation periods. This is relevant in that certain substrates have been shown to extend the active life of cysteine cathepsins, and from these studies, fibrin should be added to this list for cathepsin L. Finally, catK, L, and S appear not to hydrolyze the fibrin in one event, but successively process it into smaller fragments, and can also bind and cleave fragments produced after plasmin-mediated fibrinolysis suggesting multiple sites of cleavage along the molecule. Again, the patterns of degradation differ among the cathepsins studied here, corroborating the finding that though they are closely related, they still retain unique properties that can be relevant in physiological systems.

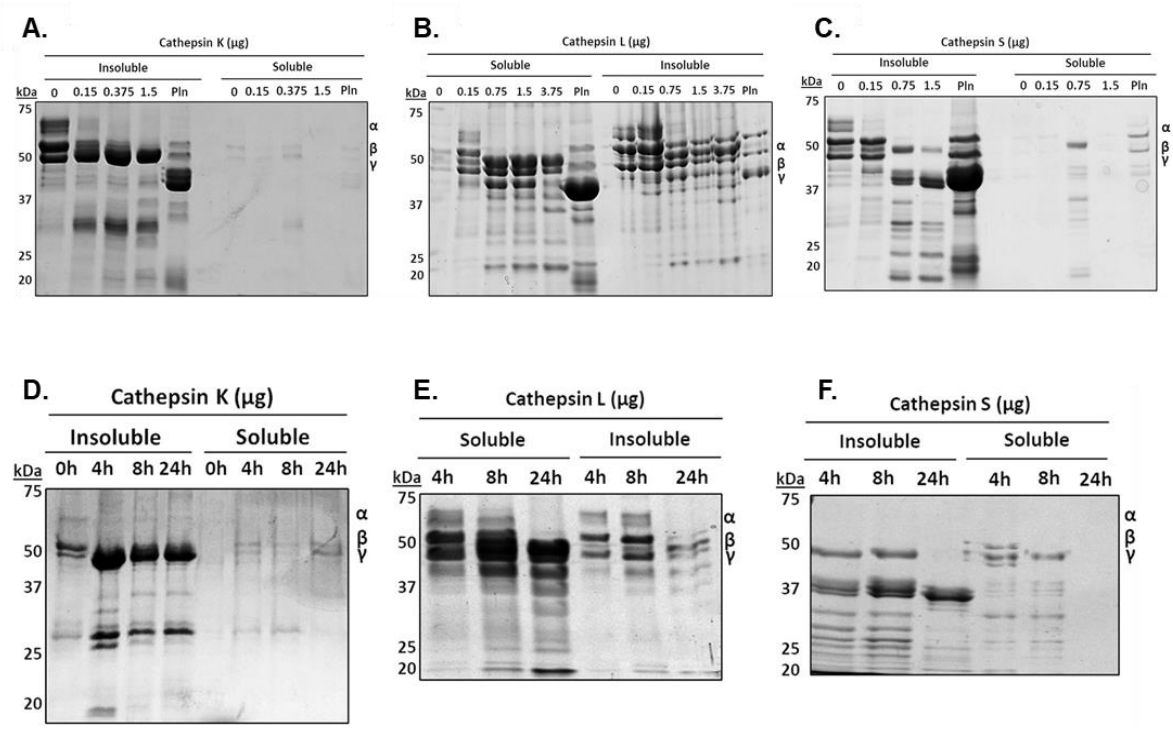

Figure 3-7: Cleavage patterns after fibrinolysis are unique for cathepsins K, L, and S compared to plasmin. (A-C) Increasing amounts of cathepsins K, L or S (catK, L or S) were incubated with fibrin gels for 24 h. After degradation, the fibrin fragments released into the supernatant (denoted as the soluble fraction) were collected and the remaining fibrin gel (insoluble fraction), was collected and solubilized with β-mercaptoethanol to prepare it for SDS-PAGE. Coomassie stained bands denote the different patterns when cleaved by each of the cathepsin**. (D-F)** 1.5 µg of cathepsins K, L or S (catK, L or S) were incubated with fibrin gels for 4, 8, or 24 h. (0 h control time points for insoluble and soluble fractions shown in catK gel). After degradation, the fibrin fragments released into the supernatant (denoted as the soluble fraction) were collected and the remaining fibrin gel (insoluble fraction), was collected and solubilized with β-mercaptoethanol to prepare it for SDS-PAGE. Coomassie stained bands denote the different patterns when cleaved by each of the cathepsin.

There is clinical relevance to these findings as fibrin is involved in the coagulation cascade after vessel injury. The proteases thrombin and plasmin are considered responsible for the initiation and degradation of fibrin [35, 36, 58], respectively, and the possibility of other enzymes being involved is understudied. Cysteine cathepsins are known to be involved in vascular related injuries [27, 151] and vascular remodeling [6, 152], and identified in atherosclerotic plaques [6, 153]. Cathepsins have been shown to be produced and secreted by endothelial cells that line the blood vessel wall [6, 152], and even catB and catD shown to play some role in cleaving other factors in the fibrinolytic system [154]. With such access to the clot, the roles of cysteine cathepsins and their putative activity to resolve these clots should be considered in physiological, and perhaps pathophysiological scenarios. As an example, elevated cysteine cathepsins are elevated in sickle cell disease [40], which is a disease that is also associated with a hypercoagulable state [155]. Cathepsin partial or complete fibrinolysis may prevent full solid clots from forming or staying in a protective way. However, our recent study also shows that cathepsins potentially can be involved in fibrin gel formation as they can hydrolyze fibrinogen as well [42]. This putative conflict will need to be resolved to understand the participation of this additional class of proteases in hemostasis.

There are specific details to highlight regarding the differences among cathepsins K, L, and S. CatS appeared to degrade the fibrin gel faster than the other proteases in this in vitro study, but it may not necessarily be a better fibrinolytic enzyme than plasmin in vivo; there are pH dependent and environmental cofactors that must be considered, but this deserves further investigation since catS is unique among cysteine cathepsins in that it retains its activity at neutral pH [7, 54]. Additionally, cathepsin S was shown to be elevated in the plasma of patients with diabetes [156, 157], associated with wound healing and hemostatic abnormalities, and other cardiovascular diseases, which may be a biomarker for these diseases [152, 158, 159]. Adsorption of active cathepsins to substrates and extension of their active lifetimes has been described for elastin [50] and collagen [147], and these

data presented here suggest fibrin be added to this list for catL. CatL and catK have had exosites identified that improve their catalysis of matrix proteins by binding them at these allosteric sites [158]. It was not identified if the fibrin binding site for catL is the same as its exosite for elastin, but the mechanism may exist. CatL adsorbs to fibrin as it was cleaved from the bulk fibrin gel, and the fibrin could be serving as a pool for active catL, thus stabilizing and sustaining its activity. As catL cleaves fibrin, it remains active and provides further hydrolysis of fibrin fragments which can prolong proteolysis within the system. These implications for fibrin acting as a reservoir for catL, to extend catL-mediated degradation in native tissue or in engineered tissue constructs, could be a design issue for tissue engineers using fibrin constructs in regenerative medicine and therapeutics research.

There is already evidence of unexplained proteolytic breakdown of fibrin-based tissue engineered constructs. Cysteine cathepsins were shown to be upregulated in engineered living systems such as a walking biological machine, composed of a skeletal muscle strip made with fibrin as part of its scaffold. Studies used aminocaproic acid (ACA), which inhibits conversion of plasminogen to plasmin, slowed degradation of the muscle strips at earlier time points, but catL was still active and a contributing factor to the breakdown of the walking biological machine [144]. Microvascular networks formed in a microfluidic device using a co-culture of endothelial cells and fibroblasts encapsulated in fibrin, formed a patent lumen. However, within days to weeks the networks collapse in an unpredictable, uncontrolled manner [15] and cathepsin mediated degradation may be involved. During vasculogenesis, proteolytic activity is required for matrix remodeling [20, 160] and uncontrolled proteases could lead to scaffold destabilization. Fibrin-based constructs for the nervous system have been developed and reviewed here [161]. Fibrin nanoparticles have also been proposed for drug delivery [162], and their degradation by cysteine proteases can affect release profiles.

To conclude, this work introduced human cysteine cathepsins as a new class of proteases for the biomaterial community to consider when developing fibrin-based

constructs. It is possible that fibrin-based constructs can sustain active cathepsins which will degrade them, causing constructs to fail. This motivates our future studies to identify the cleavage sites of cathepsin on fibrin to better understand the mechanism and develop novel cathepsin inhibition strategies to control proteolysis and meet design criteria for proper engineering. There is also clinical relevance and potential research avenues for cathepsin based mechanisms underlying aberrant clot resolution, especially since cathepsins are secreted by endothelial cells which line the blood vessel walls providing direct access to clots.

CHAPTER 4 BIOMECHANICAL AND BIOCHEMICAL REGULATION OF CYSTEINE CATHEPSINS IN MATRIX-REMODELING OF FIBRIN-BASED ENGINEERED MICROVASCULAR NETWORKS

4.1 Introduction

Vasculogenesis is the formation of *de novo microvessels*, which is usually observed in embryogenesis, tumor growth, and after extensive vascular damage [73, 74]; this differs from angiogenesis where microvessels are formed from pre-existing vessels, usually after injury [22]. These processes are complex and coordinated, involving ECM remodeling, endothelial cell (EC) migration, cytokine secretion, lumen formation, and mural cell (i.e.: pericyte) recruitment [22, 73, 74]. The mechanisms that drive vasculogenesis and angiogenesis need to be better understood, as it can help engineers develop better strategies for microvascular networks in regenerative medicine.

Cell microenvironments, which include extracellular matrix (ECM), various cell types, and factors (i.e.: signaling molecules or proteases), change cellular behavior. The ECM could act as a reservoir for bound growth factors and proteases which could indirectly regulate ECs; thus, controlling availability of biochemical signals [22]. Capillary morphogenesis requires proteolytic remodeling of ECM during EC migration, invasion into perivascular tissue, and tubulogenesis or lumen formation [22, 23, 163]. This is mediated by various cell types secreting angiogenic factors and extracellular proteases, such as matrix metalloproteinases (MMPs) [21-23].

The role of MMPs in vasculogenesis have been well studied and characterized. Following induction by pro-angiogenic factors, such as VEFG [164] and FGF [165], MMPs, secreted by ECs, degrade the surrounding ECM [21, 22]. *In vitro* and *in vivo*

models have demonstrated that MMPs are important for migration and invasion of endothelial cells (ECs) [19, 166]. MMP-1, -2, and -9, degrade ECM and basement membrane to aid in vascular remodeling, cell migration, and sprout formation [77]. They can also release ECM-bound angiogenic growth factors in pericytes from vessels undergoing angiogenesis [20]. As such, MMPs have been a common focus of study [20, 21, 77] and primary target of inhibition during the development of engineered microvessels as a strategy to enhance their development [14, 167]. However, other proteases, like cysteine cathepsins, could contribute to active ECM remodeling in the vascular niche.

Cathepsins have been implicated in angiogenesis [24-28] and in the pathogenesis of vascular diseases, including atherosclerosis and the formation of abdominal aortic aneurysms [6, 26, 143, 168]. Studies have shown that specifically, cathepsins K and S (catK and S) are involved in neovascularization, where their inhibition has impaired formation of vessels [27, 28]. Stimulation of ECs with inflammatory cytokines and angiogenic factors induced catS expression, but when catS was inhibited, cell invasion was impaired and EC tube formation was reduced [24]. Increased cathepsin L (catL) has been linked to cell invasion and neovascularization [3, 83], and catL has been identified in tip/stalk-like and phalanx-like ECs, types of invasive/migratory ECs [169]- this is discussed more in Chapter 7. Thus, cathepsins potentially play pivotal roles in angiogenesis/vasculogenesis, and they are likely to be involved in remodeling of matrix in microvascular network formation.

Here, the role of cathepsins in proteolysis during microvascular network development was determined by using a microfluidic model to perturb the network using flow and cathepsin inhibitors. ECM and vascular remodeling are dependent on biomechanical and biochemical cues within the microenvironment [21-23], and it is

important for engineers to consider the role of matrix remodeling proteases during microvessel formation. Studying these complex interactions can improve understanding their role in vasculogenesis, which can help improve design constraints for future microvascular networks. Our work demonstrates that active cathepsins decrease under fluid flow conditions while increasing their endogenous inhibitor, cystatin C. Adding cathepsin inhibitors to microvessels cultured under static conditions reduces the amount of active cathepsins. These findings suggest that cathepsin inhibitor interventions could aid in prolonging network stability, demonstrating the need for us to consider cathepsins as contributors to ECM remodeling in microvasculature network.

4.2 Materials and Methods

4.2.1 Cell Culture and Generation of Microvascular Networks

Human umbilical vein endothelial cells (ECs) were transduced by standard Lentivirus procedures to label the cytoplasm by red or blue fluorescent protein expression (RFP or BFP) and normal human lung fibroblasts (fibroblasts) which are non-fluorescent in all experiments, except for Figure 2 (cytoplasmic GFP). Both cell types were purchased from Lonza and were cultured until confluency in T150 and T75 flasks coated with rat tail collagen 1 (50mg/mL, Corning). HUVEC were cultured in VascuLife media (LL-0003) and normal human lung fibroblasts (fibroblasts) were cultured in FibroLife (LL-0011) media (Lifeline Cell Technology) that was changed every 2 days.

Once confluent, cells were dissociated using TrypLE (ThermoFisher) at concentrations of $24x10^6$ cells/mL ECs and $4.8x10^6$ cells/mL fibroblasts, which results in final cell concentrations of 6 and 1.2 $x10^6$ cells, respectively. Thus, a 5:1 ratio of EC:fibroblasts were cultured in a (fibrin gel 3mg/mL), as previously reported [170]. The

cell-gel solution was injected within a macro-scale (~100μL total gel volume) PDMS (10:1 ratio, Ellsworth adhesives) single-gel channel platform. Microvascular networks formed via a vasculogenesis-like process over ~7days, following which half of the` devices were exposed to continuous flow, inducing a low shear stress (~2Pa = 2 dynes/cm^2 – average value across vessels, as determined previously [171]) for 48hrs. Flow was maintained by a pressure head (~0.5mm H_2O) generated across the gel using an in-house built chamber fitted to the PDMS device, which was driven by a positive displacement (solenoid-driven) air pump. For sample collection for immunoblot and zymography, the hydrogel component of the PDMS devices containing microvascular networks were extracted (for both static and flow conditions) on day 9 and flash-frozen in the vapor phase using liquid nitrogen, and then stored at -80°C until further sample preparation as indicated below.

4.2.2 Cathepsin Inhibitor Experiments

Microvascular networks were grown in a scaled-down version (same as prior use [170, 172]) of the microfluidic chip (~35μL cell/gel volume). These microvascular networks were all cultured until day 7 prior to addition of 10μM E-64, or 1μM cystatin C (Molecular Innovations), or a control volume of diluent in the media. These samples were cultured until day 10 and flash-frozen in the vapor phase using liquid nitrogen, and then stored at -80°C until further sample preparation as indicated below.

4.2.3 EC and Fibroblast 2D Culture on Fibrin Gels

Fibrin gel (3mg/mL) was prepared by mixing at 1:1 ratio 6mg/mL fibrinogen (from bovine plasma, Sigma) with 4U thrombin (from bovine plasma, Sigma). A total volume of 100μL was added to the center of each well of a 12-well plate and rotated for complete coating. Fibrin was gelled for several minutes prior to addition of complete media and

incubation at 37°C overnight in a standard incubator. The following day ECs and fibroblasts were seeded onto either non-coated or fibrin coated wells, at a concentration of $5x10^4$ cells/well. HUVECs and fibroblasts were cultured for 2 days in VascuLife or FibroLife, respectively. Following that media was collected into a separate tube. The remaining cells and fibrin gel (homogenate), were collected and homogenized in zymography lysis buffer.

4.2.4 Immunofluorescence Staining and Confocal Microscopy Imaging

Microvascular networks in microfluidic devices were fixed at day 7 using 4% paraformaldehyde (PFA, 8% Electron Microscopy Science, diluted with Dulbecco's phosphate buffered saline (DPBS), VWR) for 30mins. Well-plates were fixed on day 2. Following several washes with DPBS, samples were subsequently permeabilized with Triton-x 100 (0.1% v/v in DPBS) for 10mins and incubation in blocking buffer (5% w/v BSA (Sigma), 3% v/v goat (or horse) serum in DPBS) for several hours. Primary anti-human antibodies were used at 2µg/mL in wash buffer (0.5% w/v BSA in DPBS) as follows: rabbit polyclonal anti-cathepsin K (ProteinTech), goat polyclonal anti-cathepsin L (R&D systems), goat polyclonal anti-cathepsin S (R&D systems), anti-collagen 1 (Abcam, ab34710), monoclonal mouse anti-FSP1 (Novus). Appropriate secondary antibodies (ThermoFisher) were used at dilutions of 1:200. DAPI (Invitrogen) was used at 1:1000 for 10mins. Samples were imaged on a confocal microscope (Olympus IX81) with Fluoview v4.1. Z-stack images were captured using 5µm slices (~20-30 total number) and presented as maximum z-projections, unless otherwise specified. Co-localization of antibodies was performed using the NIH ImageJ analysis tool.

4.2.5 Multiplex Cathepsin Zymography

Multiplex cathepsin zymography was used to assess active cathepsins, as previously described [148]. Samples were prepared using a non-reducing loading buffer (5×-0.05% bromophenol blue, 10% sodium dodecyl sulfate (SDS), 1.5M Tris, 50% glycerol. A 12.5% SDS-PAGE gel was used and embedded with 5 mg/ml gelatin substrate. Gels were run at 200 V at 4 °C. Proteases were renatured in 65mM Tris buffer pH 7.4 with 20% glycerol for 3 washes, 10 min each, then incubated in pH 6 (phosphate buffer, 1mM EDTA with 2mM DTT, freshly added) activity assay buffer overnight. Next, gels were stained with Coomassie Blue (4.5% Coomassie blue; Sigma-Aldrich, 10% acetic acid, and 10% isopropanol) then destained (10% acetic acid and 10% isopropanol). For inhibitor assays, 1µM of cathepsin K II inhibitor (1-(N-benzyloxycarbonyl-leucyl)-5-(N-Boc-phenylalanyl- leucyl) carbohydrazide [Z-L-NHNHCONHNH-LF-Boc], Calbiochem/Millipore Sigma) or 1µM of cathepsin L inhibitor (Z-FY-CHO, Calbiochem/Millipore Sigma) was added to the pH6 assay buffer prior to overnight incubation.

4.2.6 Immunoblotting

Samples were prepared with reduced loading dye (5× - 0.05% bromophenol blue, 10% SDS, 1.5M Tris, 50% glycerol, 25% beta-mercaptoethanol) and run on 12.5% SDS-PAGE gels. Proteins were transferred onto a nitrocellulose membrane, and then immunoblotted using the following antibodies: rabbit polyclonal anti-cathepsin K (ProteinTech), goat polyclonal anti- cathepsin L (R&D Systems), goat polyclonal anti-cathepsin S (R&D Systems), rabbit polyclonal anti-cystatin C (EMD Millipore), or goat

polyclonal anti-GAPDH (R&D Systems). Immunoblots were imaged using Odyssey CLx, LI-COR. Densitometry was performed with ImageJ (NIH).

4.2.7 Statistical Analysis

Statistical significance was determined using a two-way ANOVA (unless noted otherwise) between normalized RAW264.7 macrophage control or recombinant enzyme control, using GraphPad. All experiments were replicated at least three times and a p value < 0.05 was considered statistically significant.

4.3 Results

4.3.1 Shear, induced by flow, decreased amount of active cathepsins in microvascular networks

Generating vasculature within microfluidic devices allows for control over mechanical cues such as shear stress [23, 173, 174]. Considering the significant influence of fluid flow on vasculature [173, 175], and that mechanical cues are tied to remodeling of the vascular niche [176, 177], it is important to investigate how these mechanisms alter cathepsin activity during ECM remodeling. It has been previously reported that cathepsins are mechanosensitive [28]; catL activity is inhibited when ECs are exposed to laminar shear stress [6]. It was hypothesized that applying luminal flow through vessels would reduce active cathepsins in microvascular networks. To test this hypothesis, microvascular networks were developed in a large-scaled version of a single-gel channel PDMS device using a co-culture of human umbilical vein endothelial cells (ECs) and normal human lung fibroblasts in a fibrin gel, as previously described [170, 172]. Following microvessel formation, pressure driven recirculating fluid flow was applied from day 7 to day 9 (48hrs)

on half of the devices, with the others cultured under static conditions as controls. A pump was used to impose a shear stress averaging ~2Pa = 2 dynes/cm^2 [171]. The microvessels/networks were collected and homogenized, then samples were prepared for cathepsin zymography. Multiple active cathepsins bands were detected (37kDa, ~27kDa, and ~23kDa), which were determined to be cathepsins K and L based on known electrophoretic distances [148]. Flow significantly reduced the amount of active catK (37 kDa) by 42% ±2.3%, catK/L (27 kDa) by 52% ±4.5%, and catL (23 kDa) by 55% ±04.6 (Fig 4-1A).

Zymograms were repeated, in the presence of either a catK inhibitor (Figure Fig 4-1B) or a catL inhibitor (Fig 4-1C) to confirm the bands seen in Figure 1A. Incubation with the catK inhibitor blocked the appearance of the 37kDa, 27kDa, and 23kDa active bands. In the presence of the inhibitor, the 37kDa and 23kDa active bands no longer appeared; however, microvascular networks subjected to flow retained some active cathepsin bands at 27kDa, compared to static conditions ($p = 0.0134$). Thus, the 37kDa, 27kDa, and 25kDa bands are likely catK, and the 27kDa band is catL.

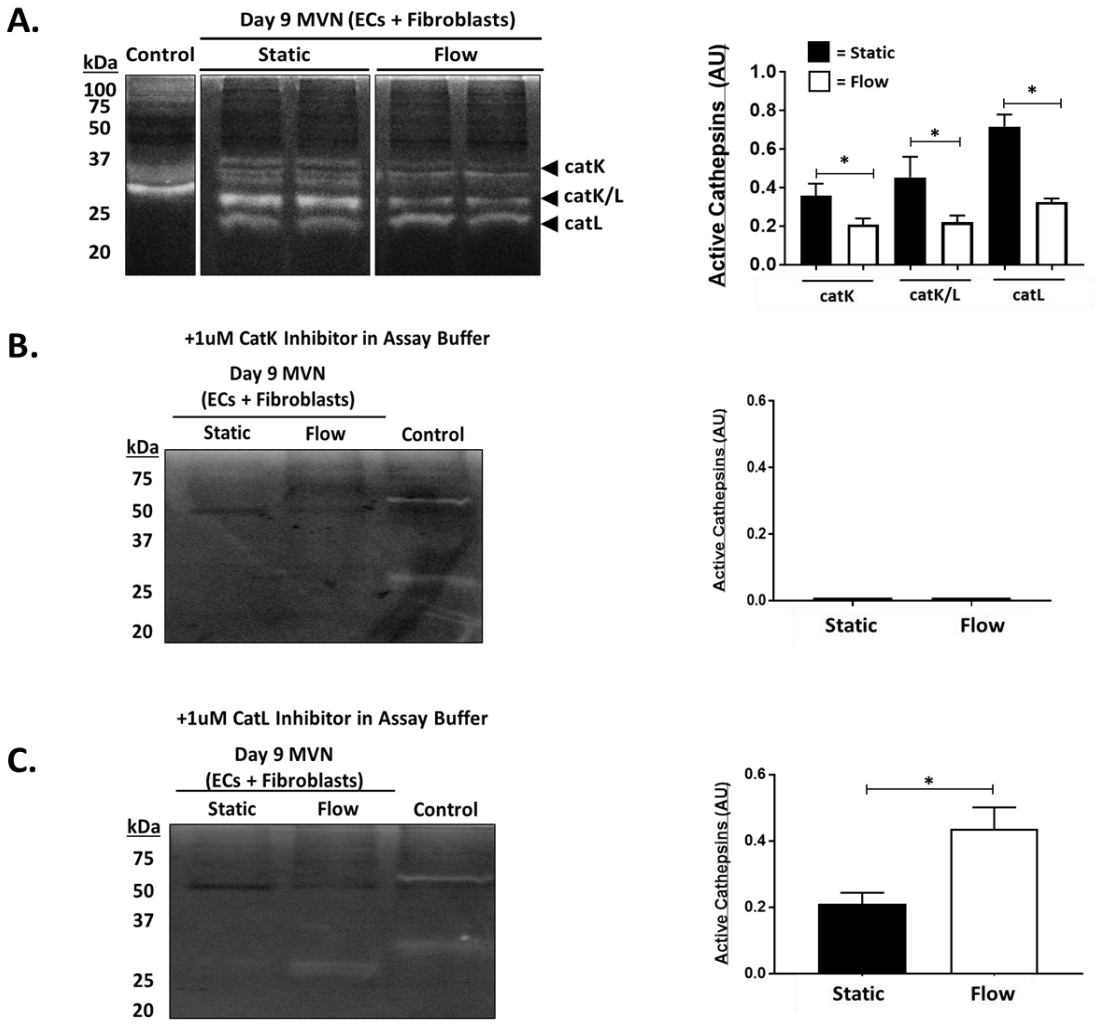

Figure 4-1: Shear flow through microvessels decreases amount of active cathepsins in microvascular networks.

ECs and fibroblasts were cultured at a 5:1 ratio in a 3mg/mL fibrin gel within a macro-scale (~100uL gel volume) PDMS platform. Microvessels (MVNs) formed via a vasculogenesis-like process over ~7days. Some devices were exposed to continuous flow, inducing a low shear stress (~2Pa) for 48hrs. Flow was maintained by a pressure drop generated across the gel using an in-house pum p. Gels containing MVNs were extracted from devices (static and shear) on day 9. Zymography was run to assess the amount of active cathepsins, as indicated by white clear bands, and western blots were done to assess for presence of cathepsins and cystatin C. **(A)** Multiple active cathepsin bands were observed in the zymogram. There was a significantly less amount of active cathepsins in MVNs formed under shear stress compared to static devices ($p < 0.05$). To identify the cathepsins in the zymogram, **(B)** cathepsin L inhibitor and **(C)** cathepsin K inhibitor was added to the assay buffer. In the zymogram with Cathepsin L inhibitor added, an active cathepsin band was identified at 25kDa, while the other bands were blocked. However, more active cathepsin is observed in MVNs made under shear compared to static suggesting that different cathepsins are affected by flow. Cathepsin K inhibitor in the assay buffer blocked all active cathepsins.

4.3.2 Flow increases cathepsin L protein levels and expression of cystatin C

Zymography is used to detect active cathepsins, but immunoblots are needed to detect the total amount of protein. It is possible that the procathepsin and mature forms of cathepsin could be present but not in an active conformation that would yield a zymographically detected signal. To assess how flow affects cathepsin expression and maturation in microvascular networks, total protein was determined by immunoblot. Flow caused a 44% ±0.14% increase in pro catL level and 53% ±2.57% increase in levels of mature catL compared to static controls (Fig 4-2A); this result was counter to the amounts of active cathepsin detected in zymography (Figure 1A). To potentially resolve this discrepancy, immunoblots were done for cystatin C, the tight binding, endogenous inhibitor of cysteine cathepsins, expressed by most nucleated cells, and previously shown to be upregulated by endothelial cells under flow conditions [178]. Consistent with these results, microvascular networks subjected to flow demonstrated a 64% ±13% increase in cystatin C compared to those cultured under static conditions ($p = 0.0219$, Fig 4-2B). This suggests that flow induced upregulated cystatin C can bind to cathepsins and reduce the amount of free, active cathepsins, aligning with the results of Figure 4-1A.

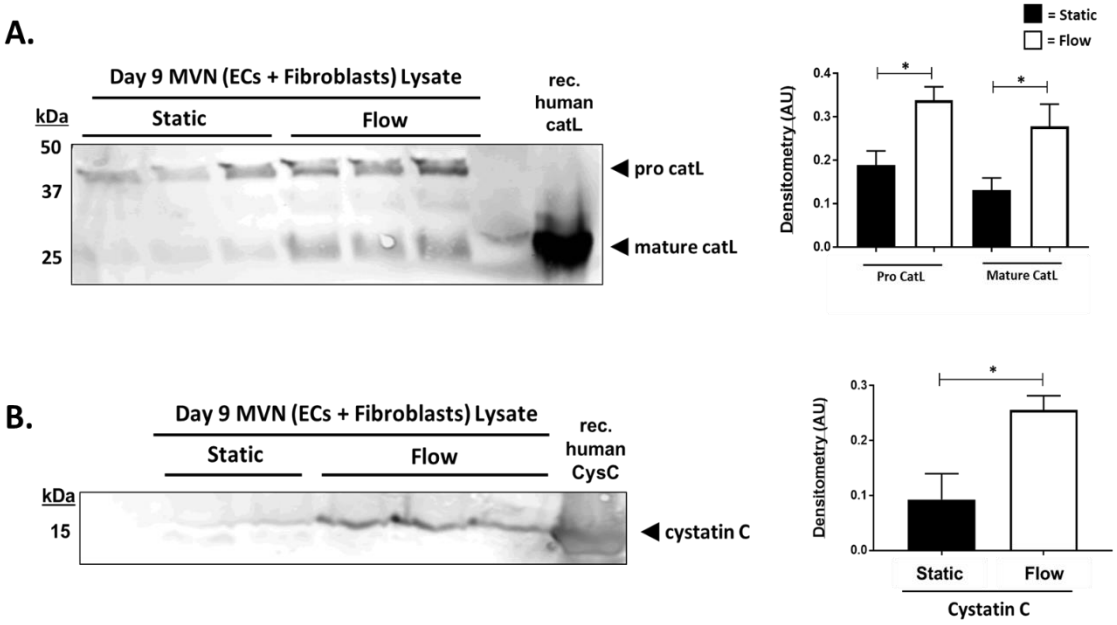

Figure 4-2: Shear flow through microvessels increased the total amount of cathepsin L and cystatin C in microvascular networks.
(A) There was significantly more pro ($p = 0.0049$) and mature cathepsin L ($p = 0.0332$) in networks formed under flow compared to static conditions. No cathepsin K or cathepsin S were detected by western blot. To understand the increase in cathepsin L present, networks were assessed for cystatin C, endogenous cysteine cathepsin inhibitor. **(B)** Cystatin C was significantly increased in MVNs formed under shear stress ($p = 0.0219$). This increase in cystatin C corroborates the decrease in active cathepsins.

4.3.3 Cathepsins K, L, and S were present in stromal and luminal regions of microvascular networks

Next immunofluorescence was used to determine locations of cat K, L, and S in the microvascular networks, and if they were associated with one cell type more than the other. Microvascular networks were fixed and labeled with antibodies against fibroblast specific protein (FSP-1) and collagen I (Fig 4-3A) to demonstrate the cell associations and organization in the formed microvascular network. Images were reconstructed using NIH ImageJ (Fig 4-3B). The left side is a maximum z-projection with orthogonal projections demonstrating open vascular lumen, and the right side is the corresponding x-y plane for the projects, demonstrating remodeling by fibroblasts (green) of ECM by reflectance imaging. This was done to see where cathepsins localized with the lumen (open circles) or stroma (surrounding area), and visualize matrix remodeling (grey) (Fig 4-3B). Cat K, L, and S were localized in the apical (arrow with 'A') and basal (arrow with 'B') side of the ECs, and in the stroma (arrow with 'S'), where fibroblasts are located (Fig 4-3C). CatK and catS were seen more on the apical side of the lumen and stroma. CatL was on both the apical and basal side of the lumen, as well as the stroma. A co-localization plugin (NIH ImageJ) was used to identify the overlapping intensity between ECs or fibroblasts and cat K, L, or S. Briefly, mean co-localization R values (acquired from z projections of n=3 images each) showed that cathepsins localize predominantly with fibroblasts, in comparison to ECs (Fig 4-3C). This result corresponds with the fact that fibroblasts are mostly responsible for degradation and remodeling of the ECM, which is seen by confocal reflectance imaging of the unlabeled gel (white/grey) in regions adjacent to vessels (Fig 4-3B).

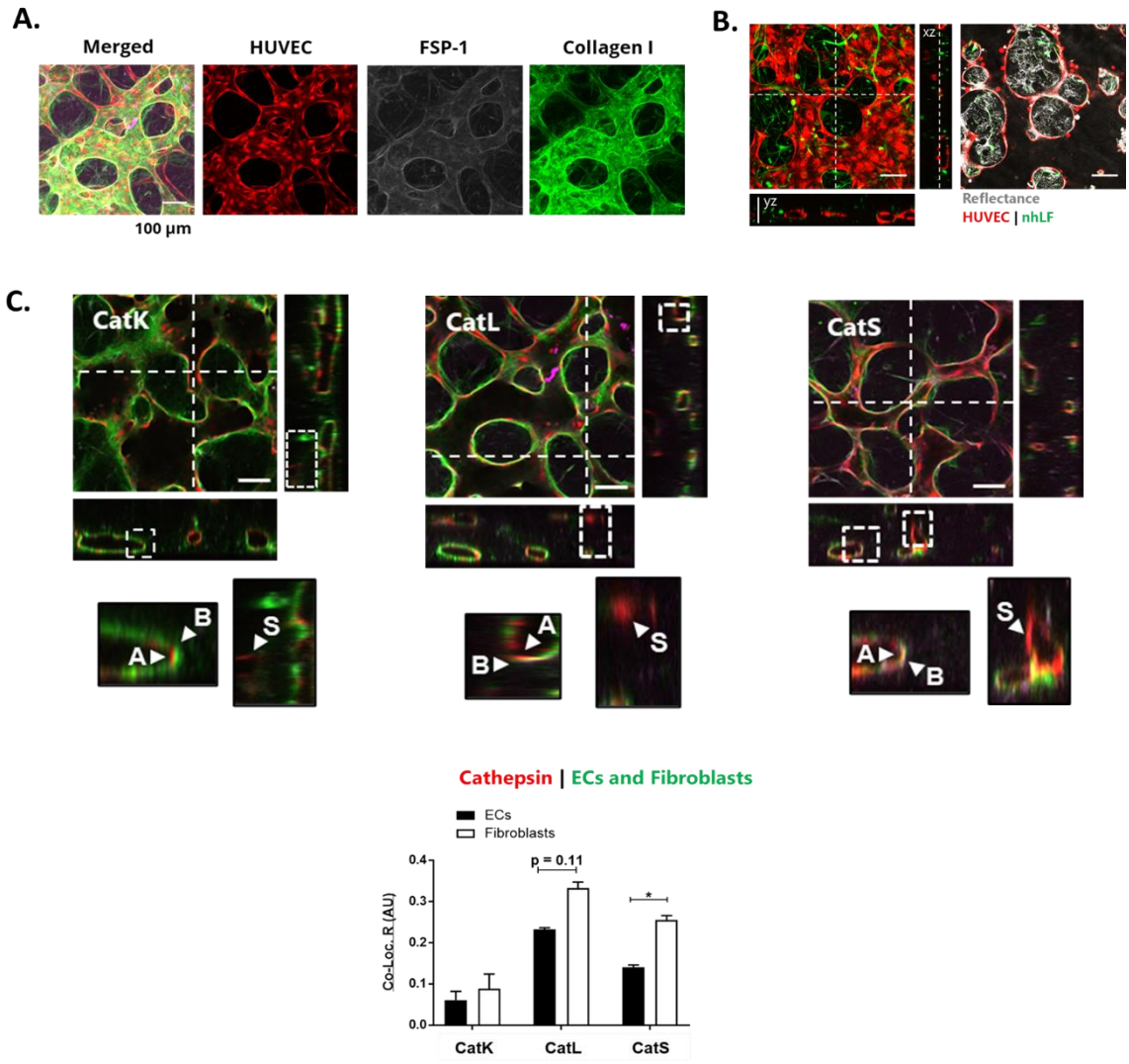

Figure 4-3: Cathepsins localize in lumen and stroma of microvascular networks.
(A) Confocal images of RFP-labelled HUVECs, FSP-1 labelled fibroblasts, and identified collagen I, and cathepsins K, L, or S. Mean co-localization of cathepsins with HUVEC (via RFP) or fibroblasts (via FSP-1). **(B)** Live confocal image showing open vascular lumen in orthogonal projections. Images were reconstructed into 3D z-stacks using to see where cathepsins localized with the lumen (open circles) or stroma (surrounding area), and visualize matrix remodeling (areas of white are reflectance of matrix). **(C)** CatK, L, and S were localized in the apical (arrow with 'A') and basal (arrow with 'B') side of the ECs, and in the stroma (arrow with 'S'), where fibroblasts are located. A co-localization plugin (NIH ImageJ) was used to identify the overlapping intensity between ECs or fibroblasts and cat K, L, or S. Cathepsins co-localize significantly more with fibroblasts compared to ECs. Significance is indicated by *$p < 0.05$ using a t-test.

4.3.4 Small molecule inhibition of cathepsins is more effective than cystatin C

To test if exogenously applied inhibitors could further reduce the active cathepsin signal in microvascular networks, biochemical inhibition strategies were done using cysteine cathepsin inhibitors: cystatin C, endogenous 13 kDa protein that is a broad cathepsin inhibitor, and E-64, a 357Da broad-spectrum inhibitor of cysteine cathepsin family members [179]. On day 8, after microvascular networks were formed, either cystatin C (1μM) or E-64 (10μM) was added to microvascular network cultures that were cultured under static conditions for 48 hours to allow time for the inhibitors to equilibrate and bind to any cathepsins already present, plus any newly synthesized. Homogenates and supernatants were collected to quantify the amounts of cell-associated and secreted active cathepsins, respectively, in the presence of these inhibitors (Fig 4-4A). Adding E-64 significantly reduced the top active band (75kDa, $p=0.0004$), active catK (37kDa, 68% ±9.7% decrease, $p=0.0271$), catK/L (27kDa, 61% ±8.7% decrease, $p=0.0155$), and catL (23kDa, 73% ±10.4% decrease, $p=0.0012$) compared to microvascular networks with no inhibitor added. However, cystatin C did not significantly reduce the amount of active cathepsins detected.

In the supernatant, there was nearly a complete reduction in the amount of active cathepsins between 0 hours (top, Fig 4-4B) and 48 hours (bottom, Fig 4-4B) in microvascular networks that had E-64 added ($p = 0.0448$). After 48 hours of inhibiting the cathepsins, there was significantly less active catK/L in E-64 samples compared to cystatin C group ($p=0.0326$) and no inhibitor group ($p = 0.0442$). Zymography also detected active cathepsin bands at 75kDa, which was reduced by 32% ±3.9% after addition of E-64, but there was little difference in amount of active cathepsins between the microvascular

networks that had no inhibitor and those with exogenous cystatin C. Previously the 75 kDa bands have been identified as active cathepsins bound to released ECM and/or tissue fragments [144], and it's also possible that cathepsin could be bound to fibrin [180].

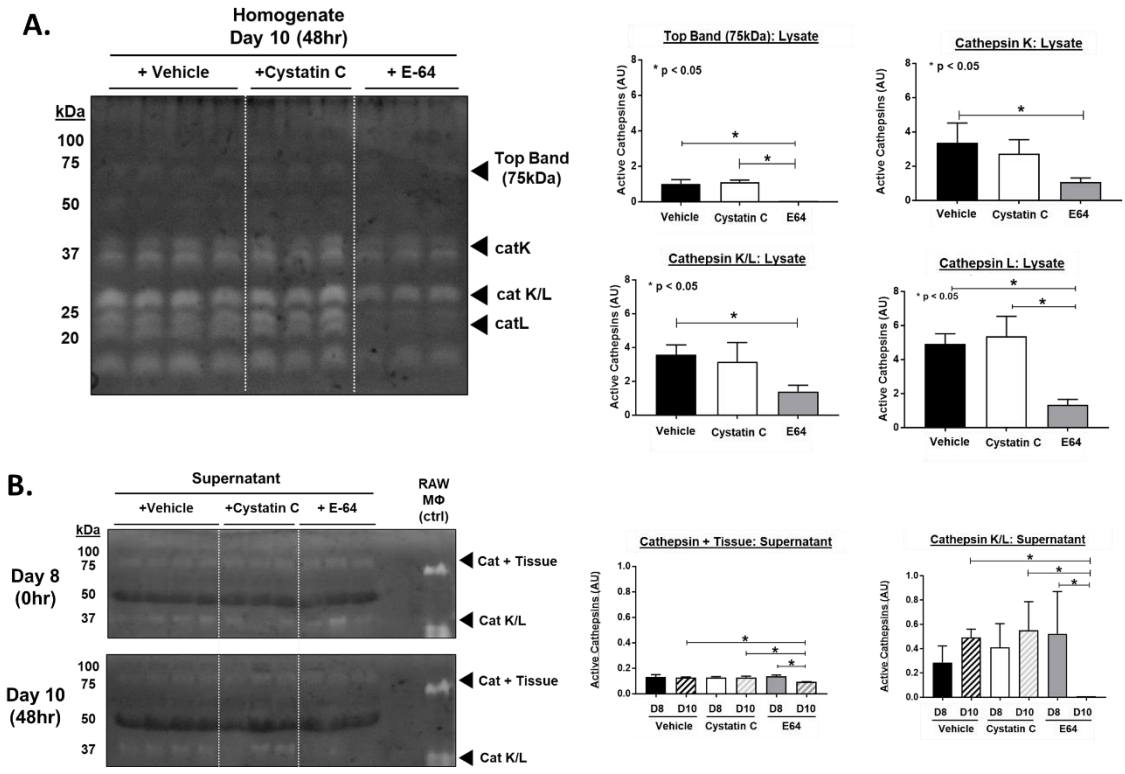

Figure 4-4: Cathepsin inhibitor, E-64, reduced active cathepsins in microvessels.
Cathepsin inhibitors, cystatin C or E-64, was added to microvascular networks for 48 hours. Lysate, containing microcascular networks, and supernatant, containing media was collected from devices. Cathepsin zymography was used to measure the amount of active cathepsins in the microvessel**. (A)** Microvascular networks with E-64, compared to vehicle, had significantly reduced active top band (75kDa, p=0.0004), catK (37kDa, p=0.0271), catK/L (25kDa, p=0.0155), and catL (20kDa, p=0.0012) in lysate, which contains microvessels. There were no significant differences between cystatin C and vehicle networks, however there was a decrease in active cathepsins in microvascular networks made with cystatin C versus E-64, except for top band (p=0.0003) and catL (p= 0.0009). **(B)** In the supernatant, there was a significant decrease in the amount of active cathepsins between day 8 and 10 in the microvessels treated with E-64 (p = 0.0448). At day 10 there was significantly less active K/L in samples with E-64 compared to vehicle (p = 0.0442) and cystatin C (p=0.0326). Zymography also detected cathepsin bound to tissue (75kDa).

Immunoblots were run on these samples to quantify the total protein amounts of catK, L, and S after adding cathepsin inhibitor to microvascular networks to assess cell feedback loops or responses to cathepsin inhibition. CatK and catS were not detected by immunoblot. From lysates, E-64 significantly reduced the amount of mature catL in microvascular networks compared to cystatin C ($p=0.0021$), or no inhibitor control ($p=0.0026$) groups. There was no significant difference in pro catL between the three groups (Fig 4-5A). There was significantly more cystatin C in homogenates of microvascular networks that had cystatin C added compared to no inhibitor (86% ±12.3%, $p<0.0001$) and E-64 (71% ±10.1%, $p<0.0001$) networks (Fig 4-5A). The supernatant of microvascular networks with cystatin C had 3-fold higher cystatin C, compared to no inhibitor ($p<0.0001$) and E-64 ($p<0.0001$) (Fig 4-5B), clearly indicating the exogenously added cystatin C was still circulating and not all taken up by the cells. Despite there being significantly more cystatin C present in microvessels with cystatin C added, there was no decrease in the amount of active cathepsins seen in Fig 4-4A.

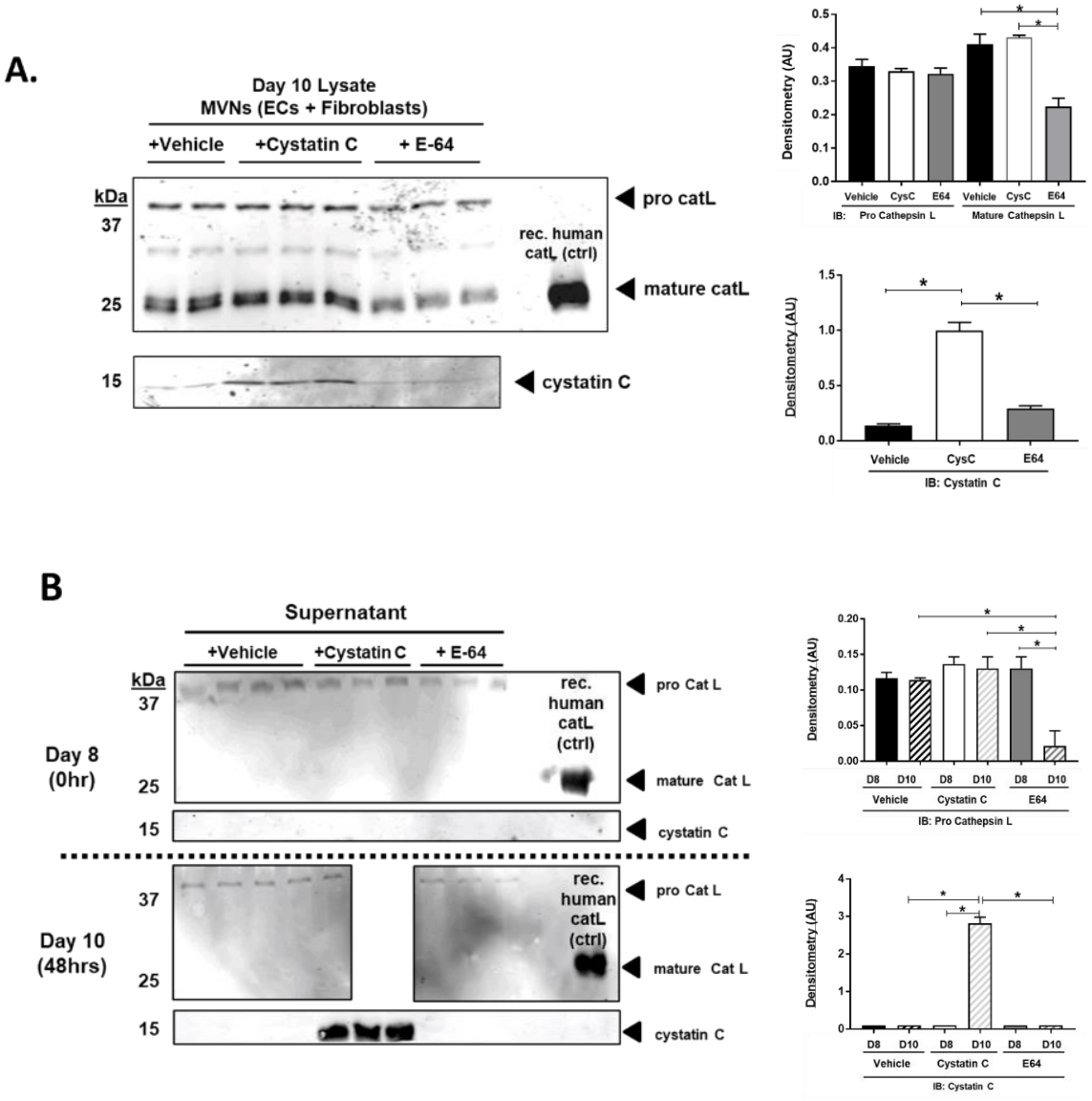

Figure 4-5: Cathepsin inhibitor, E64, reduced cathepsin L in microvessels.
(A) In lysate, there was no significant difference in pro catL between the three groups, however, microvascular networks with E-64 had significantly less mature catL compared to vehicle ($p=0.0026$) and cystatin C ($p=0.0021$) microvascular networks. At day 10, there was significantly more cystatin C in microvascular networks made with cystatin C compared to vehicle ($p<0.0001$) and E-64 ($p<0.0001$) networks. **(B)** In supernatant, no mature cathepsin L was detected, however, there was a decrease in pro catL from day 8 to day 10 in E-64 ($p=0.0161$) networks. There was significantly less pro catL in D10 E-64 networks compared to vehicle ($p=0.0053$) and cystatin C ($p=0.0002$). Between day 8 and day 10, the supernatant of cystatin C treated microvascular networks had a significant increase in cystatin C ($p < 0.0001$). There was significantly less cystatin C in vehicle ($p<0.0001$) and E-64 ($p<0.0001$) microvascular networks compared to cystatin C.

4.3.5 Fibroblasts are a dominant source of cathepsins, sustained by fibrin culture

Engineered microvessels are significantly influenced by cell types, their ratio and densities in culture, and by the containing gel, which influences vessel geometry and permeability [15, 170]. ECs (HUVECs) and fibroblasts have both been shown to produce cathepsins [28, 181]. Cathepsins localized mostly with fibroblasts in Fig 4-3C, suggesting more cathepsins were produced by them. *In vitro*, ECs and fibroblasts might increase cathepsin production in the presence of fibrin, which could be facilitate by cell integrin binding to fibrin which could stimulates cathepsin gene expression [182] or promote localization of the cathepsins to the cell surface [183]. To understand their individual contributions of HUVECs and fibroblasts, each cell was separately cultured on fibrin gels or tissue culture polystyrene (TCPS) for 24 hours. CatK and catS were not detectable by immunoblot, however, catL was identified. Fibroblasts produced more pre catL and mature catL compared to ECs (Fig 4-6), which corroborates our findings in Fig 4-3 that cathepsins mostly co-localize with fibroblasts. Interestingly, the homogenate, which contains the cell lysate, fibrin gel, and any proteins associated/bound to them, contained less pre catL and mature catL in fibroblasts cultured on fibrin gels compared to no fibrin (Fig 4-6A). The opposite was found in the supernatant; fibroblasts cultured on fibrin gel had more pro catL and mature catL (Fig 4-6B).

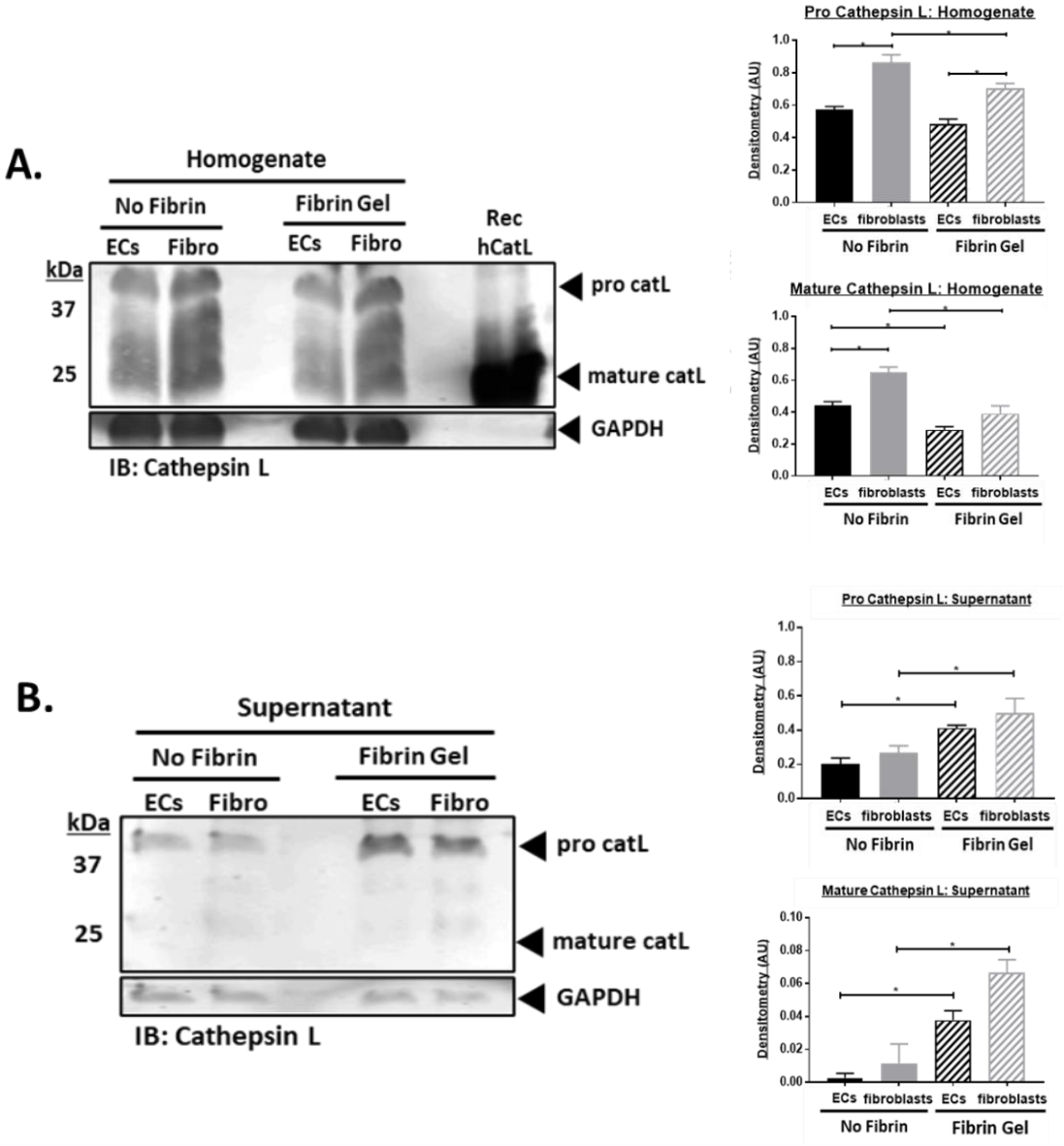

Figure 4-6: Fibroblasts contribute more cathepsins to microvascular networks. HUVECs (ECs) and normal human lung fibroblasts (fibroblasts) were separately cultured on fibrin or no gel (TCP); homogenate, containing cells and fibrin gel, and media, containing secreted proteins, were collected and prepared in reducing loading dye. Western blots were used to identify presence of cathepsins. **(A)** In homogenate, fibroblasts had significantly more pro cathepsin L compared to ECs in no fibrin ($p < 0.0001$) and on fibrin gels ($p = 0.011$). More pro cathepsin L was present in fibroblasts cultured on no fibrin compared to fibroblasts cultured on fibrin gels ($p=0.0141$). Fibroblasts had significantly more mature cathepsin L in no fibrin conditions ($p=0.0011$) compared to ECs. More mature cathepsin L was present in fibroblasts ($p<0.001$) and ECs ($p=0.0155$) on no fibrin gels conditions compared to culturing on fibrin gels. **(B)** In media, ECs and fibroblasts had significantly more pro ($p=0.0370$, $p =0.0204$) and mature ($p=0.0203$, $p=0.0003$) cathepsin L when cultured on fibroblasts.

The extracellular matrix (ECM) of microvascular networks are initially composed mostly of fibrin, but then the fibroblasts and ECs deposit other matrix proteins (i.e.: collagen, Figure 4-3A). Studies have shown that ECM substrates, including collagen and elastin, can sustain and extend cathepsin activity after they adsorb or bind upon release from cells [50, 147]. Based on our previous studies, fibrin is a substrate that can sustain active cathepsins for 24 hours [180]. It was hypothesized that ECM in the microvascular networks could serve as a bioactive reservoir to sustain cathepsin activity over longer durations. Therefore, ECs and fibroblasts were separately cultured on fibrin gels for 24 hours (in 2D well plates) to test the hypothesis that fibrin can amplify cathepsin activity. Homogenate, containing both cells and fibrin gel, and supernatants media were collected, and prepared for zymography. Multiplex cathepsin zymography was used to identify active cathepsins in the supernatant and homogenate of the individually cultured cell types. ECs and fibroblasts cultured on fibrin had significantly more active cathepsins compared to those cultured on TCPS (Fig 4-7A & 4-7B). This was observed in both homogenate and media. Based on the ratio of cells cultured on fibrin gels to cells cultured on no fibrin (Figure 4-7C), fibroblasts have more active cathepsins compared to ECs.

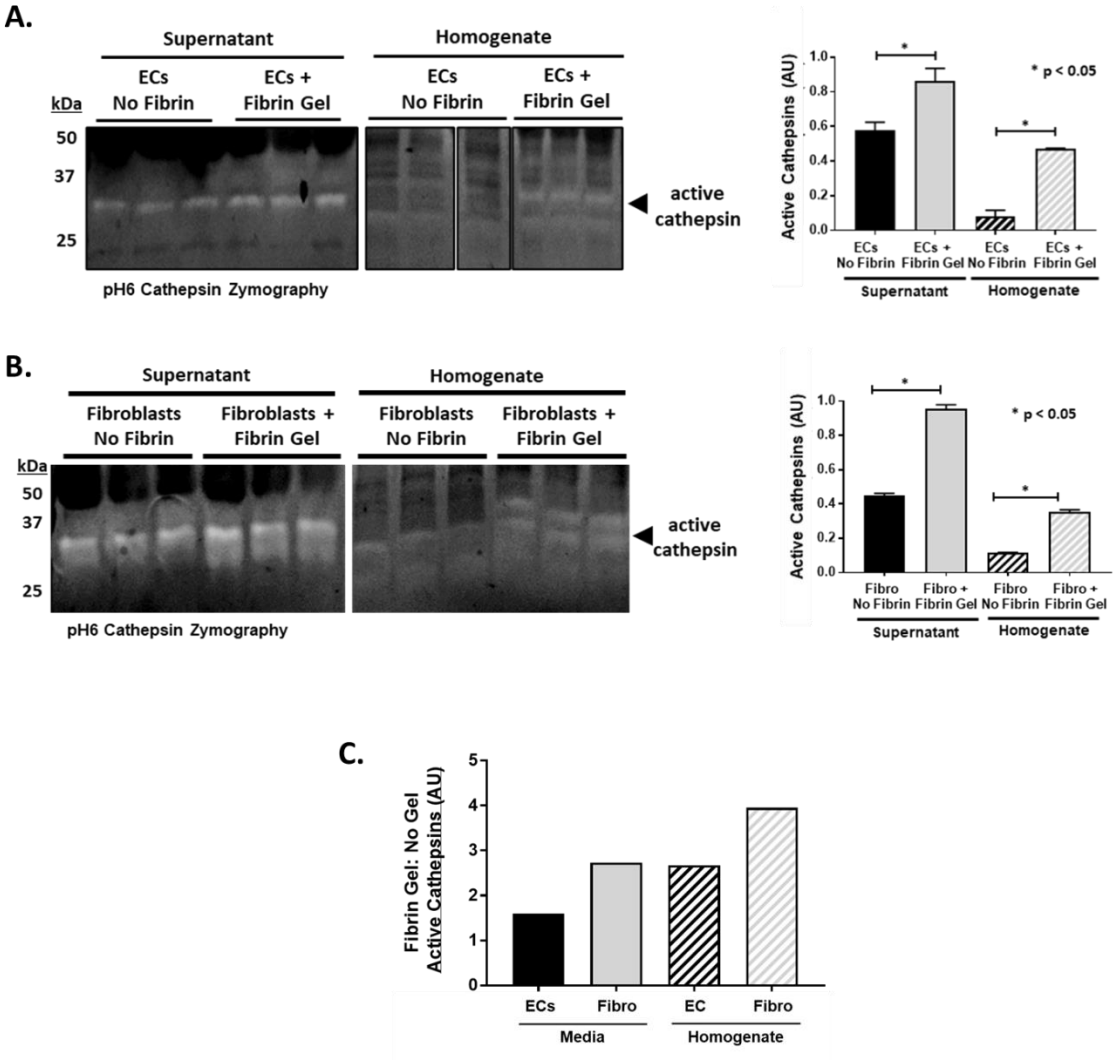

Figure 4-7: Separately culturing endothelial cells and fibroblasts on fibrin gels to identify if fibrin sustains active cathepsins in vitro.
(A) ECs and **(B)** fibroblasts were separately cultured on fibrin gels or tissue culture plates (TCP); homogenate, containing cells and fibrin gel, and media, containing secreted proteins, were collected and prepared in non-reducing loading dye. Multiplex cathepsin zymography was run to assess the amount of active cathepsins. When ECs or fibroblasts are cultured on fibrin gel, there are increased amounts of active cathepsins in media ($p=0.0023$, $p<0.0001$) and homogenate ($p<0.0001$, $p<0.0001$). In the presence of fibrin there is more active cathepsins; suggesting that fibrin helps maintains active cathepsins and enhances their activity *in vitro*. Sustaining cathepsin activity for longer periods of time makes them available to degrade matrix substrates in more complex systems, like the microvascular networks **(C)** Based on ratio quantification from zymograms in A and B, fibroblasts produce more active cathepsins compared to ECs.

4.4 Discussion and Conclusions

Here, investigated cathepsin activity during microvascular network formation was investigated. Microvessels formed in a fibrin matrix had a significant amount of active catK and catL, predominantly produced by fibroblasts. CatK, L, and S localized with ECs, associated with lumen on the apical and basal sides, as well as the fibroblasts which are associated with the stroma. When cell types were separately analyzed, fibroblasts produced more cathepsins compared to ECs, corroborating increased co-localization in stroma of microvascular networks. Defining the role of cathepsin-mediated fibrin degradation in microvascular networks suggests that cathepsin inhibitory strategies might be necessitated to improve matrix stability over long durations in culture.

Proteolytic activity is needed for matrix remodeling during vasculogenesis/angiogenesis. When developing microvasculature, researchers typically consider MMPs [14, 90, 103, 167, 184] as proteases to facilitate these processes. However, another class of proteases, cysteine cathepsins need to be considered as they have been implicated in vascular remodeling [24-28]. MMPs and cathepsins can be secreted by the same cell types involved in vascular formation including ECs [48, 169, 185] and fibroblasts [48, 186]. Both proteases interact in a proteolytic network, a coordinated cascade of events and interactions between different types of proteases connects proteases from different families into the same network [187]. While MMPs regulate the fate of ECM remodeling during microvascular network development, our data demonstrated that cysteine cathepsins do, as well. Understanding proteolytic interactions could help us uncover the roles cathepsins play in vasculogenesis and identify approaches to improve engineered microvessel design. Understanding cathepsin-mediated ECM remodeling in microvessels,

could help identify if cathepsins are a target for implanting novel microvascular network design strategies.

Microfluidic devices are advantageous for developing vasculature *in vitro*, allowing for control over the microenvironment with the ability to easily manipulate growth factors and mechanical cues; various strategies have been used to create perfusable microvasculature-on a-chip [188]. It is important for engineers to consider that as the environment is perturbed, cells will sense, adapt, and respond; and thus, other properties will emerge. Flow decreased the amount of active cathepsins and increased total amount of cystatin C in microvascular networks. This provides an example of biomechanical cues changing the properties of the proteases. Cathepsins are shear-sensitive proteases. In ECs, laminar shear stress inhibits catL activity [152]. Types and rate of flow can affect cathepsin activity. It was demonstrated that ECs under proatherogenic oscillatory 5 dynes/cm^2 with directional changes in flow) shear stress had higher amounts of cathepsin K compared to atheroprotective, unidirectional shear stress (15 dynes/cm^2) [6]. This was done *in vitro* using confluent layers of ECs with a Teflon cone to induce shear stress, and our work is done in microfluidic devices with microvascular networks that had unidirectional laminar flow (~2 dynes/cm^2). Flow also affects cystatin C; in ECs, oscillatory flow increases cathepsin expression and reduces cystatin C [178]. Flow in microvessels that increased total cathepsin present, however, cystatin C was also increased which aligned with a reduction in active cathepsins. Future directions could include assessing different types of flow or flow rates, and based on previous observations [6, 28, 152], changing these parameters could alter the amount of active cathepsins in microvascular networks.

Two different types of broad cathepsin inhibitors, cystatin C or E-64, were exogenously added to study how biochemical cues affect proteases. Cystatin C is the endogenous enzyme that reversibly binds to active sites of cathepsins to prevent substrate degradation [57]. E-64 is a small molecule inhibitor that irreversibly binds to the cathepsin active site [179]. Adding E-64 to microvascular networks significantly reduced active cathepsins, but cystatin C did not. Cystatin C was mostly in the supernatant (Fig 4-5B), suggesting that it did not cross the EC barrier. Also, there was no flow applied to these devices, so cystatin C was likely not swept away in a current. Although cystatin C is an extracellular cathepsin inhibitor; this poses a question about how permeable the EC barriers are in these microvascular networks. It is possible that transport varies due to the size differences of the inhibitors; E-64 is smaller compared to cystatin C- 0.347kDa compared to 13kDa, respectively. I hypothesize that because of the smaller size of E-64, it can pass through ECs via transcytosis, where E-64 is taken up by ECs with bulk volume during pinocytosis and exocytosis to the stroma. Conversely, cystatin C is not transported efficiently; it is likely too large for pinocytosis and could be transported to ECs via general uptake or receptor mediated endocytosis. This would limit the amount of cystatin C transported and likely why more cystatin C was found in the media the networks were cultured in (Fig 4-5B). This is worth further exploring as our lab has previously reported interesting cathepsin inhibitor behavior with E-64 [189], where breast cancer cells treated with E-64 had reduced active catL, but an increase in active catS. Also, our lab has previously observed upregulated active cathepsins in biological machines (bio-bots), another type of multi-cellular engineered living system that contains fibrin as a key matrix component. Active catL was identified in bio-bots, even when bio-bots were treated using

a serine protease inhibitor aminocaproic acid (ACA) [144], however, treatment of bio-bolts with E-64 could extend their lifetime [190]. This demonstrates that cathepsin inhibition can improve longevity of an engineered construct; an approach that can be used in the future to improve design of microvascular networks. It also should be noted that cathepsin inhibitors were added at the end of microvascular network development and there were still differences in remodeling. Perhaps earlier addition of inhibitors could lead to improved longevity of microvessels.

Microvascular networks are formed in a dynamic and complex environment, with mechanical and signaling cues from the ECM, including the production and secretion of cysteine cathepsins. Engineered microvessels form with complex interactions including cues from the surrounding ECM matrix [19, 93, 94, 166]. It is known that cell-cell interactions with matrix, cytokines, and shear stress can regulate protease expression and activity [6, 152]. A key observation is that fibroblasts produce more cathepsins compared to ECs, and their activity was increased with fibrin, suggesting that the fibrin in microvascular networks matrix could serve as a bioactive reservoir for cathepsins to maintain activity for longer periods of time. Stromal cells, such as fibroblasts, are essential for aiding the sprouting microvessels to improve development of patent microvascular networks [13, 15, 176, 191]. Eliminating fibroblasts to reduce active cathepsins may not be conducive for maintaining long term vessel viability, however, as demonstrated, the addition of flow and inhibitors can decrease active cathepsins to prevent proteolysis. This could make fibroblasts or other stromal cells an ideal cell type to target for creating an inducible cell line to control endogenous cathepsin production, which can be done by creating a “switch” to turn on cathepsins to facilitate remodeling with the ability to turn off

cathepsin production when activity is too much and causes destruction. Also, one could consider using nanoparticle microcarriers for timed delivery of E-64, seeing that this was the optimal inhibitor for cathepsins in MVNs.

Researchers have used various techniques for creating microvasculature that have varying cell sources, matrices, culturing conditions, and application of interstitial flow. One group used a 3D microfluidic device to apply interstitial flow using HUVECs. Their approach differs in that they utilized a collagen gel and increasing amounts of VEGF. They identified there is a balance between flow magnitude and VEGF concentration [103]. Similarly, manipulating flow and adding different cathepsin inhibitors can affect network formation and proteolytic activity. Studies were also done experimenting with the timing of adding broad spectrum MMP inhibitors during microvascular network formation. When added at the beginning of the angiogenic growth phase microvessel formation was blocked, however, addition after the angiogenic growth phase (day 7), helped prevent vessel regression [192]. A key difference with their approach is that a rat aortic angiogenesis model was used. Considering this, our data suggests that vascular regression is due to unbalanced proteolysis where there is continuous proteolytic activity that degrades the ECM and reduces the lifespan of the causing microvessels to fail. Another group used HUVECs or ECs derived from induced pluripotent stem cells (iPSC-ECs) and nhLFs coated on dextran microcarrier beads embedded in a fibrin matrix to examine capillary morphogenesis. Adding broad spectrum MMP inhibitor or serine inhibitor, to inhibit plasmin, the endogenous enzyme that degrades fibrin, did not eliminate sprouting of microvessels, however with both inhibitors combined, sprouting was completely blocked. The researchers suggested that these observations could be due to proteolytic interactions

between plasmin and MMP, or a third type protease involved in vasculogenesis [184]. Our experiments are similar in terms of cell source and matrix, although ours utilized a microfluidic device while the authors use a microcarrier system. Taking both studies together, this furthers the argument that cysteine cathepsins are part of the proteolytic network in regulating morphogenesis in these engineered systems.

Our work demonstrates how biomechanics, particularly fluid shear stress, control cathepsin presence and activity during microvessel formation, suggesting an approach to reduce extended proteolysis by cathepsins, which could subsequently extend microvascular network lifespan. Addition of catK or catL inhibitors during the overnight zymography assay wash demonstrated that not only are active catK and catL are present in the system, but also suggests that both cathepsins are regulated differently by flow; something to consider when identifying which cathepsin to target with inhibitors during microvessel development. This data confirms microvascular networks contain cathepsins in ECM/stroma, which could act as a bioactive reservoir to sustain proteases and making them available to degrade matrix substrate, fibrin, causing microvessel regression (i.e.: decrease in vessel diameter and vessel density). Our work demonstrates the need to consider novel cathepsin inhibition strategies to control proteolysis and meet design criteria for fibrin-based engineered tissues.

Together, these results provide insight into the role cathepsins play in ECM remodeling of microvascular networks. Cathepsins were localized, and their activity and expression were quantified in engineered microvasculature. Flow through microvascular networks not only upregulates the amount of cathepsins, but also the amount of their endogenous inhibitor, resulting in a net effect of a decreased amount of active proteases in

the system. Also, small molecular inhibitors can get through ECM barrier to block activity. Further, our work identifies an increase in active cathepsins from ECs and fibroblasts cultured on fibrin gels demonstrating, *in vitro*, a mechanism between cathepsins and fibrin, a follow up to our previous work using recombinant proteases and fibrin gels [180]. Cathepsins could bind to fibrin and it serves as a reservoir sustaining functional time of active cathepsins over longer periods of time *in vitro* and in multi-cellular engineered living systems. The long-term goal is to prevent microvessel regression, and characterizing cathepsins biomechanical and biochemical properties in microvascular networks provides insight for promising future studies.

CHAPTER 5 INCREASED FIBRINOPEPTIDE A IN A HUMANIZED SICKLE CELL MOUSE MODEL IS CAUSED BY CATHEPSIN-MEDIATED FIBRINOGENOLYSIS

5.1 Introduction

Sickle cell anemia (SCA) , red blood cell disorder, facilitates a state of chronic coagulation activation, also known as hypercoagulation, where most parts of the coagulation cascade are altered [31, 116]. Evidence of this includes increased activation of platelets and tissue factor, decreased levels of anticoagulant proteins, and abnormal fibrinolysis [33]. The cause of SCA-mediated hypercoagulation is not well understood, although there are hypotheses that it may be caused by vaso-occlusive crisis (VOC) or a secondary effect due to SCA [33, 106, 116]. Studies using anticoagulants and antiplatelet therapeutics have not helped prevent or treat hypercoagulation and vaso-occlusive conditions in SCD patients [31, 129-133, 193] and researchers need to better understand how abnormalities in coagulation activation contributes chronic coagulation activation in SCD pathophysiology and complications. Understanding underlying mechanisms of hypercoagulation in SCD could lead to the development of effective anticoagulant therapies specific to the SCD population.

In the coagulation signaling cascade, thrombin - a serine protease - cleaves fibrinopeptide A and B from fibrinogen, promoting fibrin polymerization and coagulation (Fig 2-1). It has been reported that people with SCA have increased plasma concentrations of fibrinopeptide A (FpA) [33, 39, 193] , a marker of coagulation activation, and studies suggest it is not only due to thrombin activity [39], suggesting the potential involvement of another protease.

Our lab has shown that there is an increase in cathepsin K (catK) in sickle cell anemia [40, 41]. People with SCA have increased numbers of circulating peripheral blood monocytes (PBMCs) and under the disease state, PBMCs induce catK activity in endothelial cells [40]. Also, cathepsin K-dependent arterial remodeling occurs via elastin and collagen degradation in the SCD Townes mice model [41]. Based on the increased amount of cathepsin K in SCA and increased plasma concentration of FpA in people with SCA, the connection between cat K and FpA was questioned. From computational docking algorithms, cathepsins (cat), K, L and S have putative binding and cleavage sites on fibrinogen in the central E domain, where FpA is located [42]. Furthermore, there is evidence that catK (and catS) have a unique preference to cleave proline and glycine at the P2 and P3 position [194]. Taken together, it is hypothesized that increased plasma levels of FpA in SCD is due to cysteine cathepsin activity, specifically catK, contributing to SCD hypercoagulation, and inhibiting cathepsin activity can reduce elevated FpA levels.

5.2 Materials and Methods

5.2.1 Mouse Model Experiments

Townes sickle transgenic mouse model (B6;129-Hba tm1(HBA) Tow Hbbtm2 (HBG1,HBB*) Tow/Hbbtm3 (HBG1, HBB) Tow/J) were obtained from The Jackson Laboratory. Animals were housed following a 12-hour light-dark cycle and fed Lab Diet 5001 ad lib. Pups were weaned, separated by sex at 21 days old, and their hemoglobin was genotyped using Native SDS-PAGE. All experiments were approved by Georgia Institute of Technology Institutional Animal Care and Use Committee (IACUC) with supervision of veterinarians in the Physiology Research Laboratory.

Mice were selected for daily injection with small molecule cathepsin inhibitor, E-64 (9mg/kg, Sigma-Aldrich), or vehicle (DMSO in saline) based on genotype. Mice were injected daily beginning at 1 month of age for 2 months, until age 3 month. Blood was collected from mice into heparinized tubes, at 1, 2, and 3 months of age. Samples were centrifuged at 2,000xg for 20 minutes to separate plasma.

5.2.2 Cathepsin K Deficient Mouse with Sickle Cell Anemia

Cathepsin K deficient mice B6.129X1-Ctsk^{tm1Psa} were crossed with the Townes sickle mice described above. AA $K^{-/-}$, AS $K^{-/-}$, and SS $K^{-/-}$ genotypes for mice were confirmed using PCR for presence of human hemoglobin and absence of mouse hemoglobin; cathepsin K knocked out ($K^{-/-}$), and genotypes (AA, AS, or SS) (Fig 5-1)

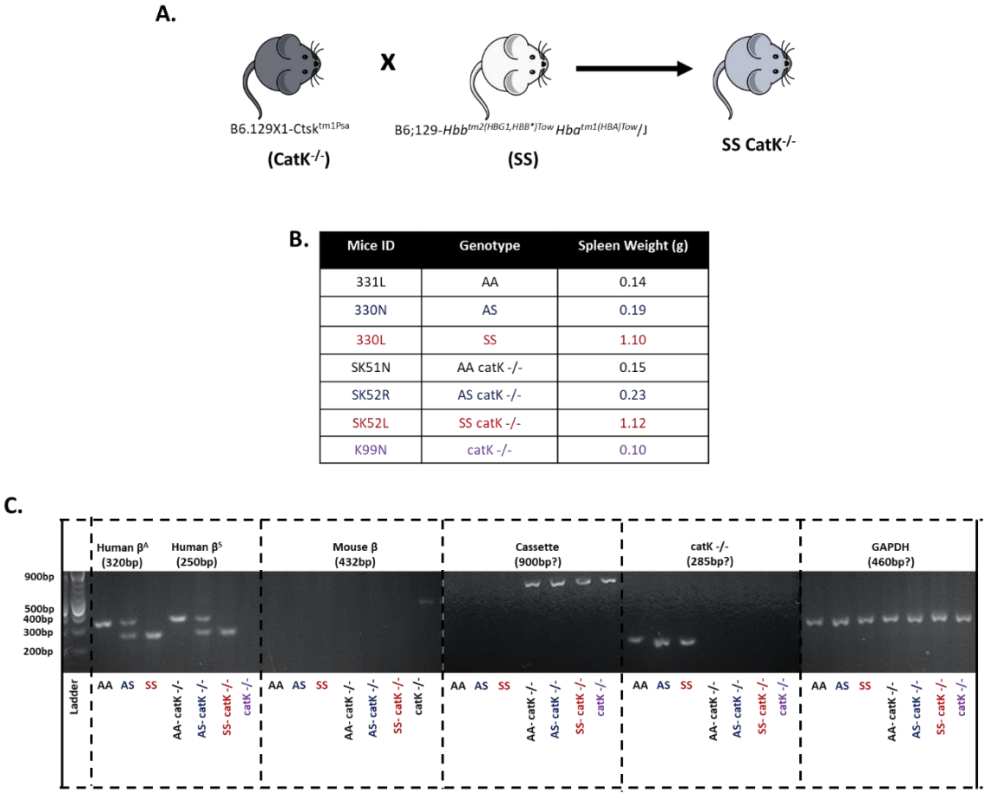

Mice ID	Genotype	Spleen Weight (g)
331L	AA	0.14
330N	AS	0.19
330L	SS	1.10
SK51N	AA catK -/-	0.15
SK52R	AS catK -/-	0.23
SK52L	SS catK -/-	1.12
K99N	catK -/-	0.10

Figure 5-1: PCR confirming generation of a cathepsin K deficient mouse with sickle cell anemia

5.2.3 Multiplex Gelatin Cathepsin Zymography

Multiplex cathepsin zymography was used to assess active cathepsins, as previously described [148]. Samples were prepared using a non-reducing loading buffer (5×-0.05% bromophenol blue, 10% sodium dodecyl sulfate (SDS), 1.5M Tris, 50% glycerol. A 12.5% SDS-PAGE gel was used and embedded with 5 mg/ml gelatin substrate. Gels were run at 200 V at 4 °C. Proteases were renatured in 65mM Tris buffer pH 7.4 with 20% glycerol for 3 washes, 10 min each, then incubated in pH 6 (phosphate buffer, 1mM EDTA with 2mM DTT, freshly added) activity assay buffer overnight. Next, gels were stained with Coomassie Blue (4.5% Coomassie blue; Sigma-Aldrich, 10% acetic acid, and 10% isopropanol) then destained (10% acetic acid and 10% isopropanol). For inhibitor assays, 1µM of cathepsin K II (1-(N-benzyloxycarbonyl-leucyl)-5-(N-Boc-phenylalanyl-leucyl) carbohydrazide [Z-L-NHNHCONHNH-LF-Boc], Calbiochem/Millipore Sigma) was added to the pH6 assay buffer prior to overnight incubation. Zymograms were imaged using Odyssey CLx, LI-COR. Densitometry was performed with ImageJ (NIH) to quantify active cathepsins.

5.2.4 Multiplex Fibrinogen Cathepsin Zymography

Recombinant cathepsin K, L, or S (10ng; Enzo), or plasmin (0.5µg; Enzyme Research Laboratories) was prepped in a non-reducing loading buffer. A 12.5% SDS-PAGE gel was embedded with 5mg/mL fibrinogen (FIB 3 Plasminogen, von Willebrand Factor and Fibronectin Depleted; Enzyme Research Laboratories) substrate. Cathepsins were renatured in the buffer and incubated in pH4 or pH6 assay buffer overnight, as described above. Plasmin was renatured in 2.5% Triton-X 100 for 2 washes, and placed in

a pH modified MMP assay buffer (0.05% Triton X 100, pH 8.58). Gels were stained, destained, and imaged as previously described.

5.2.5 Turbidity Analysis

Fibrinogen (2.5 mg/mL; FIB 3 Plasminogen, von Willebrand Factor and Fibronectin Depleted; Enzyme Research Laboratories) and cathepsins K, L, or S (1ng/µL; Enzo) or human alpha thrombin (1 NIH U/mL; Enzyme Research Laboratories) were combined in 50mM Tris-HCl/100mM NaCl. The course of gelation was assessed over the course of 2 hours using a plate reader (BioTek) with absorbance readings set to 350nm and 420nm, based on previous protocols [195].

5.2.6 SDS-PAGE

Fibrinogen and cathepsins K, L, or S, or thrombin were combined as described above. Cleavage was stopped at 0, 5, 10, 15, 30, 60, and 120 minutes. The supernatant, which contains soluble fibrinogen and cleaved fibrinogen fragments, was collected and saved. Samples were prepared with reduced loading dye (5X - 0.05% bromophenol blue, 10% SDS, 1.5 M Tris, 50% glycerol, 25% beta-mercaptoethanol) and run on 10% SDS-PAGE gels. Gels were stained with Coomassie stain (10% acetic acid, 25% isopropanol, 4.5% Coomassie blue), followed by destaining (10% isopropanol and 10% acetic acid) and imaged with an ImageQuant LAS 4000 (GE Healthcare), and densitometry performed with ImageJ (NIH) to quantify fibrin(ogen) polypeptide chains.

5.2.7 Immunoblot

For immunoblotting, samples were prepared with reduced loading dye (5X - 0.05% bromophenol blue, 10% SDS, 1.5M Tris, 50% glycerol, 25% beta-mercaptoethanol) and

run on 12.5% SDS-PAGE gel. Proteins were transferred onto a nitrocellulose membrane, and then immunoblotted using rabbit polyclonal anti-fibrinopeptide A (Abcam, for mouse plasma studies) or mouse anti-fibrinopeptide A (HyTest, for human recombinant protein studies). Immunoblots were imaged using Odyssey CLx, LI-COR. Densitometry was performed with ImageJ (NIH) to quantify cleaved fibrinopeptide A.

5.2.8 Statistical Analysis

Statistical significance was determined using a two-way ANOVA between no enzyme control or normalized 1 month AS plasma, unless indicated otherwise using GraphPad. All experiments were replicated at least three times and a p value of <0.05 was considered statistically significant.

5.3 Results

5.3.1 Fibrinopeptide A was increased in plasma of 3-month old male mice with sickle cell anemia

To examine whether the Townes Mouse model had increased fibrinopeptide A (FpA), as observed in human plasma [33, 39, 193], ELISA was used to quantify FpA in non-sickle (AA), sickle trait (AS), and sickle cell anemia (SS) mice. There was no significant increase in FpA in 1-month old SS mice compared to AA and AS mice (Fig 5-2A). At 3 months of age, the majority of mice had low FpA levels, although there was an outlier. When the data was divided by sex, it was determined that mice with low levels of FpA were all female mice. This suggested that male mice had more FpA compared to female mice, however a greater number of mice are needed to provide significance. Immunoblots were performed to quantify FpA in AA, AS, and SS mice. At 1 month, there were similar FpA levels across all samples, corroborating data from the ELISA (Fig 5-2B).

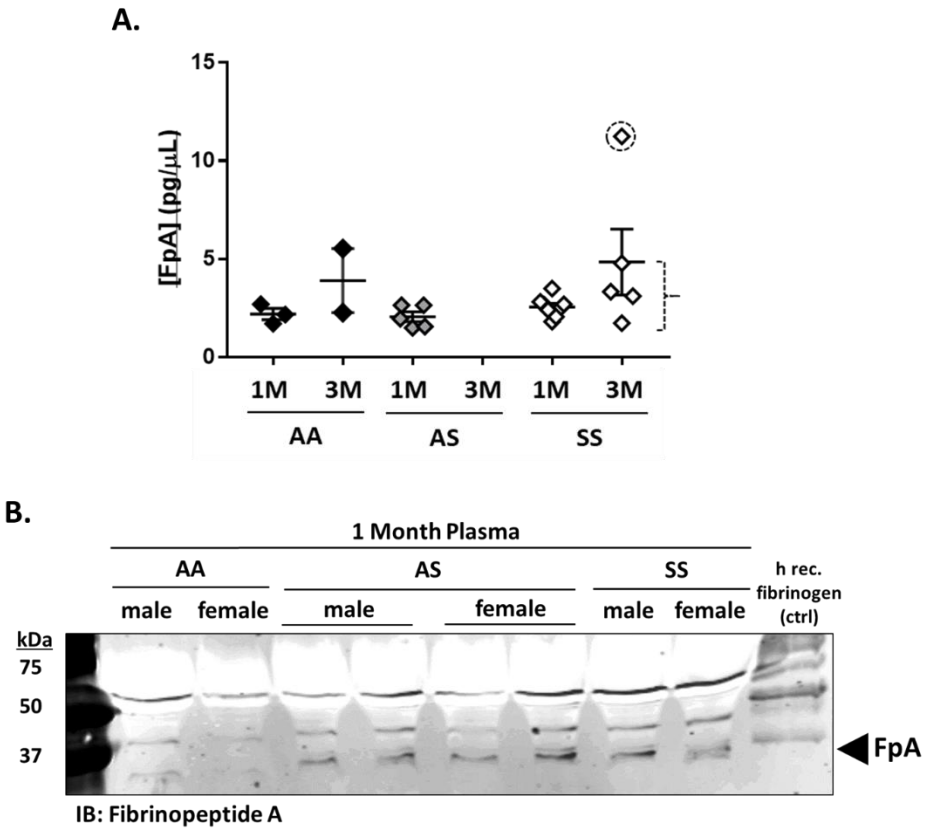

Figure 5-2: Quantifying fibrinopeptide A in Townes Sickle Mouse model.
Immunoblots and ELISA were used to identify and quantify fibrinopeptide A (FpA) in plasma of AA, AS, and SS mice. **(A)** There was no difference in FpA quantified in 1-month AA, AS, and SS mice. Interestingly, with plasma from 3-month-old mice, there are clustering of data, where the higher FpA concentration were identified as male mice (circled) and lower concentration as female mice (brackets). (n=3-6, one-way ANOVA). **(B)** Immunoblots were done on 1 month AA, AS, and SS mice. Little difference was observed between FpA in AS and SS mice. This preliminary data suggests that male mice have more FpA than female mice.

5.3.2 Mice with sickle cell anemia have increased active cathepsins in plasma compared to non-sickle and sickle cell trait mice.

Next, multiplex cathepsin zymography was used to test the hypothesis that active cathepsins in Townes mice plasma and hypothesized that mice with sickle cell anemia have more active cathepsins circulating in their plasma compared to non-sickle and sickle trait mice, and the amount of active cathepsins would increase as the mice aged. Plasma was isolated from blood collected from AA, AS, and SS mice at ages 1 and 3 months. Multiplex gelatin cathepsin zymography was used to measure amounts of active cathepsins in plasma. There was a single ~50kDa band, and 1 month and 3-month SS mice had significantly more active cathepsins compared to 1 month and 3-month AA and AS mice (Fig 5-3A). Age was a factor in SS-mediated active cathepsins, where there were elevated levels of cathepsins in plasma of 3-month SS mice compared to 1-month SS mice, and there was no significant difference in cathepsins in AA and AS mice between 1 and 3 months.

5.3.3 Male mice with sickle cell anemia have more active cathepsins compared to female mice.

As noted earlier, there was variability in the amount of active cathepsins within the mice with sickle cell anemia. To better parse this observation, AA, AS, and SS plasma samples were divided based on sex. At 1 month of age, male SS mice have more active cathepsins compared to female SS mice (Fig 5-3B). This difference in the amount of active cathepsins between sexes was sustained as the mice age. SS male mice at 3 months of age have more active cathepsins compared to 1-month old male mice (Fig 5-3C), however there was no significant difference in the amount of active cathepsins of female mice between 1 and 3 months of age in all three genotypes.

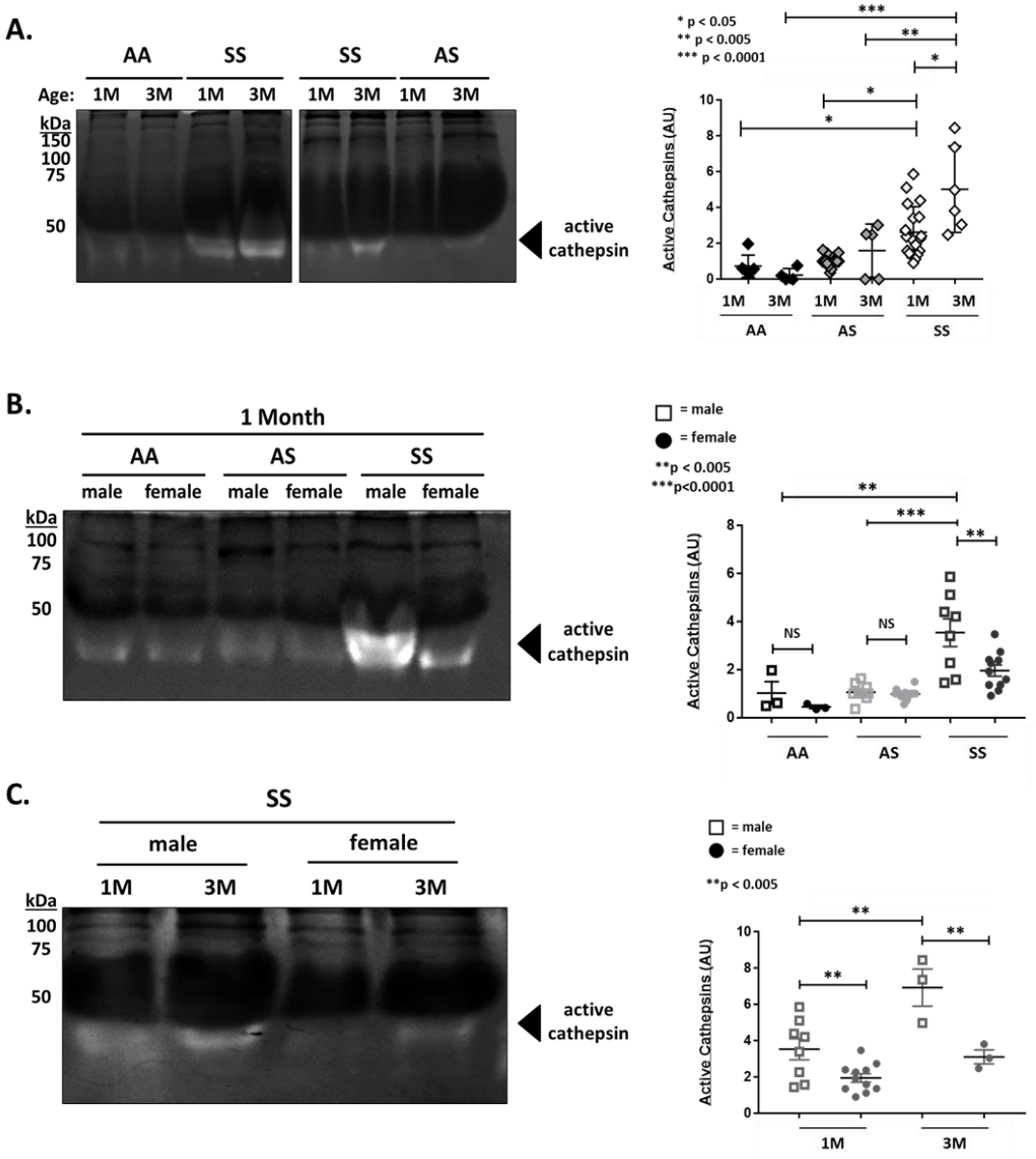

Figure 5-3: Mice with sickle cell anemia have increased active cathepsins compared to non-sickle and sickle cell trait mice, and SS male mice have more active cathepsins compared to SS female mice

Blood from AA, AS, and SS mice were collected at 1 and 3 months of age, and plasma was isolated and zymography was used to assess for active cathepsins. **(A)** There was significantly more active cathepsins in SS mice compared to AA and AS at 1 month ($p=0.0143$, $p=0.008$) and 3 months of age ($p<0.0001$, $p=0.002$). In SS mice, there was an age-related increase ($p=0.008$) in active cathepsins between 1 and 3 months. This data suggests that elevated cathepsins in plasma is abnormal and likely have some pathophysiological contribution in sickle cell anemia. **(B)** There was variability in the amount of active cathepsins detected in SS genotype mice plasma; to investigate mice were separated based on sex. At 1-month, Male SS mice plasma have significantly ($p=0.0023$) increased active cathepsins compared to female SS mice plasma. **(C)** 3-month-old male SS mice have significantly more ($p=0.0029$) active cathepsins in plasma compared to 1 month.

5.3.4 Active cathepsins in AA, AS, and SS plasma were identified as cathepsin K and L.

Based on previous work from our lab showing that cathepsin K is elevated in SCA [40, 41, 196], it was hypothesized that the active cathepsin detected in zymograms was cathepsin K. Our lab has also developed a novel cathepsin K deficient mouse model with sickle cell anemia to study how cathepsins contribute to SCA pathophysiology. Blood was collected and plasma was isolated from the cathepsin K deficient mice with SCA (AA $K^{-/-}$, AS $K^{-/-}$, and SS $K^{-/-}$) as well as control cathepsin K deficient mouse ($K^{-/-}$) and Townes mice (AA, AS, and SS genotypes). Preliminary data showed that active cathepsins were still detected in SS $K^{-/-}$ mice, however the amount of active cathepsins was less than the SS mice, suggesting that another cathepsin may also be present in the plasma (n=1, Fig 5-4A). To determine the identity of the active cathepsin in plasma, zymography was done on AA, AS, and SS mouse plasma, then zymograms were incubated with an inhibitor of cathepsin K (1µM) or L (1µM) in the assay buffer overnight. The ~50kDa band was not detected in either zymogram (n=1, Fig 5-3B), suggesting that the elevated cathepsin in plasma was cathepsin K and L.

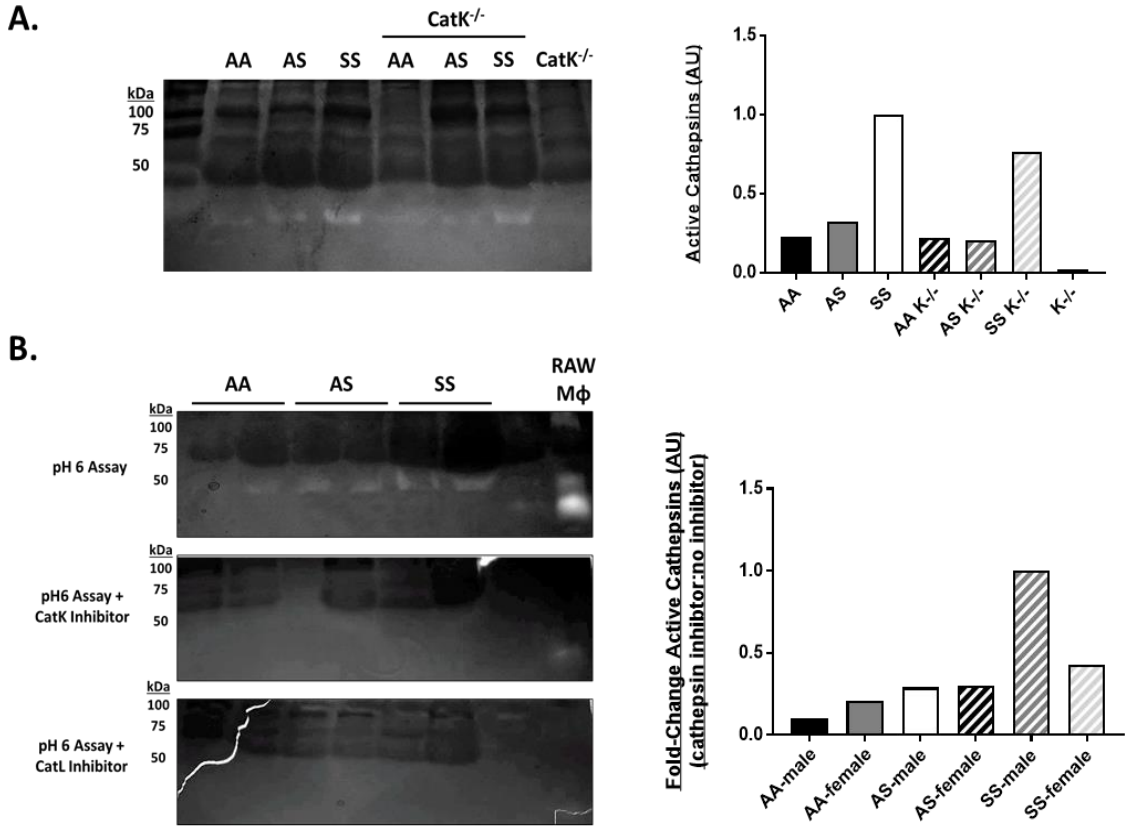

Figure 5-4: Active cathepsins in AA, AS, and SS plasma are identified as cathepsins K and L.

A novel cathepsin K deficient (K-/-) mouse with sickle cell disease was bred to identify the role of cathepsin K in disease progression, particularly in sickle cell mediated FpA generation. **(A)** Zymography was done on cathepsin K deficient AA, AS, or SS (AA $K^{-/-}$, AS $K^{-/-}$, and SS $K^{-/-}$) mouse plasma and AA, AS, or SS mouse plasma or cathepsin $K^{-/-}$ mouse plasma as controls. SS $K^{-/-}$ still had active cathepsins present, but it was less than SS mice (n=1). Cathepsin K deficient mice had no active cathepsins. Collectively, this suggests that active cathepsins were not only cathepsin K. **(B)** To determine which cathepsins were present, zymograms were incubated overnight with catK or catL inhibitor in the assay buffer (n=1). No active cathepsins were determined in either zymogram, suggesting the active cathepsin band was catK and catL.

5.3.5 Multiplex cathepsin fibrinogen zymography detected active cathepsin K, L, and S

Molecular docking and bioinformatics sequence specificity analysis can predict potential binding interactions and hydrolysis sites of cathepsin K on fibrinogen, including the central E domain where FpA is located [42]. Further, after co-incubation of purified fibrinogen and recombinant cathepsin K, cathepsin K can hydrolyze the Aα chain of fibrinogen where FpA is located [42]. To directly test the fibrinogenolytic activity of cathepsins, the multiplex cathepsin zymography assay [148] was modified to include a fibrinogen substrate and tested it with recombinant cathepsin K, L, or S. Using pH4 assay buffer, a pH that has selectivity for detecting catL [148], CatL was observed at its expected molecular size, 20kDa (n=3, Fig 5-4A-top). CatS was identified with the pH4 and pH6 assay buffer at ~25-37kDa. However, at pH6 catK was observed at 150kDa, nearly 3x higher than its expected molecular size (n=3, Fig 5-4A-middle). It is hypothesized that cathepsin K can act as a matricellular protease when cathepsin interacts with the surface of fibrinogen or, so the cathepsins K does not migrate during electrophoresis. Plasmin, a serine protease and canonical enzyme that degrades fibrin [66, 142], was used as a control. By manipulating the MMP assay buffer (Triton-X based) to pH 8.48, optimal conditions for plasma [66] there was a white band at ~86kDa, the expected molecular size of cathepsin (n=3, Fig 5-4A-bottom).

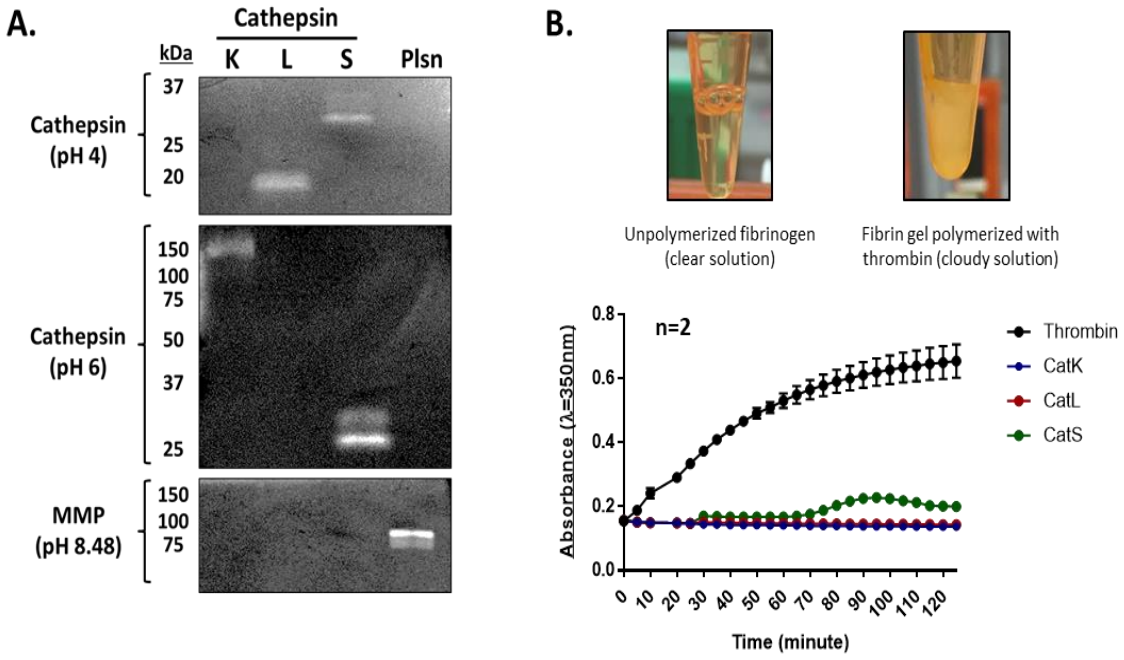

Figure 5-5: Cathepsins are fibrinogenolytic, but do not cause gelation of fibrin. Recombinant catK, L, and S were used to test fibrinogen zymography (n=3). **(A)** Active catL was observed at its expected molecular size 20kDa and catS at its expected molecular size 25kDa. CatK was found active at pH6, it is observed at 150kDa, nearly 3x higher than its expected molecular weight. Plasmin, endogenous enzyme that degrades fibrin is a serine protease with optimal activity at pH 8.5, and by manipulating the MMP assay buffer to pH 8.48, active plasmin was detected. **(B)** Turbidity analysis, a technique using absorbance to determine the turbidity or cloudiness of a solution, was performed to assess cathepsin-mediated fibrin formation using recombinant human fibrinogen and catK, L, or S. Turbidity measurements show that cathepsin K and L have no change in absorbance, indicating that both enzymes do not produce a cloudy solution, indicating catK and catL are cleaving FpA and causing fibrin gelation. However, the slight increase in absorbance with catS, suggests the initiation of fibrin gelation, which means catS could have the potential to form fibrin before degrading it.

5.3.6 Cathepsins K, L and S cleaves fibrinopeptide A on fibrinogen, however it does not cause gelation of fibrin.

With the finding that cathepsins K, L, and S are fibrinogenolytic, their role in cleaving fibrinogen to initiate fibrin polymerization was assessed. Papain causes gelation of fibrinogen [195] and since cysteine cathepsins are part of the papain-like family of peptidases, it was hypothesized that cathepsins K, L, or S could cleave fibrinogen and cause gelation. To do this, absorbance was measured to quantify the turbidity of cathepsin-mediated fibrin gels over a 2-hour time period; more absorbance would indicate fibrin gel formation. There was no change in absorbance when fibrinogen was combined with catK or catL, suggesting that neither enzyme can cleave fibrinogen to form a fibrin gel (Fig. 5-5B). With catS, there was a slight increase in turbidity starting around 70 minutes, suggesting the initiation of fibrin polymerization. However, turbidity peaked around 90-100 minutes then decreased, suggesting that a gel started to form then was likely degraded by catS.

Release of FpA from fibrinogen initiates the process to form fibrin, and after observing that cathepsins do not lead to the gelation of fibrin, the Aα, Bβ, and γ fibrinogen polypeptide chains were assessed using reducing SDS-PAGE. CatK degraded the Aα and Bβ polypeptide chains, and smaller molecular weight fragments were detected (Fig 5-6A-left). There was little to no degradation or cleavage of fibrinogen by catL (Fig 5-6A-middle). CatS degraded the Aα and part of the Bβ polypeptide chain, and smaller molecular weight fragments (Fig 5-6A- right). These experiments differ from Chapter 3, in that isolated fibrinogen was co-incubated with cathepsins K, L, or S to see if it cleaved FpA. Previous work cathepsins were co-incubated with fibrin where FpA was already cleaved

by thrombin. Overall, catK and catS produced distinct banding patterns compared to each other, suggesting they cleaved fibrinogen at different polypeptide sites.

Protein samples were separated by SDS-PAGE and transferred to a nitrocellulose membrane, then immunoblotted for fibrinopeptide A (FpA). CatL released little to no FpA (Fig 5-6B- middle), which corroborates SDS-PAGE (Fig 5-6A-middle) where a little amount of Aα chain was degraded. CatK and catS cleaved FpA. As time increased, more FpA was released by catK, but after 60 minutes there was a decrease in the amount of FpA (Fig 5-6B- left). By contrast, catS released the same amount of FpA over 2 hours (Fig 5-6B- right).

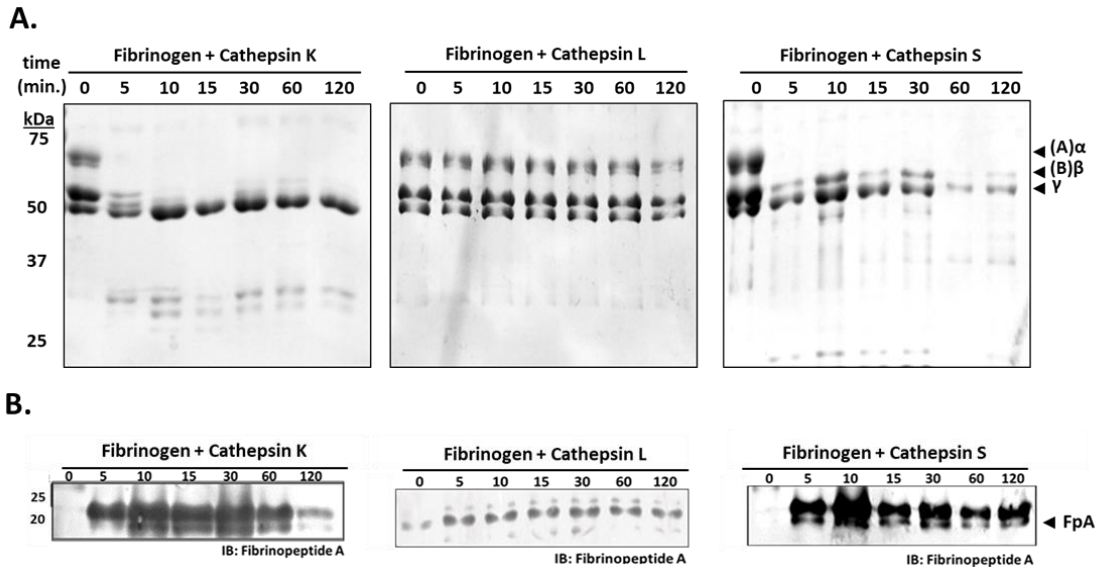

Figure 5-6: Cathepsins K, L, and S degrade the Aα and Bβ fibrinogen polypeptide chains, but only cathepsins K and S cleave fibrinopeptide A.
(A) Samples were resolved in reduced SDS-PAGE. Cathepsin K degraded the Aα and Bβ polypeptide chains, and smaller molecular weight fragments were detected. Cathepsin L degraded the Aα polypeptide chain. Cathepsin S degraded the Aα and some of the Bβ polypeptide chain, and smaller molecular weight fragments. Overall, cathepsins K and S produced distinct banding patterns compared to each other, suggesting each cleaves fibrinogen at different polypeptide sites. **(B)** As time increased catK released more FpA, as determined by immunoblots. However, after an hour there was a decrease in FpA suggesting it was degraded by catK. CatL released FpA consistently as time increased. CatS released FpA, but had a consistent concentration of released FpA. Overall, cathepsin K, L, and S cleaved fibrinopeptide A.

5.3.7 E-64 reduced the amount of active cathepsins and fibrinopeptide A in plasma of mice with sickle cell anemia.

To determine if cysteine cathepsins were responsible for increased FpA, mice were injected daily with E-64, a small molecule, broad cathepsin inhibitor, from 1 month to 3 months of age, to test the hypothesis that E-64 will inhibit catK, preventing its cleavage of fibrinogen to release FpA. Mice were treated with vehicle or E-64 from 1 to 3 months of age, and blood was collected and plasma was isolated 1 and 2 months post treatment. Multiplex cathepsin zymography was used to assess amounts of active cathepsins in plasma, and ELISA was used to quantify plasma concentrations of FpA. As early as 1 month of E-64 treatment, there was a reduction in the amount of active cathepsins in SS mice, and 2 months post treatment, there was a significant decrease in active cathepsins (Fig 5-7A). There was no significant decrease in plasma FpA levels of E-64 treated SS mice (Fig 5-7B). However, when separated by sex, there was less FpA was in the male SS mice compared to female SS mice.

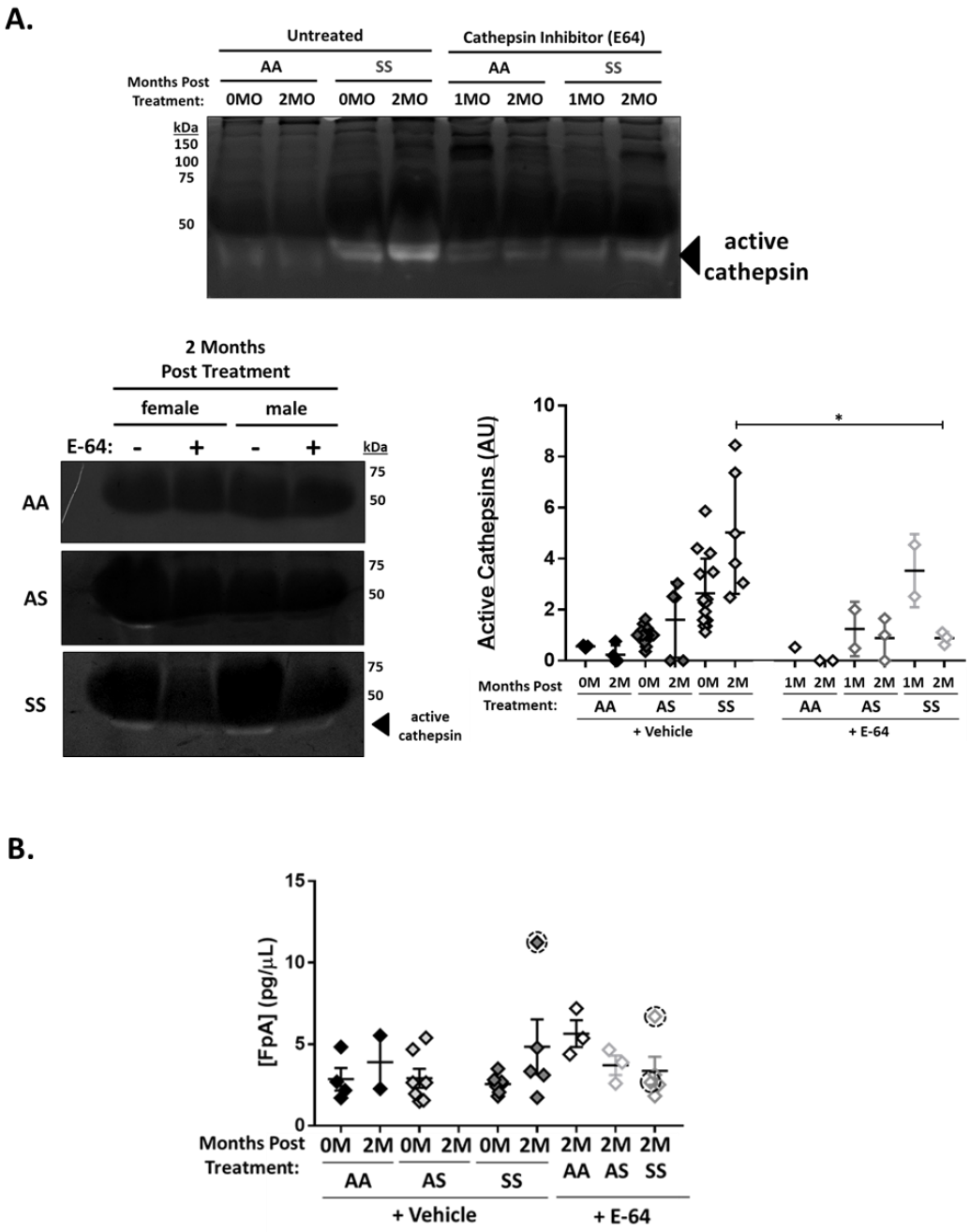

Figure 5-7: E-64 reduced the amount of active cathepsins and fibrinopeptide A in mice with sickle cell anemia.

AA, AS, and SS mice were injected daily with small molecule cathepsins inhibitor, E-64, from 1 month to 3 months of age. Blood was collected and plasma was isolated; multiplex cathepsin zymography and ELISA was used to assess the amount of active cathepsins and quantify fibrinopeptide A (FpA) in plasma. **(A)** There was significantly less (p=0.0003) active cathepsin in SS mice after 2 months of treatment. **(B)** Preliminary data suggested FpA in male (dashed-circle) SS mice is reduced with E-64.

5.3.8 People with sickle cell anemia have increased active cathepsins in their plasma

People with SCA have 3x higher the amount of FpA compared to people without SCA; and FpA levels can be 5x as higher when people with SCA experience VOC [33, 39, 193], however, to see if the cathepsin plasma levels the Townes mouse model was also observed in humans, zymography was done on AA and SS human plasma. There was more active cathepsin in SS human plasma compared to AA human plasma (Fig 5-8), which confirms the elevated cathepsin plasma results observed in the SS mice.

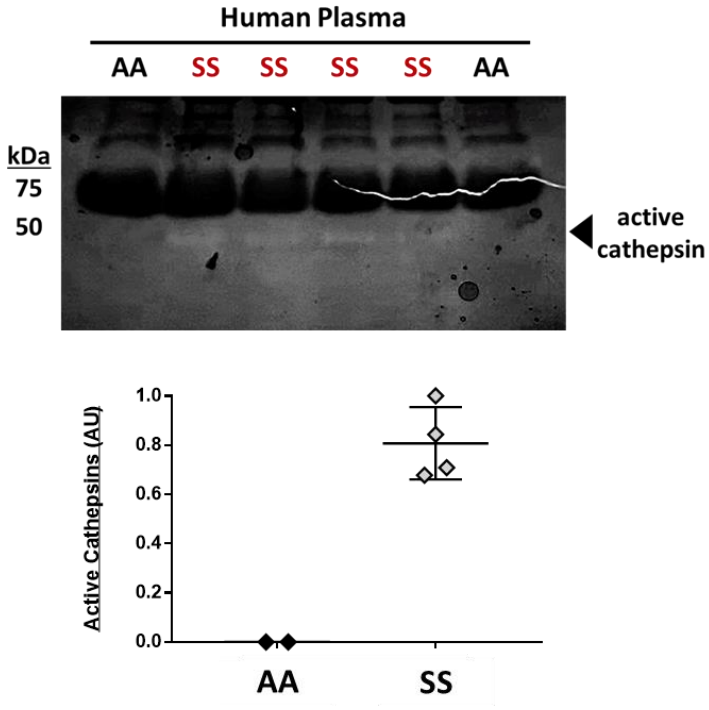

Figure 5-8: Plasma from people with sickle cell anemia had active cathepsins.
Blood was collected from AA or SS donors, and plasma was isolated. Zymography was done to assess the amount of active cathepsins. **(A)** SS human plasma has more active cathepsins compared to AA human plasma. This corroborates data from the Townes mouse model.

5.4 Discussion and Conclusions

People with sickle cell anemia (SCA) experience chronic coagulation activation, evidenced by an increase in circulating FpA in plasma. The aim was to investigate if cathepsins were casual agents of this. Results showed that SCA mediates increased levels of active cathepsins in plasma of humanized mouse model and humans. Circulating plasma FpA in Townes humanized sickle transgenic mouse model was quantified, and there was elevated FpA in plasma of SS male mice at 3 months of age. Treatment with E-64 reduced the amount of active cathepsins in the plasma, accompanied by a reduction in FpA concentrations. Cleaving FpA from fibrinogen is the first step in fibrin polymerization; even though catK and catS released FpA, it did not include fibrin polymerization. This demonstrates the potential role upregulated cathepsins can play in coagulation where they have access to cleave fibrinogen. Collectively, our data implicates cathepsin-mediated fibrinogenolysis in SCA.

Researchers are trying to identify how chronic coagulation activation in SCA contributes to pathophysiology and complications of the disease [33, 193]. It is unknown if chronic coagulation activation directly causes VOC or if it is an effect due to SCA [197]. Anticoagulant therapeutic approaches have not significantly helped prevent or treat VOC, further these types of treatments have hemorrhage and bleeding risks, which have limited their studies clinically [130]. People with SCA have increased plasma levels of FpA, which is considered a marker of increased thrombin generation and hypercoagulation. This increase in FpA is not solely due to thrombin cleaving fibrinogen, suggesting involvement of another protease [39]. Our lab has shown that inflammation of SCA causes increased amounts of catK, which has been implicated in SCA disease progression [40, 41]. Combined with our computational docking models of cathepsins on fibrinogen [42], it was

hypothesized that increased plasma levels of FpA in SCA is due to cysteine cathepsin activity, specifically catK, contributing to SCA hypercoagulation.

Amounts of active cathepsins and FpA in plasma of Townes humanized sickle cell mouse model were quantified using wildtype (AA), sickle trait (AS), and sickle cell anemia (SS) genotypes. Mice were injected daily with E-64, cathepsin inhibitor, for 2 months to determine if cysteine cathepsins were the cause of increased FpA. Blood from mice was collected from untreated and E-64 treated mice after 1 and 2 months of treatment, and plasma was isolated. Multiplex cathepsin zymography was used to assess amounts of active cathepsins in plasma, and an ELISA was used to quantify the concentrations of FpA in the plasma. To determine cathepsin-mediated fibrinogenolysis mechanisms, experiments were done with recombinant fibrinogen and recombinant cathepsins K, L, and S. Turbidity analysis was conducted to see if cathepsins could polymerize fibrin, along with SDS-PAGE and immunoblots to see if the fibrin polypeptide chains were cleaved and if FpA was released.

Mice with SCA had more active cathepsins in plasma than wild type and sickle. As SS mice age, there was an increase in active cathepsins from 1 to 3 months of age, demonstrating positive correlation between cathepsin upregulation and age. Collectively, this data suggests that elevated cathepsins in plasma is a manifestation of SCA pathophysiology, and the age-related increase in cathepsins could be biomarkers of disease progression. Interestingly, male SS mice have more active cathepsins compared to female SS mice, which may be associated with differences in how the disease presents itself in males compared to females, clinically. Specifically, it may be associated with females having less frequent and less severe sickle crisis episodes, as well as longer life spans [198].

Active cathepsins in SS human plasma were increased, corroborating data from our humanized mouse model. The age and sex of human samples are unknown; however, this information can be requested when more samples are acquired in the future. Preliminary data suggests that there was no difference in FpA plasma amount in mice at 1 month in AA, AS, and SS mice, but there was an increase in FpA plasma of male SS mice at 3 months. Not seeing a difference in FpA compared to zymography results suggests that it could take time for cathepsins, among other proteases, to start cleaving fibrinogen to release FpA. Inhibiting cathepsins with E-64 not only reduced the active cathepsins in plasma, but also reduced cleaved circulating FpA that was seen previously elevated in SS male mice plasma. Together, this demonstrated cathepsin-mediated fibrinogenolysis in SCA.

Mouse models have been used to understand the etiology of coagulation in SCA. Approaches include treating mice with coagulation cascade factor inhibitors to generating mice with genetic modifications in their coagulation factors. To test the relationship between sickle cell pathology and coagulation activation, plasminogen or fibrinogen deficient mice were crossed with sickle cell disease transgenic (SAD) mice; fibrin(ogen) helps maintain vascular integrity, tissue repair, and supports hemostasis under SCA conditions. However, the study focused on mortality; where fibrinogen deficient SAD mice had poorer survival outcomes likely due to bleeding related events [135]. Tissue factor, which triggers the extrinsic coagulation pathway, was targeted using TF-antibodies in the Berkley SCD mouse model. There was no effect on the anemic state, but coagulation activation and inflammation was reduced [136]. Mice treated with a factor II antisense "gapmer" to reduce prothrombin, died early, and genetically modified prothrombin

deficient mice saw improvements in SCA-associated end organ damage and reduced coagulation activation, as evidenced by a decrease in D-dimers [139]. While this is a significant finding in a mouse model, a clinical trial using sevuparin, which inhibits prothrombin, failed clinical trials in 2019 after failing to improve vaso-occlusive crisis resolution time with no clinical benefits or improvements in patients [133]. The results presented in this current study differ from the aforementioned models in two key ways: (1) amount of active cathepsin plasma levels were quantified and (2) genetic modifications targeted the cathepsins in a sickle cell mouse model. Aside from quantifying active cathepsins in plasma, circulating FpA was also quantified, an approach yet to be seen in mouse models. This approach targets a protease, cysteine cathepsins, which are not the central proteases for blood clotting.

The novel cathepsin K deficient mouse with sickle cell anemia provided more insight for identifying the cathepsin in the SS (Townes) mice. Previous results from our lab [40, 41] suggested that it was catK. However, there was still presence of active cathepsins in the SS catK$^{-/-}$ mice and little to none in the catK$^{-/-}$ control, meaning another cathepsin was present. Using inhibitors in the overnight assay buffers helped us identify that the active cathepsin was likely catK and catL. Normally, catL appears ~20kDa, however, as demonstrated in Chapter 3, catL can bind to fibrin and fibrin fragments. Seeing the active cathepsin band appearing at ~50kDa in SS plasma, suggests that catL could be bound to fibrin or some other plasma/coagulation protein, thus it would appear at a higher molecular weight. Perhaps this could be elucidated by injecting mice to target specific cathepsins, rather than a broad-spectrum inhibitor like E-64.

Co-incubating isolated fibrinogen and recombinant cat K, L, or S demonstrated that cathepsins do not cleave fibrinogen to polymerize fibrin. Thrombin and cat K, L, and S are all endopeptidases, meaning that their catalytic triad hydrolyzes peptides at internal peptide bonds. The main difference is the nucleophile group in the triad- serine for thrombin and cysteine for cathepsin [199, 200]. This supports the idea that cathepsins could cleave fibrinogen, and release FpA like thrombin can. In addition, our molecular docking models show that cat K, L, and S can bind to the central E domain where FpA is located [42]. However, catK and catS degrade the Aα and Bβ polypeptide chains of fibrinogen, and FpA was released and degraded over time. This suggests that cathepsins can cleave FpA, but eventually became destructive and degraded fibrinogen. Other proteases have been reported to only cleave FpA from fibrinogen. There is evidence of different types of snake venom that can cleave FpA from fibrinogen including, batroxobin (a serine protease from *Bathrops atrox* venom), arvin (snake venom isolated from *Agkistrodon rhodostoma*), and a coagulant serine proteinase from *T. flavoroviridis* venom [12]. This further supports that cat K, L, and S may only cleave FpA from fibrinogen and not result in fibrin polymerization.

Mechanisms and kinetics of fibrin formation have been identified. When thrombin cleaves fibrinogen, FpA is released faster than FpB to initiate protofibril formation and longitudinal aggregation. Lateral aggregation of fibrin is mediated by FpB release, which occurs more slowly compared to FpA [201]. There is an opposite rate of release with okinaxobin, a serine protease, which cleaves FpA and FpB; okinaxobin releases FpB at a faster rate than FpA [12]. This demonstrates that proteases might differ in the mechanisms and kinetics of fibrinogen cleavage and subsequent fibrin formation. Although cat K, L,

and S did not cleave FpA and cause fibrin gelation, our data supports that catK and catS could generate more FpA. This is possible as cathepsin L from *Fasciola hepatica*, a type of snake, created a fibrin clot with different cleavage sites on the polypeptide chains fibrinogen compared to thrombin [12]. When fibrin is formed by FpA cleavage only, thinner fibrin networks are formed compared to fibrin networks formed by cleavage of both FpA and FpB [62]. These observations demonstrate mechanisms and kinetics for fibrinogen cleavage and release of FpA, supporting the hypothesis that cathepsin cleave and release FpA. Perhaps, this is what occurred with experiments where isolated fibrinogen was co-incubated with recombinant human cathepsin K, L, or S; a different type of fibrin was formed, which is something that should be explored further in the future.

CHAPTER 6 FIBRINOLYSIS MECHANISMS IN MONOCYTES AND SIMULATED SICKLE FIBRIN CLOT DEGRADATION

6.1 Introduction

People with sickle cell anemia (SCA) are in a chronic inflammatory state as evidenced by an increase in elevated leukocytes, pro-inflammatory cytokines such as TNF-α, IL-8, and IL-17, endothelial damage, hemolysis (RBC rupture), increased reactive oxygen species production [202, 203]. Vaso-occlusive crisis (VOC) and hemolysis-dependent endothelial cell (EC) activation and inflammation increase tissue factor expression which leads to coagulation activation. It was proposed that activation of coagulation creates a loop that enhances VOC, EC activation, and inflammation via thrombosis [203]. In other words, abnormal blood clots in SCA causes vessels and tissues around the clots to become inflamed, which trigger the presence of increased levels of circulating monocytes. There is interplay between coagulation and vascular inflammation in SCA, where RBC sickling results in vaso-occlusion mediated ischemia-reperfusion injury and hemolytic anemia, which can result in increased vascular inflammation and activation of coagulation [203].

SCA is also characterized by monocytosis, where there is an increase in monocytes and circulating polymorphonuclear neutrophils (PMNs) [110, 204]. Monocytes from people with SCA are more activated and express interleukin (IL)-1β and TNF-α [110]. Production of IL-1β and TNF-α increases endothelial surface receptors and facilitates monocyte and sickle RBC adherence to endothelium, which can lead to vascular damage [106, 110, 205]. When monocytes are cultured with ECs, E-selectin, (intracellular adhesion molecule) ICAM and vascular adhesion molecule (VCAM) expression are also induced [206], another mechanism that can facilitate RBCs binding to endothelium [207].

Microvascular thrombosis, which is also associated with inflammation, is another complication in SCA that contributes to pulmonary hypertension, osteonecrosis, and stroke

[208]. Although thrombosis and inflammation have been viewed as separate systems that complement each other, cross-talk between the two systems need to be taken into consideration, especially because inflammation can stimulate thrombosis and thrombosis can promote inflammation [209]. Thrombosis with associated inflammation (thromboinflammation) is defined as a pathophysiological response in vasculature after blood vessel injury followed by a non-infectious inflammatory response; it includes activation of the coagulation system and innate immunity response [210]. It is suggested that developing thrombotic vaso-occlusion is due to sickled erythrocytes getting stuck in vessels leading to EC damage and vascular injury triggering a thrombotic response [211, 212]. Others also have hypothesized that mechanisms such as RBC adhesion, endothelial dysfunction, and leukocyte activation are contributors [208-210].

Our lab has demonstrated that SCA activates peripheral blood mononuclear cells (PBMCs), which includes mostly monocytes and lymphocytes, to induce cathepsin K activity in ECs. However, when PBMCs from AA controls were stimulated with TNF-α, catK activity was increased. Inflammation and activated circulating PBMCs upregulate cathepsin activity in SCA [40]. In Chapter 5, I demonstrated there is increased circulating cathepsins in SS mice and human plasma. Collectively, this data suggests elevated cathepsins can be a pathophysiological manifestation of SCA. This chapter contains preliminary work that investigates monocyte-mediated fibrinolysis, where I hypothesize that cathepsins secreted by monocytes are fibrin(ogen)olytic and can resolve fibrin gels. This work connects the coagulation pathway and inflammation, as potential mechanism that contributes to abhorrent clot resolution and thrombosis.

6.2 Materials and Methods

6.2.1 Multiplex Cathepsin Fibrinogen Zymography

THP-1 monocytes were lysed in zymography lysis buffer and BCA was used to quantify protein. Samples were prepared in non-reducing loading buffer. The same protocol from Section 5.2.4 was used.

6.2.2 THP-1 Monocyte 2D Culture on Fibrin Gels

Fibrin gels were formed in 12 well plates by combining fibrinogen (2.5mg/mL) and thrombin (1U/mL), for 2 hours at 37ºC. GFP-tagged THP-1 monocytes were seeded onto the fibrin gels at 200,000 cells per well, completely covering the gel, and incubated for 24 hours. Before and after cells were added, plates were imaged using the ImageQuant LAS 4000 to visualize fibrin gel degradation. Plates were also imaged using immunofluorescent imaging before and after incubation. Following a 24-hour incubation, the homogenate, containing remaining fibrin gel and monocytes, and supernatant, containing fragments released from fibrin gels insoluble fragments were saved and collected, and reduced SDS-PAGE was used to quantify fibrin degradation following the protocol described in section 3.2.4.

6.2.3 Degradation of Fibrin Clots Embedded with RBCs from AS and SS Mice

Simulated sickle fibrin clots were made with fibrinogen (5 mg/mL), thrombin (1U/mL), and RBCs from AS and SS mice (1% or 10%) in 50mM Tris-HCl/100mM NaCl, at a concentration of 2.5 mg/mL and 1 NIH U/mL in a final volume of 100 µl, then incubated for 2 hours at 37°C. Cathepsins K or S (0.15ng) were added and degraded RBC-fibrin clots overnight. The supernatant, which should contain any released fibrin fragments, was collected and saved, and the homogenate, which contains fibrin gel and monocytes, was resuspended in Tris-HCl with 25% beta-mercaptoethanol and sonicated to solubilize

it. Both supernatant and pellet were prepped for reduced SDS-PAGE, to assess fibrin degradation using the protocols described in section 3.2.4.

6.3 Results

6.3.1 Monocytes secrete cathepsins with fibrinogenolytic properties

To test if monocytes secrete cathepsins with fibrin(ogen)olytic potential, multiplex cathepsin fibrinogen zymography was used to assess the amount of active cathepsin in THP-1 monocytes. Increasing amounts of THP-1 monocytes were resolved in fibrinogen zymography and gelatin zymography was used as a control, as gelatin is the baseline substrate for the cathepsins (Fig. 6-1). Cathepsins from the THP-1 monocytes, degraded the fibrinogen substrate. The amount of active cathepsins in the zymograms increased in a dose-dependent manner and was quantified using densitometry. In the fibrinogen zymogram, active cathepsins were observed between 50 and 75 kDa, however, in the gelatin zymogram, active cathepsins were observed at ~25kDa. This indicates that the cathepsins hydrolyze fibrinogen, demonstrating the fibrinogenolytic potential of cathepsins.

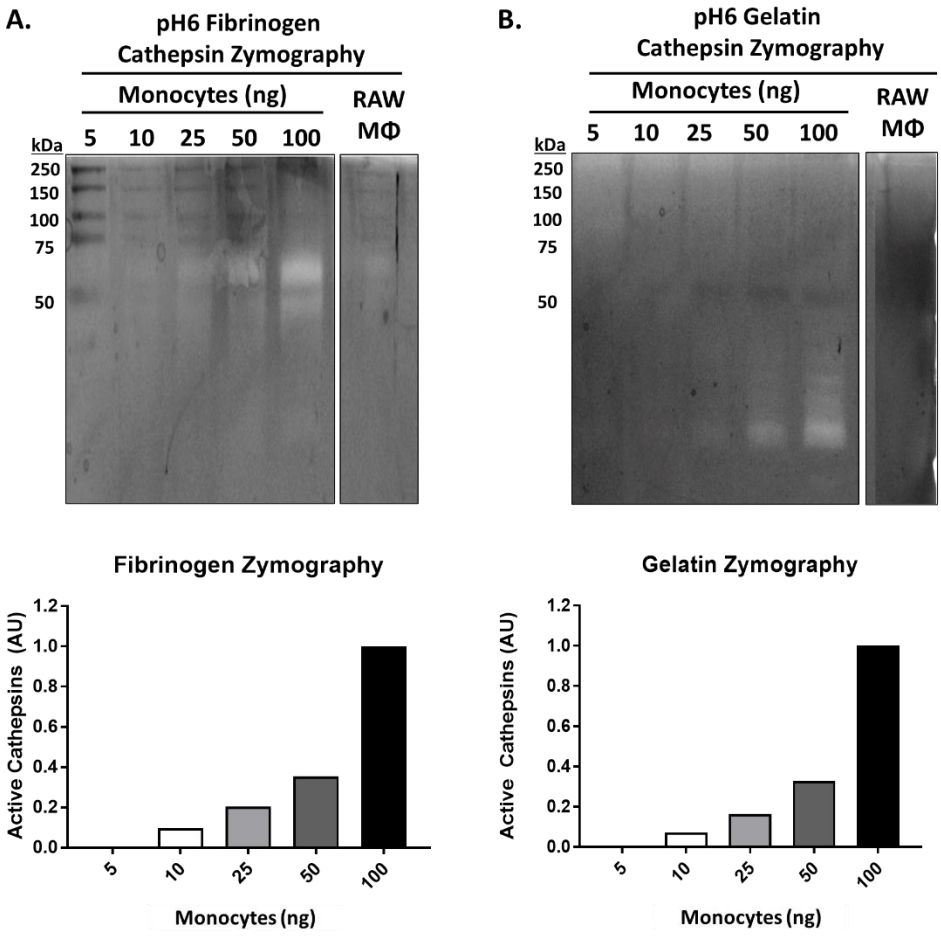

Figure 6-1: Fibrinogenolytic activity of cathepsins secreted by THP-1 monocytes
Multiplex cathepsin zymography assessed proteolytic activity of cathepsins secreted by monocytes using **(A)** fibrinogen substrate and **(B)** gelatin substrate. As the amount of monocytes added increases, the amount of active cathepsins increases as quantified using densitometry. The active cathepsin in the fibrinogen zymogram appeared at a higher molecular size compared to the gelatin control zymogram. This suggests a binding interaction between cathepsins and fibrinogen that prevents the cathepsins from migrating further through the gel.

6.3.2 Monocytes migrate into and degrade fibrin gels in 24 hours.

To test the hypothesis that monocytes could degrade fibrin gels, THP-1 monocytes transduced to express GFP were co-cultured with fibrin gels overnight. Plates were imaged using fluorescence imaging before and after to assess monocyte migration into the fibrin gel. In plates with fibrin gel and monocytes there was less fluorescence at 24 hours, as indicated by a decrease in fluorescence (Fig 6-2A). However, there was little to no change in fluorescence in plates with monocytes only (Fig 6-2B). This suggests that the monocytes co-cultured on fibrin gels migrated into the fibrin. Fibrin gels were imaged before and after degradation to visualize bulk fibrin degradation, similar to what was described in Chapter 3. In the co-culture of monocytes and fibrin gel, fibrin was degraded compared to the fibrin only control group (Fig 6-2D). Together, this suggests that as monocytes degraded the fibrin gel as they migrated into the gel.

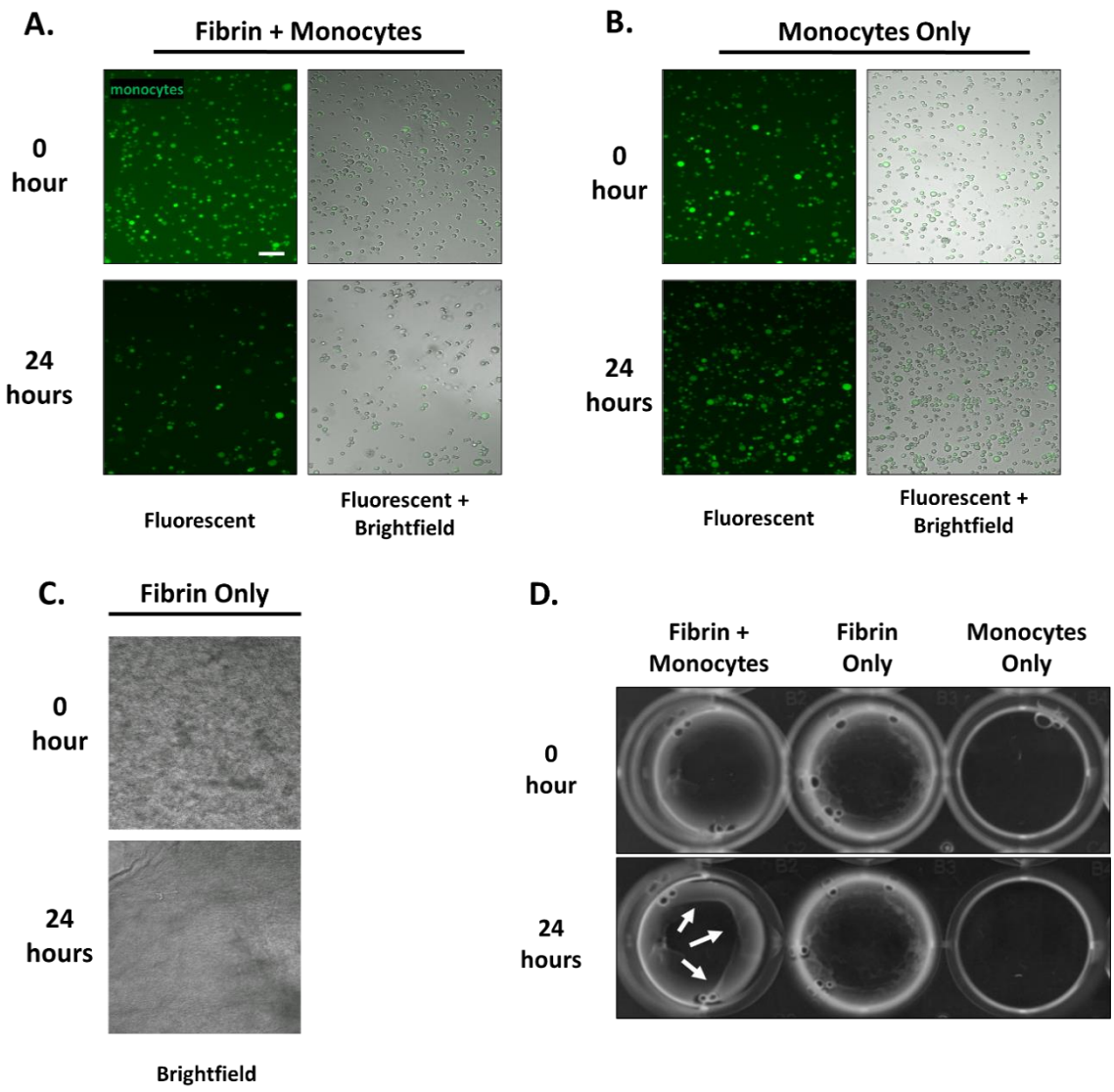

Figure 6-2: Monocytes migrate into and degrade fibrin gels
Fibrin gels were made using fibrinogen and thrombin in 12 well plates, and GFP tagged THP-1 monocytes were seeded on top of the gels for 24 hours. **(A)** Less fluorescence was observed in the THP-1s seeded on fibrin gels, compared **(B)** to the monocyte only (no fibrin gel) control. This suggests migration of the monocytes into the fibrin gels. Bulk fibrin degradation was also visualized. **(C)** At 24 hours, fibrin gel degradation (white arrows) was seen in the monocyte-fibrin gel co-culture, which could be compared **(D)** to the monocyte only (no fibrin gel) conditions.

6.3.3 Monocytes degrade the α and β fibrin polypeptide chains

To assess degradation of fibrin polypeptide chains, the homogenate, which contained monocytes and any remaining fibrin gel, was resolved in reducing SDS-PAGE. There was significantly less α polypeptide chain in monocytes seeded on a fibrin gel compared to fibrin only ($p=0.001$, $n=3$, Fig 6-3). However, there was significantly more β polypeptide chain present (Fig 6-3), suggesting that higher molecular size α polypeptide chains were degraded, giving more insight into possible cleavage sites. Proteins were also detected in the supernatant, and based on their molecular size (ranging from 50 to 75kDa) the proteins are hypothesized to be fibrin fragments.

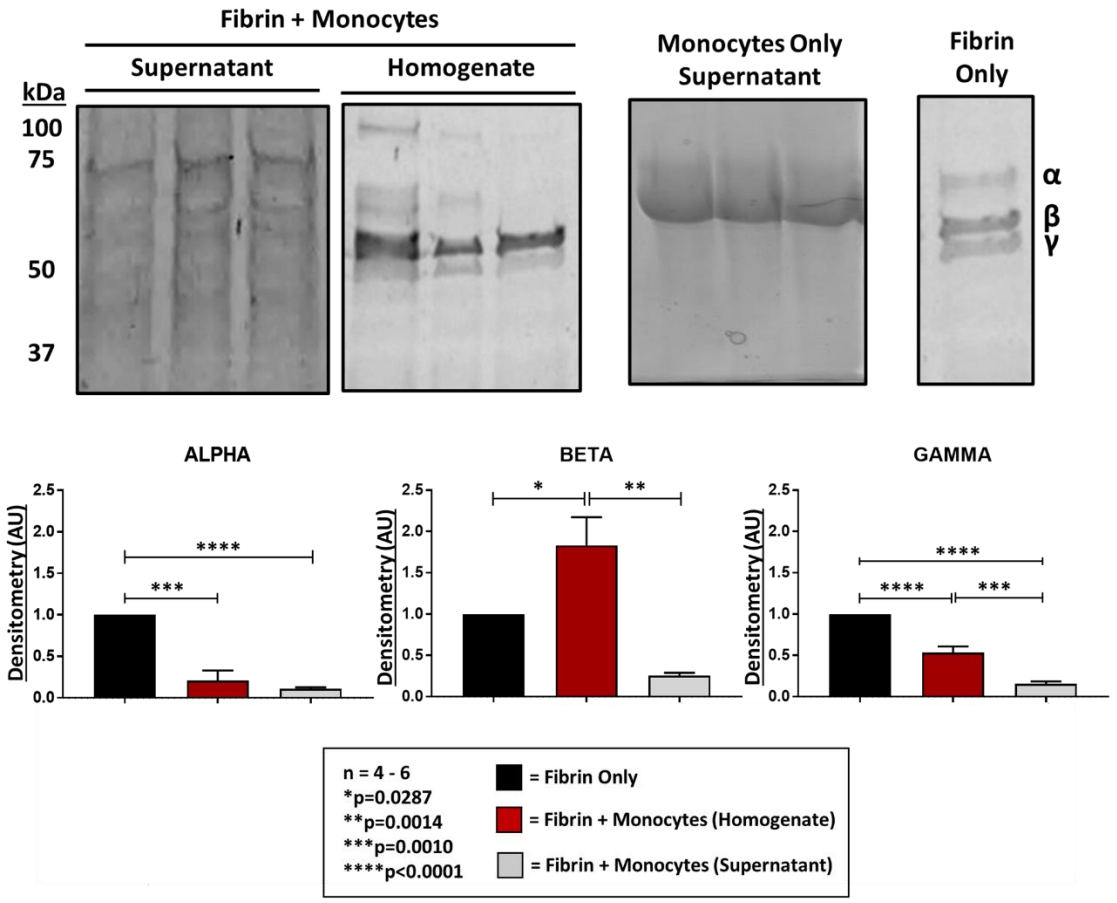

Figure 6-3: Monocytes degrade the alpha chain of fibrin gels within 24 hours.
As described in methods, fibrinogen and thrombin were combined to form fibrin gels and GFP tagged monocytes were seeded on top of the gels. Reduced SDS-PAGE was run to assess for fibrin degradation, and the α, β and γ polypeptide chains show partial fibrin degradation. Within 24 hours, monocytes degraded the alpha chain of fibrin, initializing fibrin degradation, but did not progress to degrade the beta and gamma bands of fibrin.

6.3.4 Degradation of RBC-fibrin clots with recombinant cathepsins

In vitro fibrin clots and thrombi also contain red blood cells (RBCs), which alter fibrin network structure and mechanical properties. RBCs incorporate into spaces between fibrin fibers which disrupt the network increasing the pore size and increases blood viscosity [213]. Clot mechanical properties are influenced by RBCs due to high deformability of RBCs [214, 215]. When fibrin clots had a RBC concentration of 10%, elastic and viscous moduli peaked, but then as more RBCs were added viscoelastic properties of RBCs dominate. One must also consider differences in SS RBCs mechanics; SS RBCs are less deformable [216] and the Young's modulus is stiffer compared to AA RBCs [217].

The effect of RBCs on fibrin structure should be considered in future cathepsin-mediated fibrinolysis studies. This would suggest that incorporation of SS RBCs alters fibrin network structure and mechanics which could impact fibrinolysis. I have done some preliminary work creating fibrin clots embedded with 1% or 10% of AS or SS RBCs, which were then degraded with recombinant cathepsin K or S (Fig 6-4A). Cathepsins K and S degraded AS RBC- fibrin clots (Fig 6-4B, Fig 6-4D) and SS RBC fibrin-clots (Fig 6-4C, Fig 6-4E) producing lower molecular size fragments in the pellet. There is degradation of α polypeptide chain, however proteins appear in the supernatant, which are hypothesized to be fibrin fragments that were released from the fibrin gel by proteolytic cleavage. As the amount of AS or SS RBC increased from 0% to 10% there was an increase in the amount of fibrin fragments at lower molecular sizes. The banding patterns of the lower molecular size fibrin fragments differ between cathepsin K and S, but also there is a difference in banding patterns between AS and SS clots, indicating cathepsins cleaving fibrin at different sites. Collectively, this demonstrates how RBCs alter cathepsin-mediated fibrinolysis.

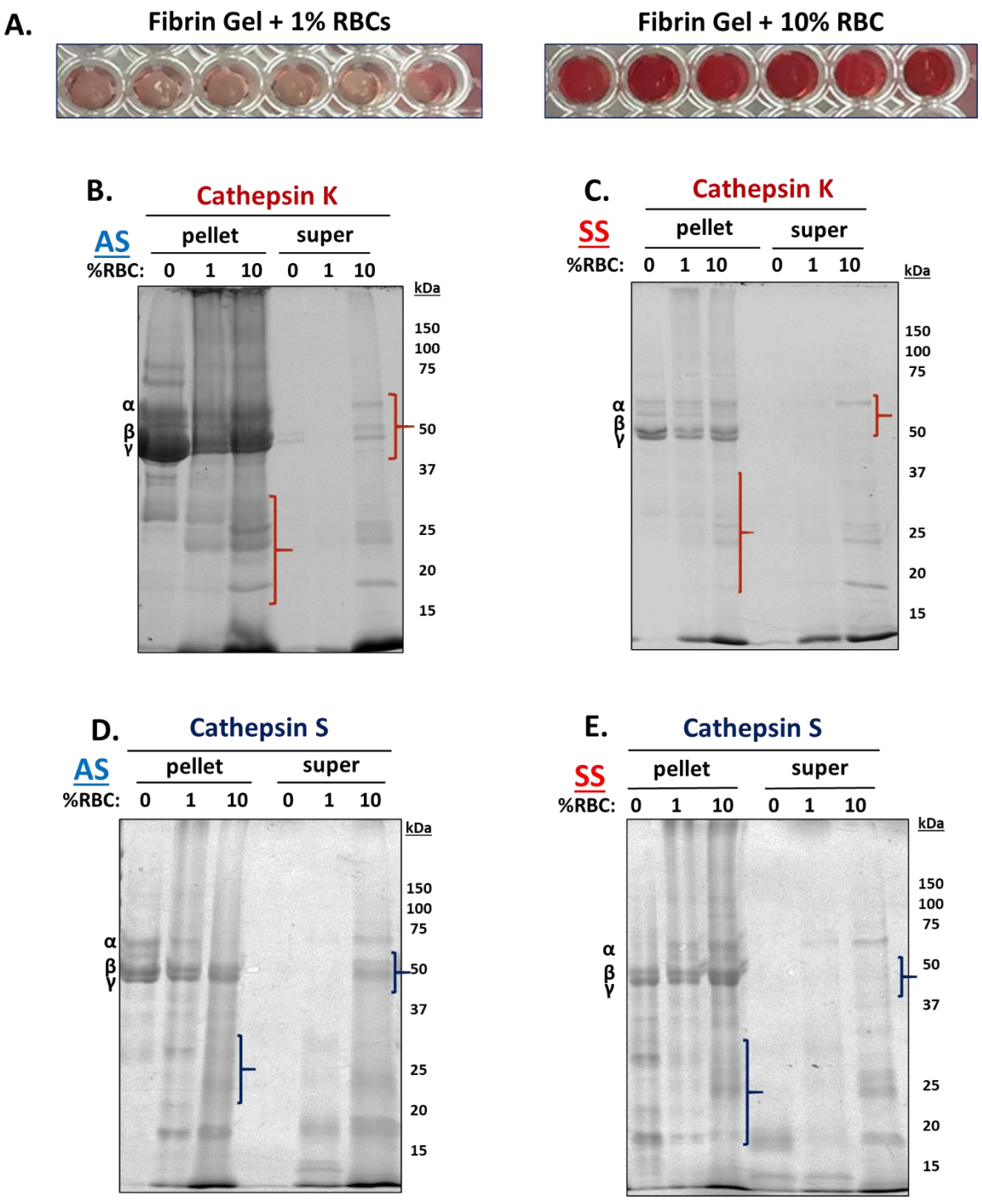

Figure 6-4: Cathepsins K and S degrade fibrin gels embedded with AS and SS, with distinct banding patterns.

(A) Stimulated clots were made with fibrin gel embedded with 1% or 10% AS or SS red blood cells (n=1). **(B,C)** Cathepsin K or **(D,E)** cathepsin S degraded stimulated AS or SS clots and produce different banding patterns, suggesting that each cathepsins cleave fibrin at different sites.

6.4 Discussion and Conclusions

Monocytes secrete cathepsins with fibrinolytic properties, demonstrating a potential mechanism in fibrinolysis. Using modified multiplex cathepsin zymography, I demonstrated fibrinogenolytic activity of cathepsins. Next, THP-1 monocytes were co-cultured on fibrin gels for 24 hours, where I demonstrated that monocytes migrate through and degrade fibrin gels. Further investigation using reducing SDS-PAGE, identified that the polypeptide chains of fibrin were degraded and released products into supernatant. Overall, this demonstrates cathepsin-mediated fibrin(ogen)olysis *in vitro* and suggests that monocytes could play a role in aberrant blood clot resolution.

Noticeably, there was a difference in the electrophoretic migration distance of active cathepsins in fibrinogen zymogram compared to gelatin zymogram; 50-75kDa and 25kDa, respectively. This is similar to what was observed in Chapter 5 (Fig 5-4) with recombinant catK in a fibrinogen zymogram appearing at a higher molecular size than expected. In Chapter 3, I demonstrated that catL adsorbs to fibrin (Fig 3-1C and Fig 3-5B). Interestingly, the cathepsin electrophoretic migration distance in the fibrinogen zymogram is the same molecular size that catL adsorbed to fibrin. This suggests the cathepsins are binding to the fibrinogen substrate in the zymogram. Together, this led me to consider that cysteine cathepsins can act in a similar manner to matricellular proteins on fibrin(ogen). Matricellular proteins are non-structural proteins that are secreted into the extracellular environment, interacting with cell-surface receptors, proteases, and cytokines [218]. The CCN (Cyr-61, connective tissue growth factor, and Nov) family of cysteine-rich matricellular proteins, is an ECM protein involved in intercellular signaling by modulating growth factors such as TNFα. TGF-β, and VEGF; specifically, CCN1 engages cell surface receptors, with emerging roles in wound healing, inflammation, and vascular disease [219]. ADAMTs (A disintegrin-like and metalloprotease with thrombospondin motif), are another family of matricellular proteases that play roles in cell migration, tissue organization, coagulation, inflammation, and angiogenesis where they are proteolytically active on cell-

surfaces [220]. I hypothesize that cathepsins bind to fibrinogen as they migrate through the gel, and the electrophoretic force cannot overcome the strong interaction between cathepsins and fibrinogen, thus the cathepsins do not migrate through the gel to its expected molecular size. Collectively, this evidence suggests cysteine cathepsins could act as matricellular proteases.

There was accumulation of the β polypeptide chain, as well as degradation of the α chain, which could suggest cathepsins degraded the α polypeptide chain into fragments that are approximately the same size as the β polypeptide chain (Fig 6-3). These results can be compared to work from Chapter 3 with the recombinant cat K, L, and S. The α chain is degraded by all three cathepsins, however only catK and catS degraded both α and β chain. Compared to recombinant studies, little to no fibrin fragments were observed in the supernatant. Also, there were no fibrin fragments below 50kDa in the PAGE for the homogenate compared to what was observed in Fig 3-7. Future work could consider doing a time course, where degradation is stopped a different time points, to see if fragments are generated at earlier time points and degraded over time.

Plasmin is the canonical protease that degrades fibrin, however, evidence suggests fibrinolysis in plasminogen activator-deficient transgenic mice occur via non-plasmin pathway [71, 72]. Cathepsins, secreted by monocytes, are in close proximity to fibrinogen, providing easy access for cathepsins to cleave fibrinogen in vasculature. This leads to the hypothesis that monocytes could play a supporting role in degrading fibrin. Even in the absence of plasmin, monocytes can internalize fibrin via Mac-1 integrin and degrade fibrin, resulting in a fibrin degradation pattern unique from plasmin [11]. Using chloroquine, which prevents endosomal acidification inhibiting lysosomal enzymes, it was concluded that fibrin degradation occurs in lysosomes of macrophages. Later, using protease inhibitors, including serine inhibitors and lysosomal cysteine inhibitors (including E-64d) determined that fibrin degradation was not blocked. However, with pepstatin A, an aspartyl protease inhibitor, inhibited fibrin degradation, leading to the identification of cathepsin D

as a fibrin(ogen)olytic protease [10]. I should note that this work was done in 1993 and 1994, when cysteine cathepsins were mostly thought of as lysosomal proteases. However, now extracellular function of cathepsins are being explored and more cathepsin-specific inhibitors have been identified, which could help us uncover mechanisms of non-plasmin fibrin degradation via monocytes. Our work demonstrated that active cysteine cathepsins are fibrin(ogen)olytic (Fig 6-1 and Fig 6-2) and future work should repeat these experiments using E-64 to target non-lysosomal cysteine proteases to further elucidate the role of cysteine cathepsins in degrading fibrin via monocytes. Monocytes would be seeded on fibrin gels, with E-64 added to the media, and fibrin degradation would be quantified using the methods described above.

This work demonstrates how two factors involved in the coagulation cascade and inflammatory pathway, fibrin and monocytes, could interact with each other. Thromboinflammation (thrombosis with associated inflammation) and microvascular thrombosis and their mechanisms warrant further studies in SCA. The interplay between coagulation and inflammation in SCA needs to be characterized, which could help provide better treatment for patients to prevent complications. Work in this chapter demonstrates that monocytes could secrete cysteine cathepsins with fibrin(ogen)olytic properties. Future studies should make the *in vitro* system more physiologically relevant by seeding an EC monolayer on top of fibrin gels, with the addition of PBMCs on top.

One must also consider using fibrin clots that are more physiologically relevant by adding RBCs to fibrin gels. Fibrin clots with RBCs from people with SCA are denser where RBCs aggregate and agglomerate fibrin networks. and displayed aggregation of the RBCs and agglomerated fibrin clusters [221]. Preliminary work simulated clots by embedding RBCs from AS or SS mice in fibrin gels that were degraded with cathepsin K or S (Fig 6-4). Distinct banding patterns of fibrin fragments corroborated findings in Chapter 3 where it was demonstrated that cathepsins K and S have unique fibrinolytic properties, suggesting that each cathepsin cleaves fibrin at unique cleavage sites. Our work identified fibrin

degradation products, however, future work could quantify fibrinolysis rate to see if cathepsins lyse fibrin faster and identify if fibrin clots with SS RBCs degrade at different rates compared to fibrin clots with AA RBCs. I hypothesize that given the altered structure of SS RBCS, lysis rates would be slower. Studies have identified that clot lysis rates are significantly lower in glycated clots from diabetic patients compared to controls [222, 223]. Future work could use similar methods with confocal microscopy [223] not only to measure fibrinolysis rates, but also to image fibrin clots with RBCs from people with SCA. Collectively, techniques presented in this chapter could be leveraged and combined to further study thrombosis and clotting mechanisms in SCA.

CHAPTER 7 QUANTIFYING PROTEOLYTIC ACTIVITY OF SPECIALIZED ENDOTHELIAL CELLS FROM EMBRYONIC STEM CELLS

Data from this chapter was published: Madfis, Lin, Kuma, Douglas SA. et al. (2018) "Co-Emergence of Specialized Endothelial Cells from Embryonic Stem Cells." Stem Cells and Development. 27(5)326-335 doi: 10.1089/scd.2017.0205.

7.1 Introduction

The endothelium layer forms the innermost layer of vessels and has a number of functions including regulation of vascular tone and structure integrity of vessels, immune cell responses, and blood clotting factors [224]. There is EC heterogeneity, where ECs can be distinguished based on phenotype, morphology, and function which vary based on their anatomical location in different tissue types and organs [225]. For example, ECs lining arteries are oriented longitudinally aligned in the direction of blood flow [226]. ECs of arteries and veins are continuous with tight junctions, whereas discontinuous layers are present in organs involved in filtration and secretion such as gastric and intestinal mucosa or glomeruli in kidneys [225]. Differences in EC function can be observed with EC permeability; constitutive flow between blood and tissue occurs via capillaries, and macromolecules can be transferred through the cells via endocytosis and exocytosis, or smaller solutes and fluids can transfer between cell-cell junctions [225, 226].

Structural and functional EC heterogeneity is also observed within a sprouting blood vessel during angiogenesis [226]. The leading edge of the sprouting vessel or "tip" ECs have more probing filopodia, and migrate toward the angiogenic stimulus [227], however they tip ECs do not proliferate of form lumen [227-229]. "Stalk" ECs are behind the tip ECs and more proliferative, form lumen, produce more ECM, and have shorter filopodia [230]. Another EC subphenotype, "phalanx EC" are non-sprouting, and less

migratory and proliferative Initially it was thought during sprouting there is plasticity and reversibility between the tip, stalk, and phalanx phenotypes. However, using staged differentiation and chemically specific media, distinct tip/stalk (Fig 7-1A) and phalanx (Fig 7-1B) cell types have been cultured and expanded for up to 9-10 passages, where the tip/stalk ECs are more migratory and proliferative, with increased angiogenic-like sprouting on Matrigel^{TM} compared to phalanx [231].

As discussed in Chapter 4, proteolytic activity facilitates angiogenesis aiding in EC migration and ECM remodeling. Matrix metalloproteinases (MMPs) aid in vascular remodeling by degrading ECM and basement membrane which facilitates EC migration and invasion, and sprout formation [19, 166, 232]. Cathepsins (cat) K, L, and S have been identified in ECs and are upregulated by ECs in areas of disturbed flow [28]. To further characterize the migratory ability of the sub-populations, we wanted to know what enzymes were responsible for differences in sprouting activity within the ECs. Here the amount of active proteolytic enzymes of tip/stalk and phalanx ECs was quantified, with the hypothesis that the more migratory tip/stalk ECs would have increased proteolytic activity compared to phalanx ECs.

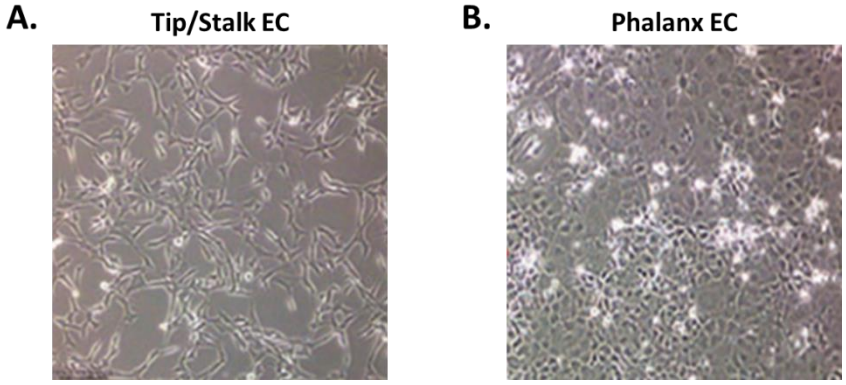

Figure 7-1: Tip/stalk and phalanx endothelial cells
Endothelial cell (EC) subtypes have heterogeneity with differences between phenotype and morphology. **(A)** Tip/stalk phalanx ECs are more migratory and proliferative, characterized by an elongated appearance. **(B)** Phalanx ECs have a "cobblestone" like morphology are less migratory and proliferative.

Adapted from Madfis et al. *Stem Cells and Development* 2018

7.2 Materials and Methods

7.2.1 Multiplex Gelatin Cathepsin and MMP Zymography

Tip/stalk and phalanx EC were lysed in zymography lysis buffer and total protein concentrations were quantified. Equal amounts of lysate were loaded for matrix metalloproteinase (MMP) or cathepsin zymography, as previously described [148, 233]. Zymograms were imaged using an ImageQuant LAS 4000 (GE Healthcare), and densitometry was performed with ImageJ (NIH) to quantify cleared white bands, indicative of proteolytic activity.

7.3 Results

7.3.1 MMP2 activity was significantly increased in tip/stalk ECs compared to phalanx ECs

MMP zymography was done on cell lysates from tip/stalk and phalanx ECs, to determine differences in active amounts of proteolytic enzymes between the two EC subphenotypes (Fig 7-2). There was significantly more active mature MMP2 in the sprouting tip/stalk-containing EC compared with phalanx EC. However, the phalanx ECs contained significantly more pro-MMP2, the inactive zymogen form that must be cleaved to be active. This shows differences in proteolytic activity, where more mature MMP which corroborates tip/stalk ECs characteristic migratory and proliferative phenotypes.

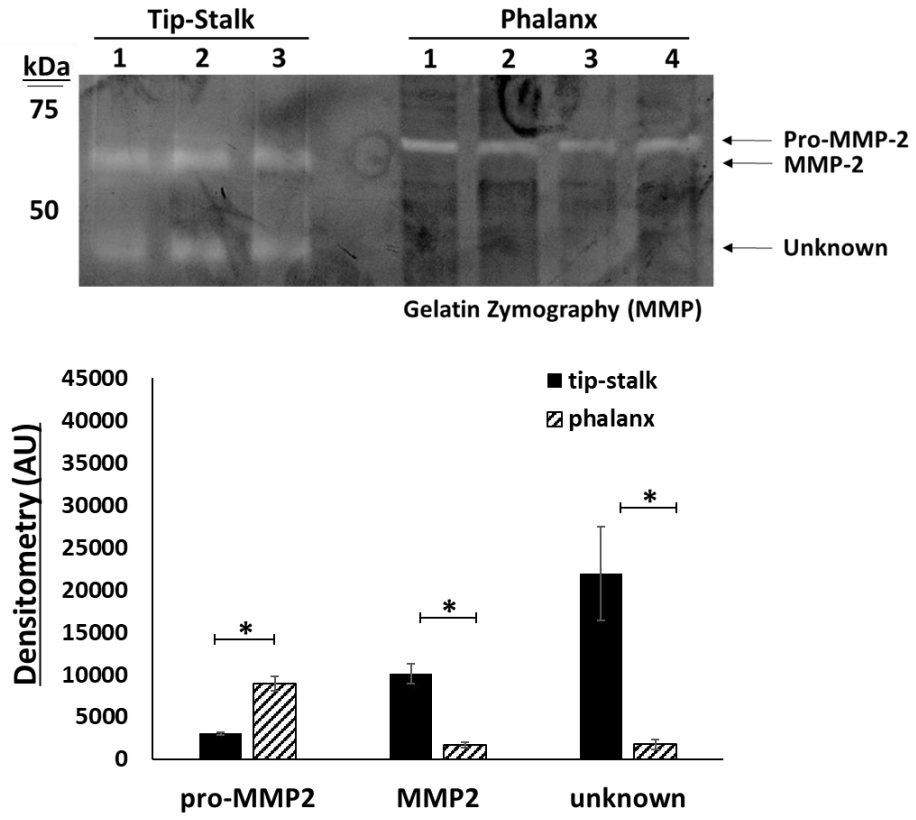

Figure 7-2: MMP proteolytic activity in tip/stalk and phalanx endothelial cells

7.3.2 Active cathepsin L was identified in tip/stalk and phalanx ECs

Both EC subtypes have increased amounts of active cathepsins. In the zymogram incubated at pH4, more catL activity was quantified in tip/stalk ECs (Fig 7-3A). This was corroborated in the zymograms incubated at pH 6 by the 20 kDa cathepsin band being significantly higher in the tip/stalk EC, while the 15 and 22 kDa fragments were only found in the phalanx EC (Fig 7-3B). Thus, increased active cathepsins are associated with sprouting ECs subphenotypes, which may be implicated in angiogenic pathways.

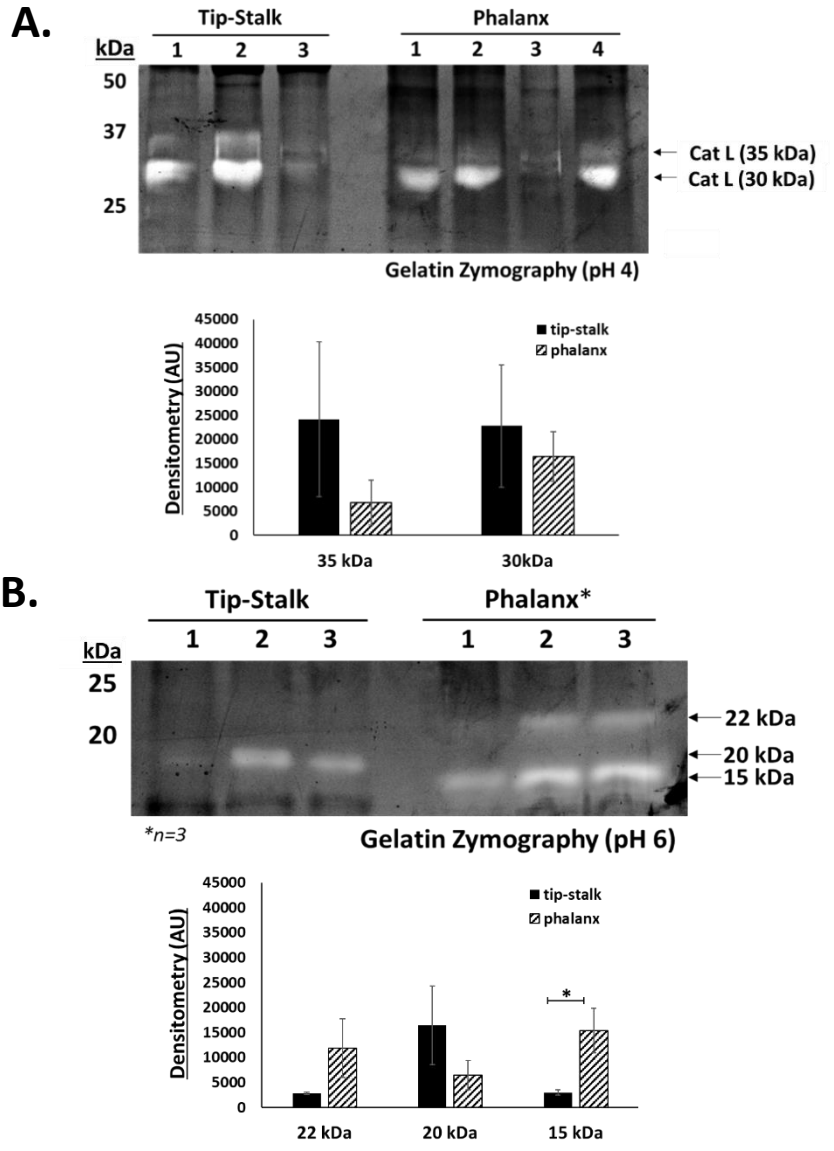

Figure 7-3: Cathepsin activity in tip/stalk and phalanx activity endothelial cells

7.4 Discussion and Conclusions

These results show distinct proteolytic activity in sprouting (tip/stalk) and non-sprouting (phalanx) EC subtypes. The more invasive and migratory EC subphenotype, tip/stalk ECs had increased MMP2 activity and catL which corroborates the sprouting characteristic. The invasive behaviors of sprouting ECs is thought to be regulated by different pathways. For example, MMP2 is activated by ADAM17 during angiogenesis [234], and overexpression of ADAM17 reduces antiangiogenic molecular expression [235], which could contribute to the invasiveness of sprouting ECs [236]. Guanylate binding protein-1 GTPase inhibits MMP1expression, which reduces the invasiveness and tube formation of ECs [237], suggesting a role for MMP1 in angiogenesis. CatL is more upregulated in endothelial progenitor cells compared to mature ECs, and has been associated with invasion and neovascularization [3, 83]. In humans, an increase in angiogenic EC behaviors has been associated with catL but the mechanism yet to be determined [84].

Tip/stalk and phalanx ECs are derived from mice, which means the cathepsins identified in the tip/stalk and phalanx ECs is specifically mouse catL, which is the ortholog for human catV; they share 75% sequence identity yet have different levels of expression and functions[3]. When incubated at pH4, mouse catL was higher in phalanx ECs compared to tip/stalk ECs, which could suggest mouse catL is multifunctional depending on the EC subphenotype. However, this angiogenic shift controlling catL activity in ECs is not clear and warrants further studies. I think this is a good opportunity to use these specialized ECs in the microvascular networks, where ECs could form via a vasculogenic-like process and cathepsin inhibitors could be added to identify the role of cathepsins during formation. Further, using tip/stalk and phalanx ECs is more physiologically accurate compared to HUVECs for studying angiogenesis, due to the more invasive and migratory phenotypes. It has been suggested that HUVECs would be better suited for studying atherosclerosis and lining small diameter vascular grafts.

Overall, cathepsins and MMPs are involved in the sprouting behavior of tip/stalk ECs, which could be associated with its migratory and invasive characteristics, likely contributing to the angiogenic pathway. Distinct proteolytic activity profiles for sprouting versus non-sprouting ECs supports the EC subpopulations are regulated differently which motivates future work to understand how proteases contribute to the invasiveness and migratory abilities of ECs during angiogenesis/vasculogenesis.

CHAPTER 8 PACMANS ANALYSIS OF CATHEPSINS K, L, AND S ON PLASMINOGEN

8.1 Introduction

Cysteine cathepsins are elevated in the plasma of SS mice, where they have access to the coagulation factors that could become substrates for the cathepsins. This mechanism could contribute to chronic coagulation activation where the cysteine cathepsins compete and interfere with the natural coagulation factors, such as plasminogen- the inactive, zymogen form of the serine protease, plasmin. The structure of plasminogen includes five kringle domains (denoted as K1, K2, etc.). Although the exact role of kringle domains is not clear, they are present in blood plasma, specifically in coagulation factors, proteases, apolipoprotein, and growth factors [238]. Kringle domain sequences differ, yet structures are highly conserved. They contain surface-exposed loops, comprised of ~80 amino acids stabilized by three disulfide bonds (Fig 8-1) [239, 240]. Single or multiple kringle domains of plasminogen bind to membranes and other proteins, which inhibit endothelial cell proliferation, tube formation, and angiogenesis [240].

Plasminogen contains a disulfide bond, C558–C566, surrounding the activation site at R561–V562 [241] . Tissue plasminogen activator (tPA) is the canonical enzyme that cleaves plasminogen at the R561 and V562 bond generating a two chain-plasmin, a heavy chain that contains the five kringle domains, and a light chain that contains the catalytic domain [241, 242]. Angiostatin, the fragment of plasminogen that contains the first 4 kringle domains, are potent inhibitors of angiogenesis by inhibits endothelial cell (EC) proliferation and migration. Plasminogen is cleaved to form angiostatin by numerous proposed mechanisms, including cleavage by MMPs- 2, 3, 7, and 9, [240, 243]. Cleavage

by different proteases suggests that there are several angiostatin isoforms or angiostatin-related proteins formed under different physiological conditions. There is evidence of cysteine cathepsins hydrolyzing plasminogen. Plasminogen cleavage by cathepsin V (catV), releases angiostatin-like products which inhibit angiogenesis. However, cathepsins K and L (catK and catL), did not generate angiostatin-like products [244], and although cathepsin S (catS) can cleave plasminogen, the released fragments do not inhibit angiogenesis on ECs [245].

Here, I analyzed the likelihood of cathepsins K, L, or S binding to plasmin(ogen) with bioinformatics site sequence specificity analysis. To do this, I used the lab's previously published PACMANS: Protease-Ase Cleavages from MEROPS ANalyzed Specificities program [246], which identifies putative sites on substrates highly susceptible to cleavage by proteases using a sliding-window approach to score amino acid sequences based on preference in the active site of the protease taken from the MEROPS database. These sequences were then mapped to kringle domains, light chain, and near known proteolytic cleavage sites on a plasminogen sequence.

8.2 Materials and Methods

8.2.1 PACMANs Analysis

PACMANs program accessed from: https://platt.gatech.edu/PACMANSuse/form and previously published [246]. The substrate input was plasminogen, which was accessed from UniProt, and protease-ase input was cathepsins K, L, or S, which were each accessed from the MEROPS database, with a pocket size upper bound 1 and lower bound 8. The higher the cumulative score, the greater the likelihood cleavage occurs; normalized scores are used to compare among the analyzed cathepsins on plasminogen.

8.2.2 Determining Kringle Domain and Known Protease Cleavage Site Sequences on Plasminogen

The kringle domains (K1, K2, K3, K4, and K5) amino acid sequences were determined based on the structure of plasminogen previously published [247], where sequences are from cysteine residues (C-C) at the base of the loop (denoted by the colored lines and circles in Fig 8-1). Known cleavage sites for elastase, aureus V8 protease, and R561-V562 (site that gets cleaved to generate plasmin) were also determined from the plasminogen figure (circled in black in Fig 8-1). It should be noted that the structure is missing the first 20 amino acid sequences, and the sequence numbers used in PACMANS align with the sites/numbers for the plasminogen site sequence in UniProt. These differences had to be taken into consideration to identify sequences from PACMANS on the structure (Appendix Table A-1) denotes these differences, which was used for the analysis.

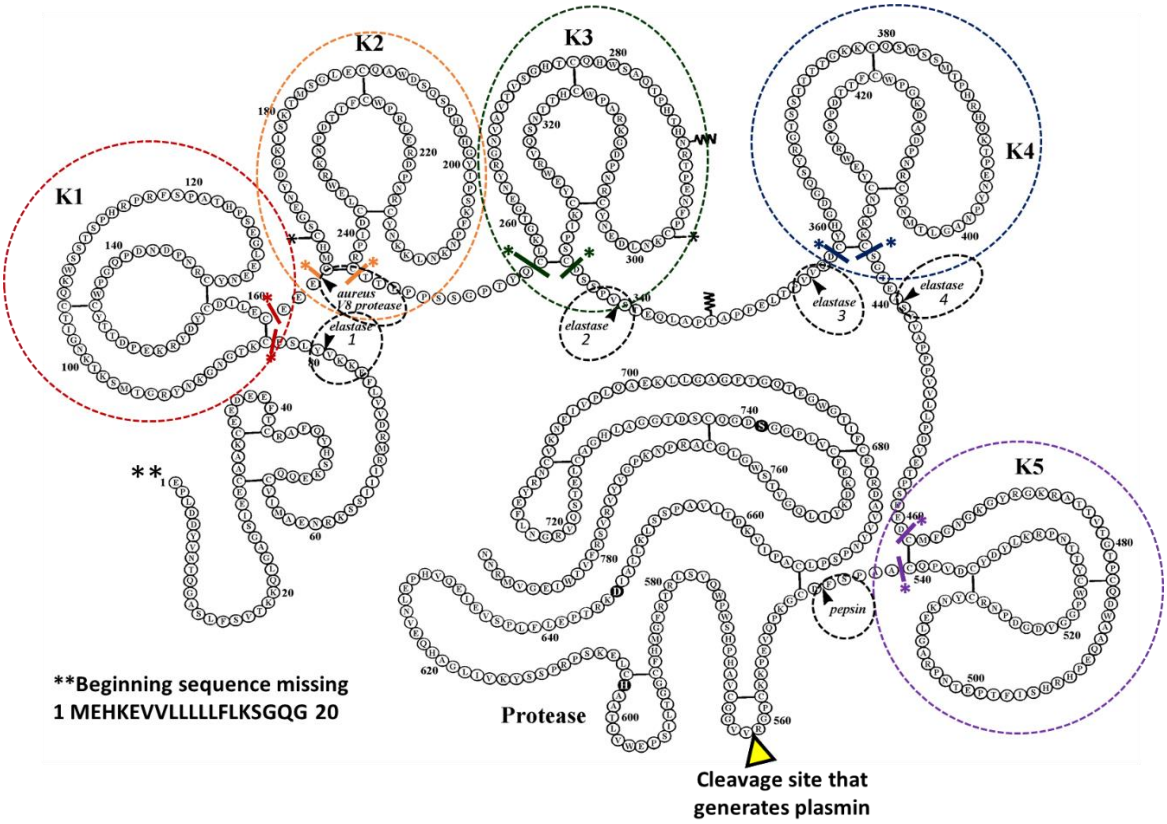

Figure 8-1: Kringle Domain and Known Protease Cleavage Sites on Plasminogen

Figure adapted from Soff et al. *Cancer and Metastasis Review*. 2000.

8.3 Results

8.3.1 Likelihood of plasminogen cleavage by cathepsin K

There were 12 top ranked PACMANS sequences in the kringle domains and 3 top ranked sequences in the light chain (Fig 8-2, Table 8-1). Based on the score, the sequences in the K3 domain at #274-281 QCLK/GTGE was the most likely location for cleavage by catK (scored at 0.934). The next top scored sequences were in the K1 domain at #177-184 DILE/CEEE (scored at 0.922), which was four residues shifted from the known cleavage site for aureus V8 protease (CEEE/CMHC). There were other top scores of catK on plasminogen where cleavage sites were located in the light chain of plasmin: #667-674 (ALLK/LSSP) scored at 0.901, #747-754 (GHLA/GGTD), and #713-720 (AGLL/KEAQ). Closer analysis of other top scored likely cleavage sites revealed there were possible cleavage sites near known elastase sites: #360-367 (EQLA/PTAP) was six residues away from elastase 2 (SSPV/STEQ) with a score of 0.771, #91-98 (VVLF/EKKV) was four residues away from elastase 1 (ESLY/VKKE) with a score of 0.763, #368-375 (PELT/PVVQ) was three residues away from elastase 3 (LTPV/VQDC) with a score of 0.735, and #98-105 (VYLS/ECKT) was two residues away from elastase 1 (ESLY/VKKE) with a score of 0.735.

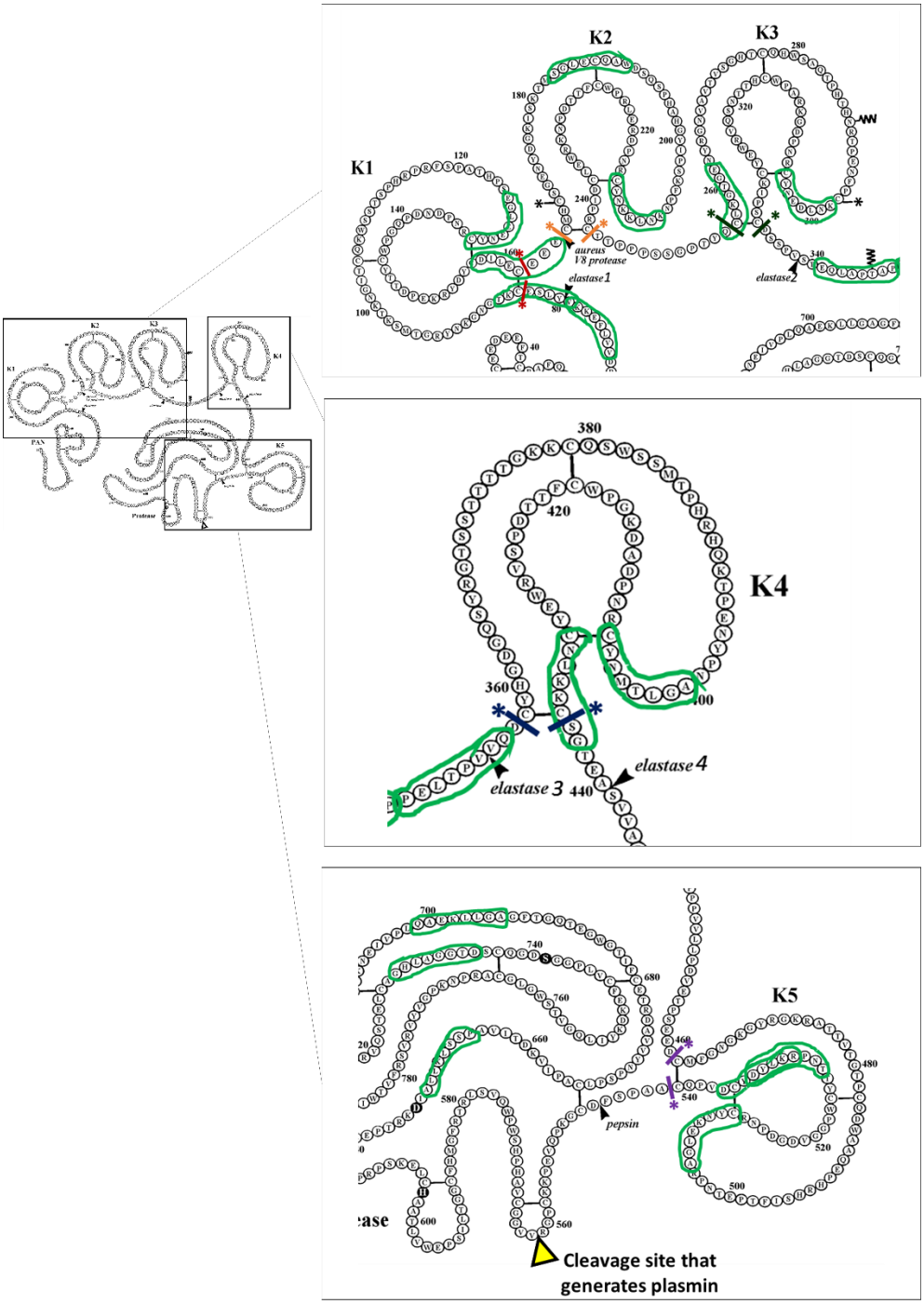

Figure 8-2: Top scored likely locations for cathepsin K cleaving plasminogen
Sites identified on plasminogen within kringle domains and near known protease cleavage sites (elastase, aureus V8 protease, pepsin, or cleavage site that generates plasmin).

Figure adapted from Soff et al. *Cancer and Metastasis Review*. 2000.

Table 8-1: Predicted plasminogen cleavage sites by cathepsin K from PACMANS

Location within Plasminogen	Plasminogen Sequence			Cumulative Score	Normalized Score
elastase 1	91	VVLFEKKV	98	1675	0.763
elastase 2	360	EQLAPTAP	367	1693	0.771
elastase 3	368	PELTPVVQ	375	1616	0.735
K1	145	EGLEENYC	152	1848	0.842
K1 & aureus V8 protease	177	DILECEEE	184	2026	0.922
K1 & elastase 1	98	VYLSECKT	105	1605	0.731
K2	227	KNLKKNYC	234	1796	0.818
K2	202	SGLECQAW	209	1621	0.738
K3	274	QCLKGTGE	281	2052	0.934
K3	317	KNLDENYC	324	1578	0.719
K4	419	AGLTMNYC	426	1688	0.77
K4	449	CNLKKCSG	456	1629	0.74
K5	549	RKLYDYCD	556	1834	0.836
K5	524	AGLEKNYC	531	1833	0.836
K5	546	ANPRKLYD	553	1558	0.711
light chain	667	ALLKLSSP	674	1980	0.902
light chain	747	GHLAGGTD	754	1979	0.901
light chain	713	AGLLKEAQ	720	1953	0.891

8.3.2 Likelihood of plasminogen cleavage by cathepsin L

There were 7 top ranked PACMANS sequences in the kringle domains and 3 on the light chains for catL on plasminogen (Fig 8-3, Table 8-2). The highest score (0.96) of catL on plasminogen was at #667-674 (ALLK/LSSP), which is located in the light chain of plasmin. Two other high scores were located in the light chain, as well #669-676 (LKLS/SPAV) and #635-642 (VILG/AHQE) with scores of 0.891 and 0.862, respectively. Similar to catK, catL also had a top scored sequence in the K1 domain at #177-184 DILE/CEEE, however it scored lower at 0.776. CatL was also the only cathepsin that had a top score (0.709) at #580-587 RVVG/GCVA and is within 3 residue shifts of the Arg-Val site that is cleaved to generate plasmin. Sequence #362-369 (LAPT/APPE) with a score of 0.728 was unique in that it is between elastase 2 and elastase 3. Other top scored likely cleavage sites, revealed close residue shifts near other elastases; #459-466 (ASVV/APPP) was two residues away from elastase 4 (GTEA/SVVA) with a score of 0.923, #360-367 (EQLA/PTAP) was six residues away from elastase 2 (SSPV/STEQ) with a score of 0.812, and #460-467 (SVVA/PPPV) was four residues away from elastase 4 (GTEA/SVVA) with a score of 0.712.

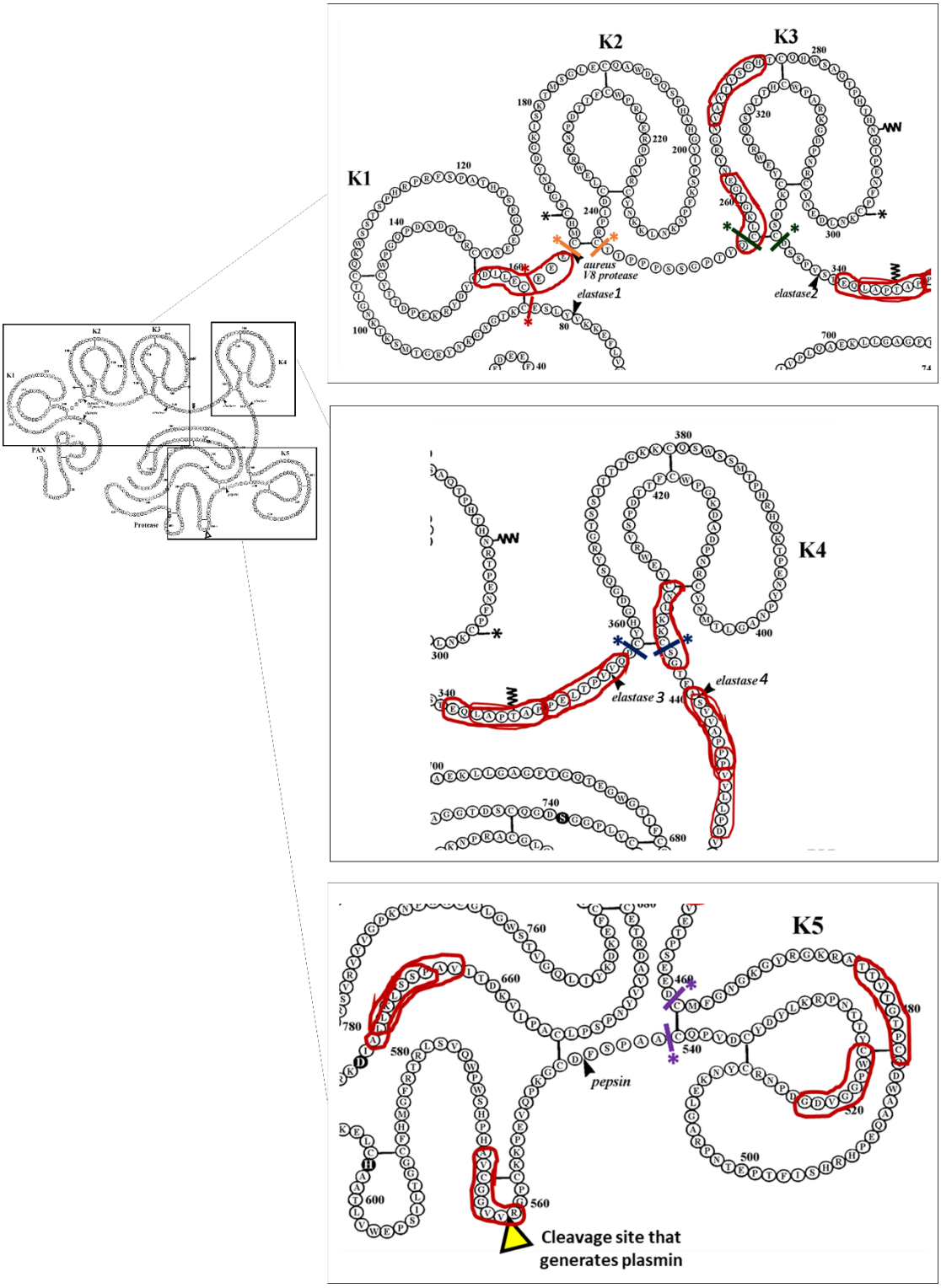

Figure 8-3: Top scored likely locations for cathepsin L cleaving plasminogen
Sites identified on plasminogen within kringle domains and near known protease cleavage sites (elastase, aureus V8 protease, pepsin, or cleavage site that generates plasmin).

Figure adapted from Soff et al. *Cancer and Metastasis Review*. 2000.

Table 8-2: Predicted plasminogen cleavage sites by cathepsin L from PACMANS

Location within Plasminogen	Plasminogen Sequence			Cumulative Score	Normalized Score
elastase 2	360	EQLAPTAP	367	2360	0.812
elastase 2	362	LAPTAPPE	369	2114	0.728
elastase 4	460	SVVAPPPV	467	2069	0.712
elastase 4	465	PPVVLLPD	472	2003	0.69
K1 & aureus V8 protease	177	DILECEEE	184	2260	0.776
K3	274	QCLKGTGE	281	2519	0.864
K3	287	VAVTVSGH	294	2026	0.698
K4	449	CNLKKCSG	456	1991	0.681
K4 & elastase 4	459	ASVVAPPP	466	2680	0.923
K5	536	GDVGGPWC	543	2076	0.715
K5	495	TTVTGTPC	502	2063	0.708
light chain	667	ALLKLSSP	674	2787	0.96
light chain	669	LKLSSPAV	676	2593	0.891
light chain	635	VILGAHQE	642	2508	0.862
plasmin generation cleavage site	580	RVVGGCVA	587	2066	0.709

8.3.3 Likelihood of plasminogen cleavage by cathepsin S

There were 6 top ranked PACMANS sequences in the kringle domains and 4 on the light chains for catS on plasminogen (Fig 8-4). Similar to catL, the highest score (0.996) of catS on plasminogen was at #667-674 ALLK/LSSP, located in the light chain of plasmin. Other light chain sequences included #714-721 GLLK/EAQL, #635-642 VILG/AHQE, and #669-676 LKLS/SPAV with scores of 0.924, 0.917, and 0.912, respectively. CatS also had a top scored sequence in the K1 domain at #177-184 DILE/CEEE, however it scored lower at 0.836. Similar to catK and catL, there were also top scores for catS cleavage on plasminogen near known elastase cleave sites. There was a top score at #360-367 (EQLA/PTAP) that was six residues away from elastase 2 (SSPV/STEQ) with a score of 0.844. Like catK, catS had a top score at #368-375 (PELT/PVVQ) that was three residues away from elastase 3 (LTPV/VQDC) with a score of 0.759. There was overlap of sequences near elastase 4: #459-466 (ASVV/APPP), #465-472 (PPVV/LLPD), and #460-467 (SVVA/PPPV) with a scores of 0.869, 0.763, and 0.734, respectively.

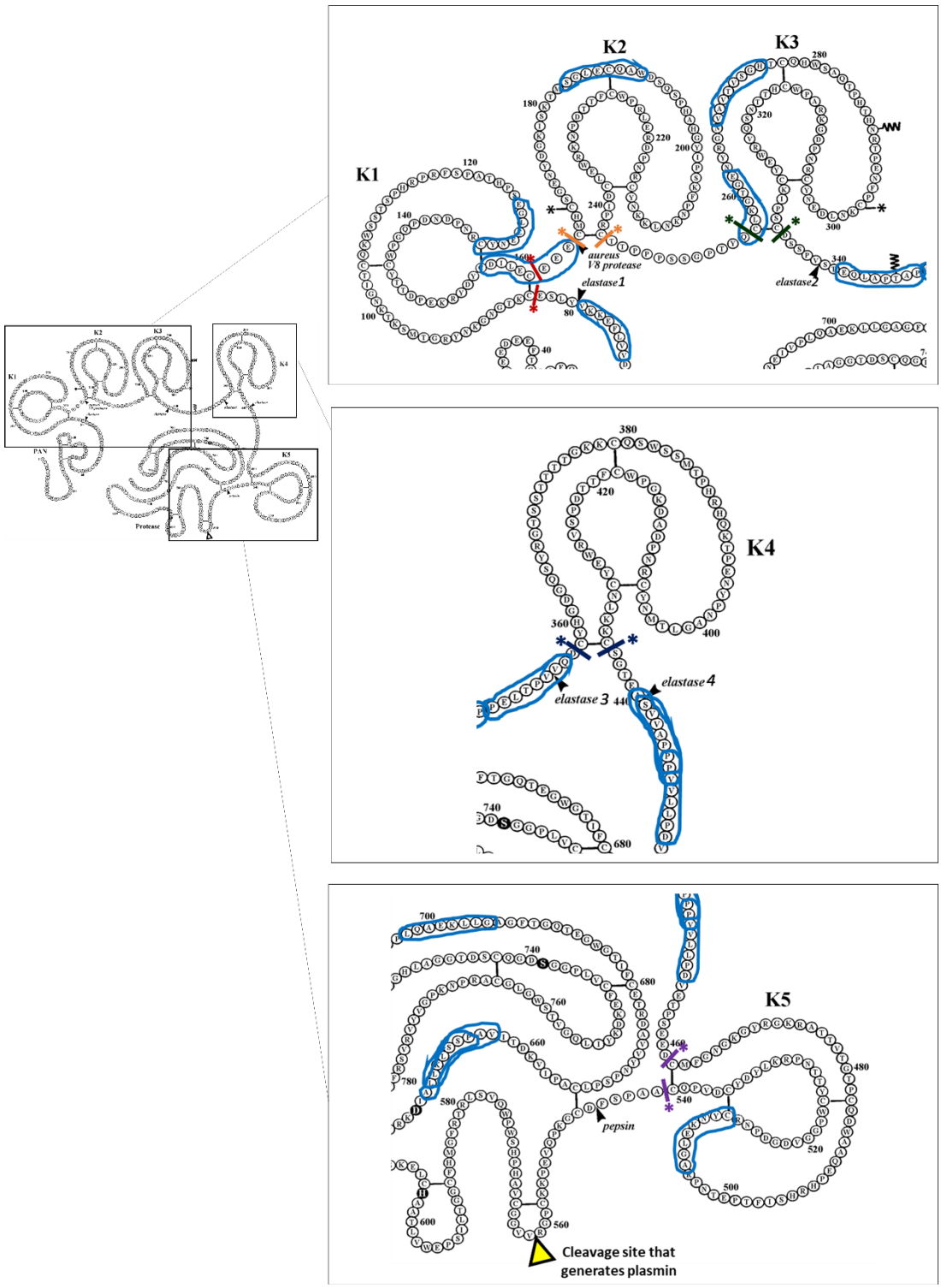

Figure 8-4: Top scored likely locations for cathepsin S cleaving plasminogen
Sites identified on plasminogen within kringle domains and near known protease cleavage sites (elastase, aureus V8 protease, pepsin, or cleavage site that generates plasmin).

Figure adapted from Soff et al. *Cancer and Metastasis Review*. 2000.

Table 8-3: Predicted plasminogen cleavage sites by cathepsin S from PACMANS

Location within Plasminogen	Plasminogen Sequence			Cumulative Score	Normalized Score
elastase 1	91	VVLFEKKV	98	2267	0.731
elastase 2	360	EQLAPTAP	367	2617	0.844
elastase 3	368	PELTPVVQ	375	2354	0.759
elastase 4	459	ASVVAPPP	466	2693	0.869
elastase 4	465	PPVVLLPD	472	2364	0.763
elastase 4	460	SVVAPPPV	467	2275	0.734
K1	145	EGLEENYC	152	2410	0.777
K1 & aureus V8 protease	177	DILECEEE	184	2595	0.836
K2	202	SGLECQAW	209	2327	0.75
K3	274	QCLKGTGE	281	2929	0.943
K3	287	VAVTVSGH	294	2483	0.8
K5	524	AGLEKNYC	531	2266	0.732
light chain	667	ALLKLSSP	674	3090	0.996
light chain	714	GLLKEAQL	721	2867	0.924
light chain	635	VILGAHQE	642	2847	0.917
light chain	669	LKLSSPAV	676	2831	0.912

8.3.4 Comparing plasminogen cleavage by cathepsins K, L, and S to cathepsin V

It has been previously reported that catV cleaves plasminogen and produces angiostatin-like products, unlike catK, L, and S [244, 245]. PACMANS identifies the putative site of a protease on a substrate, scoring the likelihood of a protease cleaving at a specific amino acid sequence. The higher the score, the more likely the cleavage event, and normalized scores allows for comparison between the different cathepsins on the same substrate [42, 246]. I hypothesized that the top score cleavage sites for catV on plasminogen would be higher than that of catK, L, and S on plasminogen. To test this, I ran PACMANS analysis with catV as the protease-ase and plasminogen as the substrate (Fig 8-5, Table 8-4) and compared it to the results for catK, L, or S (Appendix Table A-6). Interestingly, the highest score for catV was 0.914 at #667-674 ALLK/LSSP in the light chain; this sequence also overlapped with catK, L, and S with scores of 0.902, 0.96, and 0.996, respectively. Thus, catL and catS had higher scores than catV for this sequence. Another sequence that overlapped was #274-281 QCLK/GTGE where some of the scores were higher than catV; scores included 0.934 for catK, 0.864 for catL, 0.934 for catS, and 0.884 for catV. These scores are normalized so they could be compared between different cathepsins; the higher the score the higher the likelihood of cleavage at that site. The highest scores for catK, L, and S were 0.934, 0.96, and 0.996, respectively and all of these high scores overlapped with the highest scores for catV. These computational predictions suggest that further experiments are warranted to study the mechanisms behind plasminogen cleavage by cathepsins.

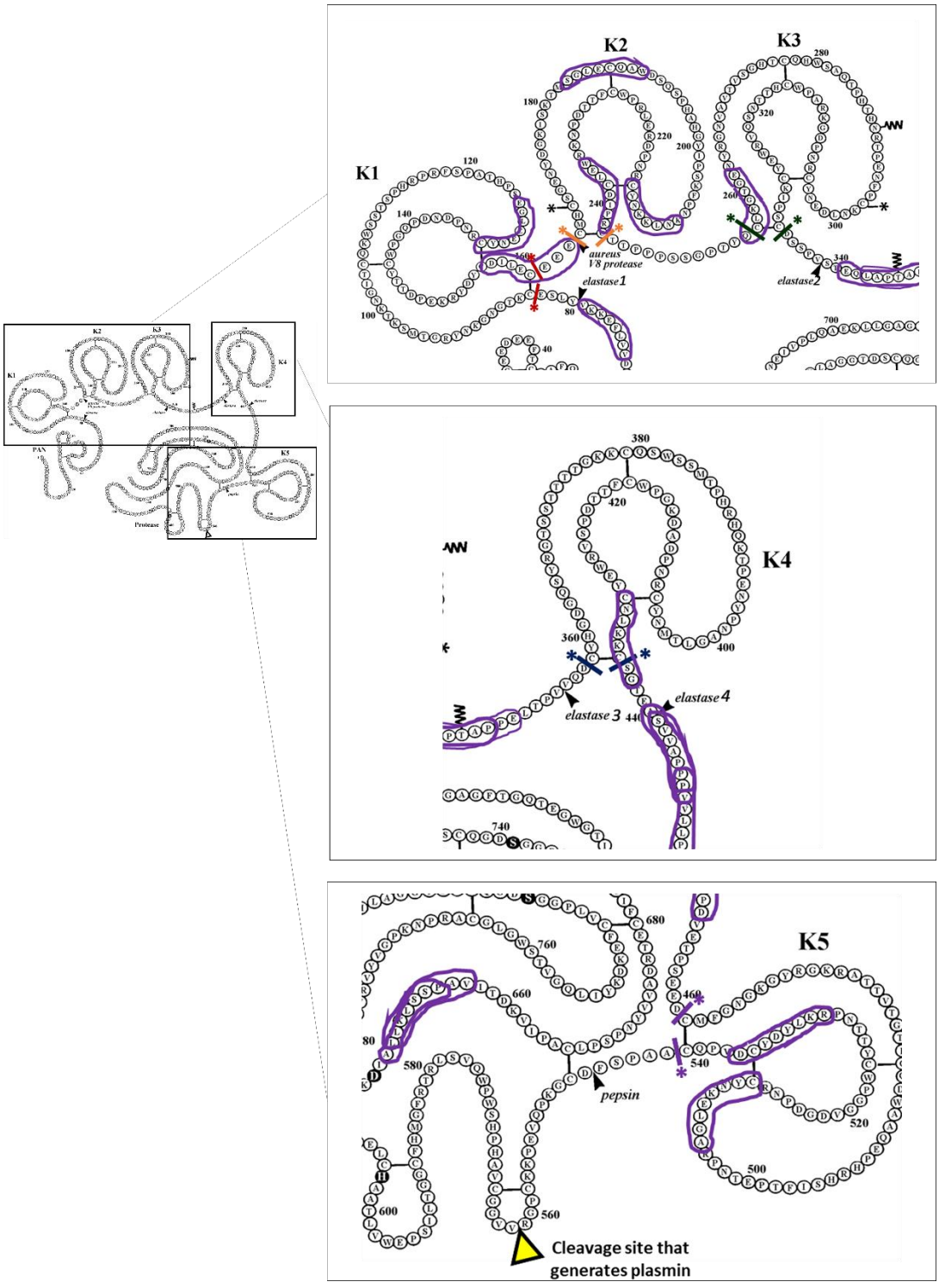

Figure 8-5: Top scored likely locations for cathepsin V cleaving plasminogen
Sites identified on plasminogen within kringle domains and near known protease cleavage sites (elastase, aureus V8 protease, pepsin, or cleavage site that generates plasmin).

Figure adapted from Soff et al. *Cancer and Metastasis Review*. 2000.

Table 8-4: Predicted plasminogen cleavage sites by cathepsin V from PACMANS

Location within Plasminogen	Plasminogen Sequence			Cumulative Score	Normalized Score
elastase1	91	VVLFEKKV	98	1203	0.728
elastase2	360	EQLAPTAP	367	1303	0.789
elastase2	362	LAPTAPPE	369	1231	0.746
elastase4	459	ASVVAPPP	466	1447	0.877
elastase4	460	SVVAPPPV	467	1159	0.702
elastase4	465	PPVVLLPD	472	1157	0.701
K1	145	EGLEENYC	152	1175	0.711
K1 & aureus V8 protease	177	DILECEEE	184	1405	0.851
K2	227	KNLKKNYC	234	1265	0.766
K2	254	WELCDIPR	261	1139	0.69
K2	202	SGLECQAW	209	1128	0.683
K3	274	QCLKGTGE	281	1460	0.884
K4	449	CNLKKCSG	456	1252	0.758
K5	524	AGLEKNYC	531	1234	0.747
K5	549	RKLYDYCD	556	1228	0.744
light chain	667	ALLKLSSP	674	1509	0.914
light chain	669	LKLSSPAV	676	1442	0.873

8.4 Discussion and Conclusion

Cleavage of plasminogen at various sites can generate angiostatin isoforms or angiostatin-related proteins forms. Plasmin is cleaved into two chains; the heavy chain that contains the kringle domains and light chain with catalytic domain that degrades fibrin. Here, I computationally analyzed the likelihood of cathepsins K, L, and S cleavage sites on plasminogen using bioinformatics cleavage site predictions. The sequences from the PACMANS analysis were then identified on plasminogen sequences with respect to the locations within kringle domains, light chains, and known cleavage sites for elastase.

Cysteine cathepsins showed preference for cleaving sequences within the kringle domains and had potential cleavage sites within two to six residues of known elastase cleavage sites on plasminogen. Cleavage at various sites within the kringle domain of plasminogen could release angiostatin-like products or isoforms [240, 243], and elastase cleaves plasminogen is an alternative pathway to generate angiostatin and inhibit fibrinolysis [248, 249]. I hypothesize that cathepsins could also cleave plasminogen and generate angiostatin-like products in a similar manner. It has been shown previously that catV does not produce active plasmin, rather it cleaves plasminogen producing fragments with anti-angiogenic properties, however, catK and catL do not degrade plasminogen [244]. The protocol co-incubated plasminogen and catK, L, or V for 1 hour using 30nM of catK or catL with 4.5μM of plasminogen. However, based on computational predictions, I would not completely rule out that catK, L, and S cannot hydrolyze plasminogen, especially considering catK, L, and S had higher top scores compared to catV (Appendix Table A-6). Future experiments could use isolated plasminogen and recombinant cathepsins in increasing concentrations and varying degradation time, to see if there is a threshold amount of cysteine cathepsins and time to degrade plasminogen. I propose this, because of evidence where low concentrations of papain can generate fibrin clots from fibrinogen, but higher concentrations degrade fibrin [195]. I hypothesize that catK, L, or S could cleave plasminogen within kringle domains, which could generate isoforms or

“kringle-like” domains, and new properties could emerge which could interfere with the naturally occurring coagulation factors.

CatK, L, and S also showed preferential cleavage in the light chain of plasminogen. The light chain of plasmin contains the catalytic domain that hydrolyzes fibrin. If cysteine cathepsins could degrade the light chain of plasmin, then plasmin would lose its fibrinolytic potential. This could be a problem as plasmin degrades fibrin into fibrin degradation products (FDP) which aid in angiogenesis, including pro-angiogenic factors that stimulate angiogenesis, such as fibrin E fragment. I hypothesize if plasmin is degraded by cysteine cathepsins, then plasmin-generated pro-angiogenic fibrin fragments are not produced; in other words, cathepsins can act indirectly to inhibit angiogenesis.

There were some overlapping sites with top scores where cathepsins K, L, or S could bind to plasminogen: DILE/CEEE (catK score 0.922, catL score 0.776, catS score 0.836), QCLK/GTGE (catK score 0.934, catL score 0.864, catS score 0.934), and EQLA/PTAP (catK score 0.771, catL score 0.812, catS score 0.844). There were also some overlapping sites between two cathepsins. These overlapping sites can be seen in the same image in Appendix A (Figure A-1 and Figure A-2). Overlapping sequences or redundancy in hydrolysis sites, highlights a property of cathepsins K, L, and , as they are known to have substrate specificity redundancies [2].

Future directions should include a more robust modeling approach using 3D molecular docking instead of the “manual” approach I used. Not only would there be more accuracy with identifying cleavage sites/sequences on plasminogen, but this would provide a better visualization of binding interactions, which could be cross analyzed with the PACMANS analysis. Further, molecular modeling could identify areas on plasminogen that are more difficult to access. However, I hypothesize that because the large kringle domains are loop structures protruding on the outside of plasminogen [241], cathepsins are more likely to bind to these sites, as predicted by PACMANS. Eventually work can move

into the wet lab, where cathepsins can degrade plasminogen, and their degradation products can be added to endothelial cell proliferation assays to see if generated sequences impair endothelial cell sprouting. This preliminary modeling work provides a foundation to continue to pursue modeling cathepsin-plasminogen binding sites and mechanisms more in depth.

CHAPTER 9 CONCLUSIONS AND FUTURE DIRECTIONS

9.1 Major Findings

The objective of this thesis was to study cathepsin-mediated fibrin(ogen)olysis to identify the roles cathepsins play in polymerization and degradation of fibrin. Cysteine cathepsins are collagenases and elastases [9, 50, 250], and for the first time I am showing that human cathepsin (cat) K, L, and S are fibrin (ogen)olytic proteases. Thrombin and plasmin, are the canonical proteases that cleave fibrinogen and degrade fibrin, respectively. Here, I studied the enzymology of cathepsins hydrolyzing fibrin(ogen) and placed it in the context of fibrin-based microvascular networks and abhorrent blood clotting mechanisms.

I questioned if cathepsins could degrade fibrin, driven by evidence that novel non-plasmin proteases could be involved in destabilization of fibrin-based constructs including biological robots [144] and microvascular networks [14, 15, 184]. My work provides insight into why these types of fibrin-based constructs collapse and fail, by proposing that cathepsin-mediated fibrinolysis mechanisms could be involved in degrading the fibrin in the matrix. For the first time, I have shown that human cat K, L, and S were fibrinolytic proteases and successively hydrolyze fibrin into smaller fragments, suggesting cathepsins had multiple cleavage sites on fibrin. Although the cathepsins are closely related, they had unique cleavage patterns and varying rates of fibrinolysis. CatS was the most fibrinolytic, compared to catK and catL. Interestingly, catL was bound to fibrin, demonstrating that fibrin is another substrate that can sustain the active life of cathepsins. These findings helped introduce a new class of proteases to the biomaterial community. Hydrolysis of fibrin by cathepsins and their mode of action properties must be considered when

developing fibrin-based constructs. Furthermore, this work has clinical implications for cathepsin based mechanisms underlying aberrant clotting mechanisms.

To understand the role of cathepsins in proteolysis and matrix remodeling during microvascular network development, I used a microfluidic model to perturb the network using flow and cathepsin inhibitors as a potential target to prolong vessel stability. Microvessels formed in a fibrin matrix with ECs and fibroblasts have a significant amount of catK and catL activity. These upregulated active cathepsins destabilize microvascular networks causing vessels to regress. Applying luminal unidirectional flow induces low shear which decreases active cathepsins and increases endogenous cystatin C inhibitor; a potential mechanism to help reduce upregulation proteolysis. Cat K, L, and S localized with ECs, associated with lumen on the apical and basal sides, as well as the fibroblasts which were present in the stromal area. Next, parts of the microfluidic network were assessed separately using an *in vitro* model through culturing ECs or fibroblasts on fibrin gels. Here, I identified that fibroblasts produced more cathepsins compared to ECs, corroborating increased co-localization of cathepsins with fibroblasts in stroma of microvascular networks. Further, this showed that fibrin is another substrate that can extend the activity of cathepsins over longer periods of time. In microvascular networks, fibrin in the matrix can serve as a bioactive reservoir sustaining activity of cathepsins over longer periods. If the cathepsins remain adsorbed to fibrin and continue to degrade fibrin, the cycle will continue. Fibrinolysis of the matrix cause destabilization and eventual construct failure. This observation has implications in other multi-cellular engineered living systems, such as the biological robots.

To determine the role cysteine cathepsins play in abnormal blood clotting, active cathepsins were quantified in the Townes humanized transgenic mouse model of wild type (AA), sickle trait (AS), and sickle cell anemic (SS) mice. I identified a significant increase in the amount of active cathepsins in SS mice as early as 1 month of age compared to AA and AS mice. Active cathepsins increased in plasma of SS mice from 1 to 3 months of age. This shows there was an age-related increase in cathepsins, which could contribute to accelerated damage in SCA. Male SS mice had increased active cathepsins compared to female mice. Seeing these sex-related differences mirrors what is seen clinically, where men have a higher severity of clinical complications compared to women; men have more episodes of sickle pain crisis and lower life expectancies compared to women [198, 251]. Perhaps different cathepsins activity levels can contribute to these sex-related differences in SCA.

The amount of circulating FpA, a marker of coagulation, was also quantified in AA, AS, and SS mice. Preliminary data showed that male mice at 3 months of age could have more FpA compared to female mice, however no differences in FpA were observed at 1 month. Cathepsins were fibrinogenolytic and released FpA, however, they cannot cleave FpA from fibrinogen and cause gelation of fibrin. Mice were injected with E-64 to inhibit cathepsins from cleaving circulating fibrinogen. After 2 months of treatment, active cathepsin levels were reduced, as well as circulating FpA in male mice. Together, this showed implications for SCA-induced cathepsin-mediated fibrinogenolysis.

9.2 Future Directions

9.2.1 Elucidate cathepsin-mediated fibrin(ogen)olysis mechanisms

Cathepsins K, L, and S degrade fibrin in unique ways compared to each other and plasmin. Future work could include sequencing sites of fibrin degraded by cathepsins compared to cathepsins cleaving fibrinogen to identify if there are any overlapping hydrolysis sites. Studies can also be done to assess dissociation and association constants of cathepsins with fibrin(ogen), to identify if cathepsins prefer to cleave fibrinogen or degrade fibrin. Distinguishing between these two mechanisms can elucidate if cathepsins can cleave FpA to cause fibrin gelation, as there was no gelation of fibrin in our studies using cathepsin.

There are limitations with my approach, for example, the amount of cathepsins was not varied to find optimal concentrations. Higher concentrations of papain degrade the fibrinogen; thus, a maximum concentration of 1ug/mL was used. My studies used 1ng/μL, so future directions should include working with serial concentrations of cathepsins K, L, and S to identify cleavage sites and characterize the fibrin structures formed.

9.2.2 Biomechanical and biochemical properties of cathepsins

My dissertation identified unique biomechanical regulatory properties of cathepsins using the microvasculature networks corroborating previous work about cathepsin mechanosensitive properties [6, 28, 152]. Although flow (~2Pa) increased total cathepsin L, it also increased cystatin C the endogenous inhibitor and reduced the amount of active cathepsins. In this case, flow served as a protective mechanism by reducing cathepsin activity. Cystatin C and cathepsins play a role in elastin degradation and atherosclerosis [26]. Future work can include using a bioreactor to induce shear stress on ECs or fibroblast

cultured on fibrin to see how the presence of fibrin affects cathepsin activity while underflow. Identifying cathepsin mechanism of sensitivity biomechanical properties of cathepsins could have implications in vascular remodeling.

9.2.3 Understand the role of cathepsins in vasculogenesis/angiogenesis

Active cathepsins were identified in microvascular networks, and their active was inhibited using biomechanical and biochemical approaches. There was also some preliminary evidence of using cathepsin inhibitors as an approach to prevent network regression (i.e.: decreased lumen diameter and vessel density). Future work could consider adding cathepsin inhibitors during earlier stages of development to see the role of cathepsins in initial stages of vascularization. There is already evidence that cathepsins are involved in vascular remodeling during wound healing [27, 29, 53, 252]. Using a microfluidic model for vascularization could be a way to identify putative roles of cathepsins in ECM remodeling during vascularization with applications in understanding uncontrolled vasculogenesis and angiogenesis in diseases.

Tip/stalk (sprouting) ECs can be derived from embryonic stem cells [169], and have increased active MMP-2 and cathepsin L compared to phalanx (non-sprouting) ECs. Knowing that cathepsins in endothelial cells are biomechanically regulated [28], these EC subtypes could be further characterized by using a bioreactor to see how laminar and oscillatory shear stress increases or decreases cathepsin and MMP expression and activity. Using a more proliferative EC phenotype would be better for studying vasculogenesis and angiogenesis, and the microfluidic device used to develop engineered microvascular networks is a good platform to study this. Biochemical and biomechanical properties can

be altered to study mechanisms of cathepsins in determining their role in the angiogenic switch in sprouting and non-sprouting ECs.

9.2.4 Control cathepsin-mediated fibrinolysis in fibrin-based constructs

One major finding is that catL adsorbs to fibrin. A study using *Fasciola hepatica* catL demonstrates that during clotting, there are interactions between catL and fibrinogen that are resistant to boiling even with SDS and mercaptoethanol present [12]. This appears to be a conserved mechanism of catL between different species and is worth exploring further. This interaction was demonstrated using recombinant proteases, as well as *in vitro* with endothelial cells and fibroblasts, which suggests it can occur in more complex systems, like microvascular networks. Fibrin serving as a substrate to sustain active cathepsins over extended periods of time can hinder the development of fibrin-based engineered constructs.

This is how I envision a bioactive reservoir is formed in microvascular networks and potentially other fibrin-based constructs: Engineers place cells in a fibrin-based matrix; remodeling will occur which is facilitated by proteases, including cathepsins, continually being secreted by these cells. Cathepsins will remodel the matrix creating lumen, but because fibrin is present their active lifetime is extended. Eventually, cathepsins will remodel the matrix to the point where the cathepsins start degrading the matrix, which causes the matrix to destabilize and eventually collapse, no longer able to support the lumen. Researchers now have a new class of proteases to consider inhibiting, aside from MMPs and plasmin, and I hope with the information collected, they will consider novel cathepsin inhibition strategies to help improve design for longevity.

Fibroblasts made more cathepsins compared to ECs, suggesting they are key producers of cathepsins in microvascular networks. Addition of stromal cells has been a proven strategy to improve microvessel architecture [15], so it would not be a good approach to reduce active cathepsins in these systems. Addition of flow increased cystatin C production, which bound to upregulated cathepsins and reduced its activity. To control proteolytic activity of microvascular networks over time, perhaps fibroblasts can be engineered using tetracycline systems to control expression of cystatins. The engineered fibroblasts can be combined with ECs and fibrin in a microfluidic device where tetracycline free media can be used during initial development period then switched to tetracycline growth media to induce cystatin C production until the tetracycline is depleted. This will give engineers more control over proteases in systems, similar to how other design parameters are used to control network architecture (i.e.: using stromal cells for paracrine signaling to increase branching).

One of the goals I initially set was preventing microvessel regression in microvascular networks to improve their longevity, but chose to focus on quantifying cathepsin activity in microvascular networks. Regenerative medicine's promise of replacement tissue and organ development has been challenged by lack of vascularization, as required for thick, complex tissues to overcome diffusional transport limitations [91, 93]. Pre-vascularization using microfluidic systems may be one strategy for generating more complex, highly organized microvascular networks. These systems are advantageous for generating microvessels *in vitro*, allowing for their development and maintenance within a controlled environment [100-102, 176]. These microvessels are easily maintained, but show regression [14, 15], as characterized by decreased microvessel diameter, number

of perfusable branches, and vessel density, following several weeks in culture. There were preliminary results adding E-64 to microvascular networks for 48 hours- it was observed that vessel diameter was preserved in microvascular networks with cystatin C or E-64 added, with little decrease in microvessel density. This is exciting, as I might have identified a novel approach using cathepsin inhibitors to prevent regression which can help maintain *in vitro* vessels for prolonged periods of growth in the future, something the fields of tissue engineering can benefit from.

9.2.5 Elucidate the role of human cysteine cathepsins in the coagulation cascade

There is clinical relevance for cathepsin-mediated fibrin(ogen)olysis in the coagulation cascade after vessel injury. The proteases thrombin and plasmin are considered responsible for the initiation and degradation of fibrin, respectively, However, this work shows cysteine cathepsins should be studied especially because cysteine cathepsins are known to be involved in other vascular related injuries and vascular remodeling [2, 24, 83, 143, 151, 153, 181, 252-254]. My thesis has some foundational evidence for the roles of cysteine cathepsins in the coagulation cascade. I should acknowledge the limitation with my studies is that I looked at one aspect of the coagulation cascade. Figure 9-1 illustrates additonal parts in the coagulation cascade that lead up to fibrinogen cleavage, including inhibitors which block the cascade.

In the sickle cell disease model I hypothesized that increased plasma levels of FpA in SCD is due to cysteine cathepsin cleaving fibrinogen. This case studies cathepsins serving only as a procoagulant, which is a limited scope considering the complexity of the coagulation cascade. Studies focused on cathepsin G, a serine protease, in the neutrophils which are involved in thrombosis response. Interestingly, cathepsin G served as both a pro-

and anti-coagulant during the same thrombin generation time course [255]. It is possible cathepsins K, L, or S could cleave or degrade other factors in the coagulation cascade, serving as a pro- and/or anti-coagulant. Our work showed that there is an increased amount of active cathepsins circulating in plasma under sickle cell anemia conditions, and they can be acting on any substrates (i.e.: factor X or thrombin-antithrombin) present. Even the proteases, thrombin or plasmin, could be substrates for cathepsins, which would inhibit fibrin formation and degradation. As an example, plasminogen as a substrate for cathepsin cleavage was explored briefly in Chapter 8. Cathepsins could hinder aspects of fibrin formation or fibrin degradation directly or indirectly. Direct mechanisms are defined as cathepsins cleaving fibrinogen or degrading fibrin; both of which were studied using recombinant proteases in Chapters 3 and 5. Indirect mechanisms for fibrin formation could include cathepsins degrading natural anticoagulants.

Prothrombin time, a measure of how long it takes for blood to clot which can indicate if abnormal clotting is occurring, is elevated in sickle cell anemia [31, 116, 256]. Elevated prothrombin times mean blood is taking longer to clot. This led me to hypothesize that cathepsins are competing with existing proteases in the coagulation cascade (Fig 9-1A), rather than working together. One would assume the opposite is happening- more proteases means faster clotting times. However, our lab has shown that because more proteases are present, does not mean their effects are additive [257]. In other words, if two or more cathepsins are in the presence of the same substrate, simultaneously, it does not mean more substrate will be degraded. Cathepsins could be blocking the "normal coagulation proteases", thus slowing the clotting process down.

Cathepsins have been shown to be produced and secreted by endothelial cells that line the blood vessel [28]. With cathepsins in close proximity to access the clots, the roles of cysteine cathepsins and their putative activity to degrade clots should be considered in physiological and pathophysiological conditions. Plasmin degrades fibrin into two main fragments, D-dimer and fibrin E fragment, and cells with higher levels of fibrin degradation products (FDP) are at the front or leading of wounds and aortic atherosclerotic plaques during invasion [258]. FDPs aid angiogenesis; specifically, fibrin E fragment is a pro-angiogenic factor that stimulates angiogenesis in wounds and plaque development [259], and has also been shown to stimulate proliferation, migration, and differentiation of microvascular ECs [260]. Cathepsins K, L, and S produce different banding patterns compared to plasmin, suggesting that cathepsins cleave fibrin at different sites compared to plasmin; this was discussed in Chapter 3. I hypothesize that if cathepsins compete with plasmin and cleave fibrin (Fig 9-1B), cathepsins will not produce FDPs that are pro-angiogenic (i.e.: fibrin E fragment) and hinder angiogenesis during wound healing.

There is also clinical evidence of depletion of natural anticoagulants, protein C and protein, which work together to inhibit conversion of prothrombin to thrombin. [116, 193, 261, 262]. Without inhibition, thrombin is continually produced, which cleaves fibrinogen and contributes to chronic coagulation conditions seen in sickle cell disease. Currently, the mechanisms of lowered protein C and protein S are unknown [262], and can be pursued in a future study. The underlying disease conditions of SCA upregulates cathepsins, which could degrade protein C and protein S, reducing their circulating levels (Fig 9-1C).

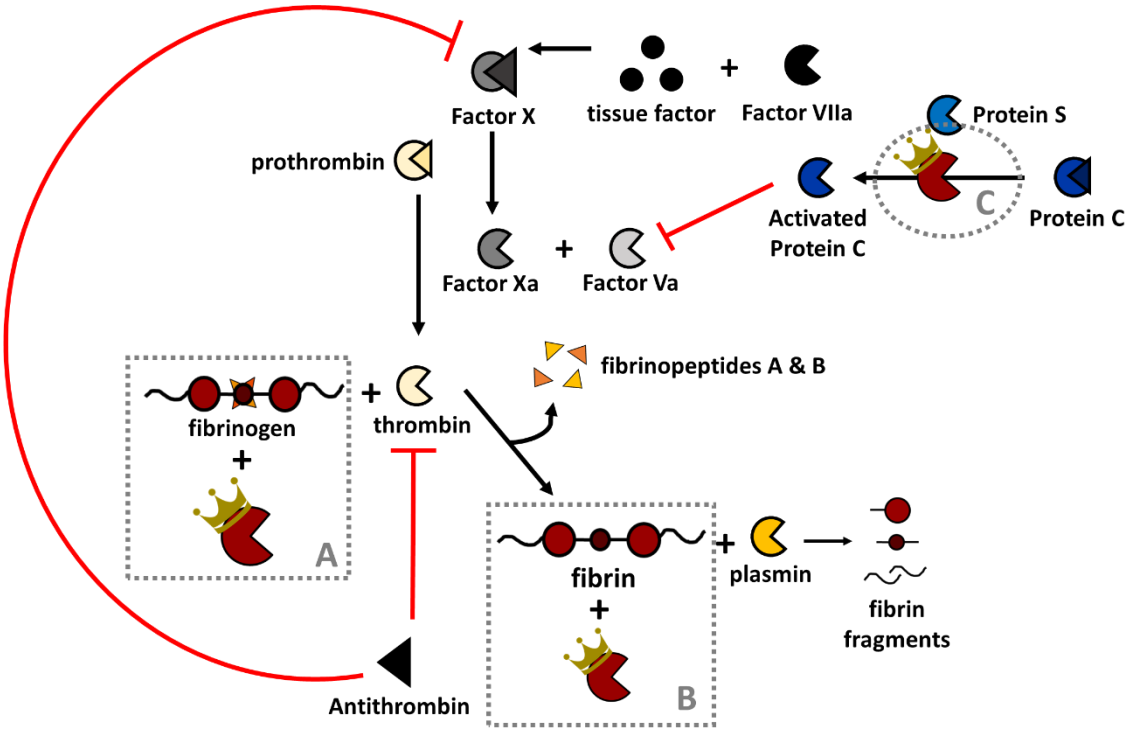

Figure 9-1: Future considerations for cysteine cathepsins in the coagulation cascade
This schematic illustrates possible locations cathepsins (represented by the red PACMEN) where cathepsins could perturb the coagulation cascade based on clinical findings. **(A)** People with SCA have increased prothrombin time, which means it takes longer for their blood to coagulate; I hypothesize that there is competition between cathepsins and canonical coagulation proteases on fibrinogen Cathepsins could be blocking the "normal coagulation proteases" which slows the clotting process. **(B)** Plasmin is the canonical enzyme that degrades fibrin into fibrin fragments that contain pro-angiogenic properties**.** However, if cysteine cathepsins degrade fibrin at different sites and generate fibrin degradation products that impair angiogenesis during wound healing. **(C)** Clinically, people with SCA present with lower amounts of anticoagulants, protein C and protein S. I hypothesize that cysteine cathepsins can degrade these anticoagulants, and thus clots are not resolved which drives chronic coagulation activation.

This is a unique opportunity to study cathepsin plasma levels by treating mice with anticoagulants or inhibitors for tissue factor, prothrombin/thrombin, factor X etc. or cross breeding cathepsin deficient mice with some of the mouse models discussed in Section 2.4.5 of the literature review (i.e.: fibrinogen deficient, protease active receptor (PAR) -1 and -2 (thrombin receptors). Blood could also be taken from the SCD mouse models, and their coagulation factors could be depleted from their plasma. Then the plasma can be spiked with increasing amounts of cathepsins, and clotting can be assessed to see if cathepsins serve as pro- or anti-coagulants.

A question yet to be answered is identifying which cell types are secreting the cathepsins. Past work in the lab has identified cathepsins in the arteries of SS mice [89], suggesting that ECs could secrete cathepsins basally, into the artery wall. This work quantified the amount of active cathepsins in plasma, suggesting that cathepsins are also being secreted from ECs on the apical side into the lumen. Also, SS PBMCs induce active cathepsins in endothelial cells [40]. To understand the role of the monocytes, sickle mice can be treated with clodronate liposomes to deplete monocytes. An approach to understand the role of ECs, could include creating a sickle cell mouse with EC-specific deletion of a cathepsin gene. Also, bone marrow transplants (BMT) can be used, where bone marrow containing hematopoietic stem cells, can be transplanted from SS mice into catK KO mice. These mice would contain SS RBCs and myeloid cells (monocytes/macrophages) and resident catK KO ECs, and if active cathepsins are identified in the plasma this would suggest the source of the cathepsins are from PBMCs. The model could also be flipped where bone marrow from catK KO mice are transplanted into SS mice. These BMT models would also have clinical relevance, as bone marrow transplants are used for treatments with

people with sickle cell anemia have seen success with disease-free and overall survival rates of 85% and 97%, respectively [263]. BMTs as a treatment option for many patients is limiting as it is hard to find donor matches [264], however, BMT experiments could be leveraged to provide answers to understanding cathepsins role in SCA.

9.2.6 SCA treatment approaches with cathepsin inhibitors

In the humanized Towne's model, cathepsins are biomarkers that can be pharmacological targets, with their plasma levels reduced by using E-64. Anticoagulant approaches to reduce vaso-occlusion and chronic coagulation activation have not been very successful, particularly because of bleeding complications [129, 130]. By targeting the cathepsins as a treatment strategy, there is no reduction in natural coagulants, thus bleeding and hemorrhagic risks are lowered. This could have broader impacts for eliminating use of anticoagulants for treatment of other blood disorders.

9.2.7 Correlating cathepsins and coagulation markers in Townes sickle mice

Another idea that was not fully explored in my dissertation was looking at additional coagulation markers with our SCD mouse model, aside from quantifying FpA. Future work should consider correlating active cathepsins with other markers of coagulation action activation, such as TAT, D-dimers, protein C, and protein S. To see if there is any relation between active cathepsins before and after sickle pain crisis, mice can be placed in a deoxygenation chamber to simulate pain crisis condition, with blood collected/plasma isolated immediately before and after. These experiments could also be done with the cathepsin deficient mouse with sickle cell disease mouse to further elucidate the role of cathepsins in blood clotting mechanisms.

9.2.8 Sex as a basis for variability in future studies

A noteworthy finding in this dissertation was male and female differences in active cathepsins in SS mice. Sex differences exist in cardiovascular diseases [265, 266]. Lorenz et al. [267] did whole genome expression analysis in HUVECs subjected to shear, and compared gene transcription levels between males and females. Female HUVECs had more of a transcription response compared to male HUVECs, where numerous genes were regulated in the opposite direction, demonstrating sexual dimorphisms in gene expression in ECs could contribute to differences in EC function. Moreover, our studies and this work demonstrates the importance of differentiating between male and female for *in vitro* and *in vivo* research. This can help us understand why there are differences in how SCD and other cardiovascular related disease manifest itself in men versus women.

APPENDIX A. FULL PACMANS TOP SCORING TABLES FOR CATHEPSIN ON PLASMINOGEN

The following tables are the top 5% of PACMANS scores for plasminogen cleaved by cathepsins K (Table A-1), L (Table A-2), S (Table A-3), and V (Table A-4).

The kringle domains (K1, K2, K3, K4, and K5) amino acid sequences were determined based on an image in Figure 8-1 (denoted by the colored lines and circles). Known cleavage sites for elastase, aureus V8 protease, and cleavage site that generates plasmin were also determined from the plasminogen figure (circled in black in Figure 8-1). Figure 8-1 is missing the first 20 amino acid sequences, and the sequence numbers used in PACMAN align with the sites/numbers for the plasminogen site sequence in Uniprot; Table 8-1 denotes these differences, which was used for the analysis.

TABLE A-1. Sequences for Kringle Domain and Known Protease Cleave Sites

Kringle Domain / Known Protease Cleavage Sites	Figure 8-1 Sequence	Aligned PACMANs Sequence (AA sequence from Uniprot)
K1	84 – 163	104 – 183
K2	165 – 265	185 – 265
K3	255 - 335	275 - 355
K4	357 - 436	377 - 456
K5	461 - 541	481 - 561
elastase 1	76 - 83	96 - 103
aureus V8 protease	162 - 169	182 - 189
elastase 2	335 - 342	355 - 362
elastase 3	351 - 358	371 - 378
elastase 4	437 - 445	457 - 465
pepsin	542 - 549	562 - 569
cleavage site that generates plasmin	558 - 566	578 - 586

TABLE A-2. Top 5% of PACMANS predicted plasminogen cleavages sites by cathepsin K

Location within Plasminogen	Plasminogen Sequence			Cumulative Score	Normalized Score
K3	274	QCLKGTGE	281	2052	0.934
K1 & aureus V8 protease	177	DILECEEE	184	2026	0.922
light chain	667	ALLKLSSP	674	1980	0.902
light chain	747	GHLAGGTD	754	1979	0.901
light chain	713	AGLLKEAQ	720	1953	0.891
light chain	714	GLLKEAQL	721	1909	0.869
light chain	635	VILGAHQE	642	1878	0.855
light chain	669	LKLSSPAV	676	1866	0.85
---	39	KQLGAGSI	46	1859	0.847
K1	145	EGLEENYC	152	1848	0.842
---	467	VVLLPDVE	474	1838	0.837
K5	549	RKLYDYCD	556	1834	0.836
K5	524	AGLEKNYC	531	1833	0.836
---	12	LFLKSGQG	19	1822	0.829
K2	227	KNLKKNYC	234	1796	0.818
light chain	780	WGLGCARP	787	1731	0.787
light chain	596	VSLRTRFG	603	1711	0.779
elastase 2	360	EQLAPTAP	367	1693	0.771
K4	419	AGLTMNYC	426	1688	0.77
---	51	AKCEEDEE	58	1678	0.767
elastase 1	91	VVLFEKKV	98	1675	0.763
light chain	655	SRLFLEPT	662	1667	0.76
light chain	733	EFLNGRVQ	740	1654	0.754
---	468	VLLPDVET	475	1653	0.753
K4	449	CNLKKCSG	456	1629	0.74
light chain	719	AQLPVIEN	726	1628	0.742
K2	202	SGLECQAW	209	1621	0.738
elastase 3	368	PELTPVVQ	375	1616	0.735
---	31	ASLFSVTK	38	1611	0.735
light chain	772	YILQGVTS	779	1609	0.732
light chain	622	HCLEKSPR	629	1607	0.731
K1 & elastase 1	98	VYLSECKT	105	1605	0.731
---	20	EPLDDYVN	27	1579	0.719
K3	317	KNLDENYC	324	1578	0.719
light chain	657	LFLEPTRK	664	1575	0.717
K5	546	ANPRKLYD	553	1558	0.711
light chain	616	WVLTAAHC	623	1555	0.707
light chain	609	GTLISPEW	616	1552	0.707
light chain	666	IALLKLSS	673	1545	0.703
---	10	LLLFLKSG	17	1545	0.704

TABLE A-3. Top 5% of PACMANS predicted plasminogen cleavages sites by cathepsin L

Location within Plasminogen	Plasminogen Sequence			Cumulative Score	Normalized Score
light chain	667	ALLKLSSP	674	2787	0.96
K4	459	ASVVAPPP	466	2680	0.923
light chain	669	LKLSSPAV	676	2593	0.891
K3	274	QCLKGTGE	281	2519	0.864
light chain	635	VILGAHQE	642	2508	0.862
light chain	747	GHLAGGTD	754	2504	0.862
light chain	714	GLLKEAQL	721	2491	0.858
---	39	KQLGAGSI	46	2440	0.839
---	12	LFLKSGQG	19	2385	0.819
light chain	780	WGLGCARP	787	2369	0.811
elastase 2	360	EQLAPTAP	367	2360	0.812
light chain	713	AGLLKEAQ	720	2333	0.804
K1 & aureus V8 protease	177	DILECEEE	184	2260	0.776
light chain	609	GTLISPEW	616	2193	0.756
---	471	PDVETPSE	478	2190	0.753
light chain	655	SRLFLEPT	662	2140	0.736
light chain	737	GRVQSTEL	744	2118	0.73
elastase 2	362	LAPTAPPE	369	2114	0.728
light chain	763	PLVCFEKD	770	2103	0.725
---	10	LLLFLKSG	17	2091	0.72
light chain	772	YILQGVTS	779	2078	0.712
K5	536	GDVGGPWC	543	2076	0.715
elastase 4	460	SVVAPPPV	467	2069	0.712
plasmin generation cleavage site	580	RVVGGCVA	587	2066	0.709
---	468	VLLPDVET	475	2064	0.711
K5	495	TTVTGTPC	502	2063	0.708
---	467	VVLLPDVE	474	2038	0.702
---	31	ASLFSVTK	38	2037	0.703
light chain	709	GTFGAGLL	716	2029	0.7
K3	287	VAVTVSGH	294	2026	0.698
light chain	775	QGVTSWGL	782	2024	0.696
light chain	596	VSLRTRFG	603	2008	0.691
light chain	623	CLEKSPRP	630	2006	0.688
light chain	616	WVLTAAHC	623	2005	0.686
elastase 4	465	PPVVLLPD	472	2003	0.69
light chain	622	HCLEKSPR	629	2002	0.686
K4	449	CNLKKCSG	456	1991	0.681
light chain	733	EFLNGRVQ	740	1976	0.68
light chain	684	ACLPSPNY	691	1975	0.681
light chain	666	IALLKLSS	673	1970	0.677

TABLE A-4. Top 5% of PACMANS predicted plasminogen cleavages sites by cathepsin S

Location within Plasminogen	Plasminogen Sequence			Cumulative Score	Normalized Score
light chain	667	ALLKLSSP	674	3090	0.996
K3	274	QCLKGTGE	281	2929	0.943
light chain	714	GLLKEAQL	721	2867	0.924
light chain	635	VILGAHQE	642	2847	0.917
light chain	669	LKLSSPAV	676	2831	0.912
---	39	KQLGAGSI	46	2771	0.892
---	12	LFLKSGQG	19	2739	0.882
light chain	747	GHLAGGTD	754	2725	0.878
elastase 4	459	ASVVAPPP	466	2693	0.869
light chain	780	WGLGCARP	787	2648	0.851
elastase 2	360	EQLAPTAP	367	2617	0.844
light chain	713	AGLLKEAQ	720	2604	0.84
K1	177	DILECEEE	184	2595	0.836
light chain	655	SRLFLEPT	662	2568	0.828
light chain	616	WVLTAAHC	623	2533	0.814
K3	287	VAVTVSGH	294	2483	0.8
---	10	LLLFLKSG	17	2428	0.782
---	467	VVLLPDVE	474	2417	0.779
K1	145	EGLEENYC	152	2410	0.777
---	466	PVVLLPDV	473	2408	0.777
---	471	PDVETPSE	478	2403	0.775
---	31	ASLFSVTK	38	2402	0.775
light chain	737	GRVQSTEL	744	2392	0.772
light chain	622	HCLEKSPR	629	2385	0.767
light chain	609	GTLISPEW	616	2379	0.768
---	8	LLLLLFLK	15	2379	0.767
light chain	772	YILQGVTS	779	2375	0.764
light chain	775	QGVTSWGL	782	2369	0.764
elastase 4	465	PPVVLLPD	472	2364	0.763
---	7	VLLLLLFL	14	2364	0.762
light chain	742	TELCAGHL	749	2363	0.761
elastase 3	368	PELTPVVQ	375	2354	0.759
light chain	596	VSLRTRFG	603	2336	0.753
K2	202	SGLECQAW	209	2327	0.75
light chain	733	EFLNGRVQ	740	2281	0.736
---	6	VVLLLLLF	13	2280	0.735
elastase 4	460	SVVAPPPV	467	2275	0.734
---	468	VLLPDVET	475	2274	0.733
elastase 1	91	VVLFEKKV	98	2267	0.731
K5	524	AGLEKNYC	531	2266	0.732

TABLE A-5. Top 5% of PACMANS predicted plasminogen cleavages sites by cathepsin V

Location within Plasminogen	Plasminogen Sequence			Cumulative Score	Normalized Score
light chain	667	ALLKLSSP	674	1509	0.914
K3	274	QCLKGTGE	281	1460	0.884
elastase 4	459	ASVVAPPP	466	1447	0.877
light chain	669	LKLSSPAV	676	1442	0.873
K1 & aureus V8 protease	177	DILECEEE	184	1405	0.851
light chain	747	GHLAGGTD	754	1403	0.85
light chain	635	VILGAHQE	642	1402	0.849
light chain	713	AGLLKEAQ	720	1400	0.848
---	12	LFLKSGQG	19	1378	0.834
light chain	714	GLLKEAQL	721	1365	0.826
---	39	KQLGAGSI	46	1365	0.826
elastase 2	360	EQLAPTAP	367	1303	0.789
light chain	609	GTLISPEW	616	1286	0.779
light chain	655	SRLFLEPT	662	1285	0.778
light chain	622	HCLEKSPR	629	1283	0.777
---	471	PDVETPSE	478	1273	0.771
light chain	780	WGLGCARP	787	1269	0.768
K2	227	KNLKKNYC	234	1265	0.766
light chain	596	VSLRTRFG	603	1261	0.763
K4	449	CNLKKCSG	456	1252	0.758
---	10	LLLFLKSG	17	1243	0.753
K5	524	AGLEKNYC	531	1234	0.747
light chain	666	IALLKLSS	673	1231	0.745
elastase 2	362	LAPTAPPE	369	1231	0.746
K5	549	RKLYDYCD	556	1228	0.744
---	467	VVLLPDVE	474	1223	0.741
---	468	VLLPDVET	475	1213	0.735
---	31	ASLFSVTK	38	1204	0.729
elastase 1	91	VVLFEKKV	98	1203	0.728
K1	145	EGLEENYC	152	1175	0.711
elastase 4	460	SVVAPPPV	467	1159	0.702
elastase 4	465	PPVVLLPD	472	1157	0.701
light chain	763	PLVCFEKD	770	1156	0.7
light chain	733	EFLNGRVQ	740	1152	0.698
K2	254	WELCDIPR	261	1139	0.69
light chain	719	AQLPVIEN	726	1138	0.689
light chain	742	TELCAGHL	749	1137	0.688
light chain	772	YILQGVTS	779	1137	0.688
light chain	684	ACLPSPNY	691	1129	0.684
K2	202	SGLECQAW	209	1128	0.683

TABLE A-6. PACMANS top scored plasminogen cleavage sites by cathepsins K, L, S or V

Cathepsin	Location within Plasminogen	Plasminogen Sequence			Cumulative Score	Normalized Score
S	light chain	667	ALLKLSSP	674	3090	0.996
L	light chain	667	ALLKLSSP	674	2787	0.96
S	K3	274	QCLKGTGE	281	2929	0.943
K	K3	274	QCLKGTGE	281	2052	0.934
S	light chain	714	GLLKEAQL	721	2867	0.924
L	K4 & elastase 4	459	ASVVAPPP	466	2680	0.923
K	K1 & aureus V8 protease	177	DILECEEE	184	2026	0.922
S	light chain	635	VILGAHQE	642	2847	0.917
V	light chain	667	ALLKLSSP	674	1509	0.914
S	light chain	669	LKLSSPAV	676	2831	0.912
K	light chain	667	ALLKLSSP	674	1980	0.902
K	light chain	747	GHLAGGTD	754	1979	0.901
L	light chain	669	LKLSSPAV	676	2593	0.891
K	light chain	713	AGLLKEAQ	720	1953	0.891
V	K3	274	QCLKGTGE	281	1460	0.884
V	elastase4	459	ASVVAPPP	466	1447	0.877
V	light chain	669	LKLSSPAV	676	1442	0.873
S	elastase 4	459	ASVVAPPP	466	2693	0.869
L	K3	274	QCLKGTGE	281	2519	0.864
L	light chain	635	VILGAHQE	642	2508	0.862
V	K1 & aureus V8 protease	177	DILECEEE	184	1405	0.851
S	elastase 2	360	EQLAPTAP	367	2617	0.844
K	K1	145	EGLEENYC	152	1848	0.842
S	K1 & aureus V8 protease	177	DILECEEE	184	2595	0.836
K	K5	549	RKLYDYCD	556	1834	0.836
K	K5	524	AGLEKNYC	531	1833	0.836
K	K2	227	KNLKKNYC	234	1796	0.818
L	elastase 2	360	EQLAPTAP	367	2360	0.812
S	K3	287	VAVTVSGH	294	2483	0.8
V	elastase2	360	EQLAPTAP	367	1303	0.789
S	K1	145	EGLEENYC	152	2410	0.777
L	K1 & aureus V8 protease	177	DILECEEE	184	2260	0.776
K	elastase 2	360	EQLAPTAP	367	1693	0.771
K	K4	419	AGLTMNYC	426	1688	0.77
V	K2	227	KNLKKNYC	234	1265	0.766
S	elastase 4	465	PPVVLLPD	472	2364	0.763
K	elastase 1	91	VVLFEKKV	98	1675	0.763
S	elastase 3	368	PELTPVVQ	375	2354	0.759
V	K4	449	CNLKKCSG	456	1252	0.758
S	K2	202	SGLECQAW	209	2327	0.75
V	K5	524	AGLEKNYC	531	1234	0.747
V	elastase2	362	LAPTAPPE	369	1231	0.746
V	K5	549	RKLYDYCD	556	1228	0.744
K	K4	449	CNLKKCSG	456	1629	0.74
K	K2	202	SGLECQAW	209	1621	0.738
K	elastase 3	368	PELTPVVQ	375	1616	0.735
S	elastase 4	460	SVVAPPPV	467	2275	0.734
S	K5	524	AGLEKNYC	531	2266	0.732
S	elastase 1	91	VVLFEKKV	98	2267	0.731
K	K1 & elastase 1	98	VYLSECKT	105	1605	0.731
V	elastase1	91	VVLFEKKV	98	1203	0.728
L	elastase 2	362	LAPTAPPE	369	2114	0.728
K	K3	317	KNLDENYC	324	1578	0.719
L	K5	536	GDVGGPWC	543	2076	0.715
L	elastase 4	460	SVVAPPPV	467	2069	0.712
V	K1	145	EGLEENYC	152	1175	0.711
K	K5	546	ANPRKLYD	553	1558	0.711
L	plasmin cleavage site	580	RVVGGCVA	587	2066	0.709
L	K5	495	TTVTGTPC	502	2063	0.708
V	elastase4	460	SVVAPPPV	467	1159	0.702
V	elastase4	465	PPVVLLPD	472	1157	0.701
L	K3	287	VAVTVSGH	294	2026	0.698
V	K2	254	WELCDIPR	261	1139	0.69
L	elastase 4	465	PPVVLLPD	472	2003	0.69
V	K2	202	SGLECQAW	209	1128	0.683
L	K4	449	CNLKKCSG	456	1991	0.681

REFERENCES

1. Brix, K., et al., *Cysteine cathepsins: Cellular roadmap to different functions.* 2008. **90**(2): p. 194-207.
2. Turk, V., et al., *Cysteine cathepsins: From structure, function and regulation to new frontiers.* Biochimica et Biophysica Acta (BBA) - Proteins and Proteomics, 2012. **1824**(1): p. 68-88.
3. Reiser, J., B. Adair, and T. Reinheckel, *Specialized roles for cysteine cathepsins in health and disease.* J Clin Invest, 2010. **120**(10): p. 3421-31.
4. Sukhova, G.K., et al., *Deficiency of cathepsin S reduces atherosclerosis in LDL receptor-deficient mice.* Journal of Clinical Investigation, 2003.
5. Sloane, M.M.M. and F. Bonnie, *Cysteine cathepsins: multifunctional enzymes in cancer.* Nature Reviews Cancer, 2006. **6**(10): p. 764-75.
6. Platt, M.O., et al., *Expression of cathepsin K is regulated by shear stress in cultured endothelial cells and is increased in endothelium in human atherosclerosis.* 2006. **292**(3): p. H1479-H1486.
7. Chapman, H.A., R.J. Riese, and G.-P. Shi, *Emerging Roles For Cysteine Proteases in Human Biology.* 1997. **59**(1): p. 63-88.
8. Seto, S.P., et al., *Cathepsins in Rotator Cuff Tendinopathy: Identification in Human Chronic Tears and Temporal Induction in a Rat Model.* Annals of biomedical engineering, 2015. **43**(9): p. 2036-2046.
9. Garnero, P., et al., *The Collagenolytic Activity of Cathepsin K Is Unique among Mammalian Proteinases.* 1998. **273**(48): p. 32347-32352.
10. Simon, D., A. Ezratty, and J. Loscalzo, *The fibrin(ogen)olytic properties of cathepsin D.* Biochemistry, 1994. **33**(21): p. 6555-6563.
11. Simon, D., et al., *Fibrin(ogen) is internalized and degraded by activated human monocytoid cells via Mac-1 (CD11b/CD18): a nonplasmin fibrinolytic.* Blood, 1993. **82**(8): p. 2414-2422.
12. Dowd, A.J., S. McGonigle, and J.P. Dalton, *Fasciola Hepatica Cathepsin L Proteinase Cleaves Fibrinogen and Produces a Novel Type of Fibrin Clot.* 1995. **232**(1): p. 241-246.
13. Kim, S., et al., *Engineering of functional, perfusable 3D microvascular networks on a chip.* Lab on a Chip, 2013. **13**(8): p. 1489.
14. Park, Y.K., et al., *In Vitro Microvessel Growth and Remodeling within a Three-Dimensional Microfluidic Environment.* 2014. **7**(1): p. 15-25.
15. Whisler, J.A., M.B. Chen, and R.D. Kamm, *Control of Perfusable Microvascular Network Morphology Using a Multiculture Microfluidic System.* Tissue Engineering Part C: Methods, 2014. **20**(7): p. 543-552.
16. Brown, A.C. and T.H. Barker, *Fibrin-based biomaterials: Modulation of macroscopic properties through rational design at the molecular level.* 2014. **10**(4): p. 1502-1514.
17. Janmey, P.A., J.P. Winer, and J.W. Weisel, *Fibrin gels and their clinical and bioengineering applications.* Journal of The Royal Society Interface, 2009. **6**(30): p. 1-10.
18. Rohani, M.G. and W.C. Parks, *Matrix remodeling by MMPs during wound repair.* Matrix Biology, 2015. **44-46**: p. 113-121.

19. Bonnans, C., J. Chou, and Z. Werb, *Remodelling the extracellular matrix in development and disease.* Nature Reviews Molecular Cell Biology, 2014. **15**(12): p. 786-801.
20. Van Hinsbergh, V.W.M., *Pericellular Proteases in Angiogenesis and Vasculogenesis.* 2006. **26**(4): p. 716-728.
21. Rundhaug, J.E., *Matrix metalloproteinases and angiogenesis.* Journal of Cellular and Molecular Medicine, 2005. **9**(2): p. 267-285.
22. Ucuzian, A.A., et al., *Molecular Mediators of Angiogenesis.* Journal of Burn Care & Research, 2010. **31**(1): p. 158-175.
23. Lamalice, L., F. Le Boeuf, and J. Huot, *Endothelial Cell Migration During Angiogenesis.* Circulation Research, 2007. **100**(6): p. 782-794.
24. Shi, G.P., et al., *Deficiency of the Cysteine Protease Cathepsin S Impairs Microvessel Growth.* Circulation Research, 2003. **92**(5): p. 493-500.
25. Joyce, J.A., et al., *Cathepsin cysteine proteases are effectors of invasive growth and angiogenesis during multistage tumorigenesis.* 2004. **5**(5): p. 443-453.
26. Sukhova, G.K., G.-P. Shi, and P. Libby, *Role of elastolytic cathepsins in vascular remodeling.* 2004. **1262**: p. 498-501.
27. Hu, L., et al., *Cathepsin K Activity Controls Injury-Related Vascular Repair in Mice.* 2014. **63**(3): p. 607-615.
28. Platt, M.O. and W.A. Shockey, *Endothelial cells and cathepsins: Biochemical and biomechanical regulation.* Biochimie, 2016. **122**: p. 314-323.
29. Vidak, E., et al., *Cysteine Cathepsins and their Extracellular Roles: Shaping the Microenvironment.* Cells, 2019. **8**(3): p. 264.
30. Ataga, K.I. and N.S. Key, *Hypercoagulability in sickle cell disease: new approaches to an old problem.* Hematology Am Soc Hematol Educ Program 2007: p. 91-96.
31. Manwani, D., J. Davila, and C.P. Minniti, *Coagulopathy in Sickle Cell Disease*. 2019, Elsevier. p. 757-760.
32. Nasimuzzaman, M. and P. Malik, *Role of the coagulation system in the pathogenesis of sickle cell disease.* Blood Advances, 2019. **3**(20): p. 3170-3180.
33. Noubouossie, D., N.S. Key, and K.I. Ataga, *Coagulation abnormalities of sickle cell disease: Relationship with clinical outcomes and the effect of disease modifying therapies.* Blood Reviews, 2016. **30**(4): p. 245-256.
34. Piel, F.B., M.H. Steinberg, and D.C. Rees, *Sickle Cell Disease.* New England Journal of Medicine, 2017. **376**(16): p. 1561-1573.
35. Doolittle, R.F., *Fibrinogen and Fibrin.* Annual Review of Biochemistry, 1984. **53**: p. 195-229.
36. Herrick, S., et al., *Fibrinogen.* The International Journal of Biochemistry & Cell Biology, 1999. **31**(7): p. 741-746.
37. Mosesson, M.W., K.R. Siebenlist, and D.A. Meh, *The Structure and Biological Features of Fibrinogen and Fibrin.* 2006. **936**(1): p. 11-30.
38. Leichtman, D.A. and G.J. Brewer, *Elevated plasma levels of fibrinopeptide a during sickle cell anemia pain crisis–evidence for intravascular coagulation.* American Journal of Hematology, 1978. **5**(3).

39. Ekwere, T., et al., *Relevance of fibrinolytic protein (D-dimer) and fibrinopeptide A as markers of sickle cell anaemia vaso-occlusive crisis.* Niger Postgrad Med Journal, 2014. **21**(3): p. 225-230.
40. Keegan, P.M., S. Surapaneni, and M.O. Platt, *Sickle Cell Disease Activates Peripheral Blood Mononuclear Cells to Induce Cathepsins K and V Activity in Endothelial Cells.* 2012. **2012**: p. 1-7.
41. Hannah Song, P.M.K., Suhaas Anbazhakan, Christian P. Rivera, Yundi Feng, Victor O. Omojola, Alexus A. Clark, and J.S. Shuangyi Cai, Rudolph L. Gleason Jr, Edward A. Botchwey, Yunlong Huo, Wenchang Tan, Manu O. Platt, *Sickle Cell Anemia Mediates Carotid Artery Expansive Remodeling That Can Be Prevented by Inhibition of JNK (c-Jun N-Terminal Kinase).* Arteriosclerosis, Thrombosis, and Vascular Biology, 2020.
42. Ferrall-Fairbanks, M.C., et al., *Computational predictions of cysteine cathepsin-mediated fibrinogen proteolysis.* Protein Science, 2017.
43. Bond, J.S., *Proteases: History, discovery, and roles in health and disease.* Journal of Biological Chemistry, 2019. **294**(5): p. 1643-1651.
44. López-Otín, C. and J.S. Bond, *Proteases: Multifunctional Enzymes in Life and Disease.* Journal of Biological Chemistry, 2008. **283**(45): p. 30433-30437.
45. Turk, B., D. Turk, and V. Turk, *Protease signalling: the cutting edge.* The EMBO Journal, 2012. **31**(7): p. 1630-1643.
46. McGrath, M.E., *The lysosomal cysteine proteases.* Annual review of biophysics and biomolecular structure, 1999. **28**: p. 181-204.
47. Repnik, U., et al., *Lysosomes and lysosomal cathepsins in cell death.* Biochimica et Biophysica Acta (BBA) - Proteins and Proteomics, 2012. **1824**(1): p. 22-33.
48. Mohamed, M.M. and B.F. Sloane, *multifunctional enzymes in cancer.* Nature Reviews Cancer, 2006. **6**(10): p. 764-775.
49. McGrath, M.E., *The Lysosomal Cystein Proteases.* Annual Review of Biophysics and Biomolecular Structure, 1999. **28**(1): p. 181-204.
50. Novinec, M., et al., *Interaction between Human Cathepsins K, L, and S and Elastins: MECHANISM OF ELASTINOLYSIS AND INHIBITION BY MACROMOLECULAR INHIBITORS.* 2007. **282**(11): p. 7893-7902.
51. Chen, B. and M.O. Platt, *Multiplex Zymography Captures Stage-specific Activity Profiles of Cathepsins K, L, and S in Human Breast, Lung, and Cervical Cancer.* 2011. **9**(1): p. 109.
52. Sukhova, G.K., et al., *Expression of the elastolytic cathepsins S and K in human atheroma and regulation of their production in smooth muscle cells.* 1998. **102**(3): p. 576-583.
53. Fonović, M. and B. Turk, *Cysteine cathepsins and their potential in clinical therapy and biomarker discovery.* PROTEOMICS - Clinical Applications, 2014. **8**(5-6): p. 416-426.
54. Shi, G.P., et al., *Molecular cloning and expression of human alveolar macrophage cathepsin S, an elastinolytic cysteine protease.* J Biol Chem, 1992. **267**(11): p. 7258-62.
55. Novinec, M. and B. Lenarcic, *Cathepsin K: a unique collagenolytic cysteine peptidase.* Biol Chem, 2013. **394**(9): p. 1163-79.

56. Bromme, D., *Production and activation of recombinant papain-like cysteine proteases.* 2004. **32**(2): p. 199-206.
57. Magnus Abrahamson, M.A.-F.a. and C.-M. Nathanson, *Cystatins*. Biochemical Society Symposium, 2003. **70**: p. 179-199.
58. Standeven, K.F., R.A.S. Ariëns, and P.J. Grant, *The molecular physiology and pathology of fibrin structure/function.* 2005. **19**(5): p. 275-288.
59. Weisel, J.W., *Fibrin assembly. Lateral aggregation and the role of the two pairs of fibrinopeptides.* 1986. **50**(6): p. 1079-1093.
60. Davie, E.W., et al., *The Role of Serine Proteases In The Blood Coagulation Cascade.* Advances in Enzymology and Related Areas of Molecular Biology, 2009. **228**: p. 277-320.
61. Weisel, J.W., Y. Veklich, and O. Gorkun, *The Sequence of Cleavage of Fibrinopeptides from Fibrinogen is Important for Protofibril Formation and Enhancement of Lateral Aggregation in Fibrin Clots.* Journal of Molecular Biology, 1993. **232**(1): p. 285-297.
62. Weisel, J.W. and R.I. Litvinov, *Fibrin Formation, Structure and Properties*. 2017, Springer International Publishing. p. 405-456.
63. Medved, L. and J.W. Weisel, *Recommendations for nomenclature on fibrinogen and fibrin.* Journal of Thrombosis and Haemostasis, 2009. **7**(2): p. 355-359.
64. Yang, Z., I. Mochalkin, and R.F. Doolittle, *A model of fibrin formation based on crystal structures of fibrinogen and fibrin fragments complexed with synthetic peptides.* 2000. **97**(26): p. 14156-14161.
65. Corte, A.L.C.L., H. Philippou, and R.A.S. Ariens, *Role of Fibrin Structure in Thrombosis and Vascular Disease.* Advances in Protein Chemistry and Structural Biology, 2011. **83**.
66. Donald Raum, D.M., Chester A. Alper, Raphael Levey, Paul D. Taylor, & Thomas E. Starzl, *Synthesis of Human Plasminogen by the Liver.* Science, 1980. **208**(4447): p. 1036-1037.
67. Doolittle, R.F., *Clotting of Mammalian Fibrinogens by Papain: A Re-examination.*
68. Eagle, H., and Harris, T. N., *Studies in blood coagulation. V. The coagulation of blood by proteolytic enzymes (trypsin, papain).* Journal of General Physiology, 1937. **20**: p. 543-560.
69. Steiner, R.F., and Laki, K, *Light scattering studies on the clotting of fibrinogen.* Archives of Biochemistry and Biophysics, 1951. **34**: p. 24-37.
70. Plow, E.F. and T.S. Edgington, *An alternative pathway for fibrinolysis. I. The cleavage of fibrinogen by leukocyte proteases at physiologic pH.* 1975. **56**(1): p. 30-38.
71. Carmeliet, P., et al., *Physiological consequences of loss of plasminogen activator gene function in mice.* 1994. **368**(6470): p. 419-424.
72. Carmeliet, P., et al., *Plasminogen activator inhibitor-1 gene-deficient mice. II. Effects on hemostasis, thrombosis, and thrombolysis.* 1993. **92**(6): p. 2756-2760.
73. Balaji, S., et al., *The Role of Endothelial Progenitor Cells in Postnatal Vasculogenesis: Implications for Therapeutic Neovascularization and Wound Healing.* Advances in Wound Care, 2013. **2**(6): p. 283-295.
74. Brown, J.M., *Vasculogenesis: a crucial player in the resistance of solid tumours to radiotherapy.* 2014. **87**(1035): p. 20130686.

75. Risau, W. and I. Flamme, *Vasculogenesis.* 1995. **11**(1): p. 73-91.
76. Chopra, H., et al., *Insights into Endothelial Progenitor Cells: Origin, Classification, Potentials, and Prospects.* Stem Cells International, 2018. **2018**: p. 1-24.
77. Sang, Q.X.A., *Complex role of matrix metalloproteinases in angiogenesis.* Cell Research, 1998. **8**(3): p. 171-177.
78. Campbell, N.E., et al., *Extracellular Matrix Proteins and Tumor Angiogenesis.* 2010. **2010**: p. 1-13.
79. PA, A., et al., *The urokinase-type plasminogen activator system in cancer metastasis: a review.* International Journal of Cancer, 1997. **72**.
80. Stepanova, V., et al., *Urokinase-type Plasminogen Activator (uPA) Promotes Angiogenesis by Attenuating Proline-rich Homeodomain Protein (PRH) Transcription Factor Activity and De-repressing Vascular Endothelial Growth Factor (VEGF) Receptor Expression.* Journal of Biological Chemistry, 2016. **291**(29): p. 15029-15045.
81. Brodsky, S., et al., *Plasmin-dependent and -independent effects of plasminogen activators and inhibitor-1 on ex vivo angiogenesis.* American Journal of Physiology- Heart and Circulatory Physiology, 2001. **281**(4): p. 1784-1792.
82. Devy, L., et al., *The pro- or antiangiogenic effect of plasminogen activator inhibitor 1 is dose dependent.* FASEB, 2002. **16**(2): p. 147-154.
83. Urbich, C., et al., *Cathepsin L is required for endothelial progenitor cell–induced neovascularization.* Nature Medicine, 2005. **11**(2): p. 206-213.
84. Sudhan, D.R., et al., *Cathepsin L in tumor angiogenesis and its therapeutic intervention by the small molecule inhibitor KGP94.* 2016. **33**(5): p. 461-473.
85. Orlando, G., et al., *Will Regenerative Medicine Replace Transplantation?* 2013. **3**(8): p. a015693-a015693.
86. A. Heidary Rouchi and M. Mahdavi-Mazdeh, *Regenerative Medicine in Organ and Tissue Transplantation: Shortly and Practically Achievable?* International Journal of Organ Transplantation Medicine, 2015. **6**(3): p. 93-98.
87. Khademhosseini, A., J.P. Vacanti, and R. Langer, *Progress In Tissue Engineering.* Biotechnology, 2009. **300**(5): p. 64-71.
88. Pellegata, A.F., A.M. Tedeschi, and P. De Coppi, *Whole Organ Tissue Vascularization: Engineering the Tree to Develop the Fruits.* Frontiers in Bioengineering and Biotechnology, 2018. **6**.
89. Song, H.H.G., et al., *Vascular Tissue Engineering: Progress, Challenges, and Clinical Promise.* Cell Stem Cell, 2018. **22**(3): p. 340-354.
90. Sharma, D., et al., *Upgrading prevascularization in tissue engineering: A review of strategies for promoting highly organized microvascular network formation.* Acta Biomaterialia, 2019. **95**: p. 112-130.
91. Laschke, M.W. and M.D. Menger, *Prevascularization in tissue engineering: Current concepts and future directions.* Biotechnology Advances, 2016. **34**(2): p. 112-121.
92. Jain, R.K., et al., *Engineering vascularized tissue.* Nature Biotechnology, 2005. **23**(7): p. 821-823.
93. Lovett, M., et al., *Vascularization Strategies for Tissue Engineering.* Tissue Engineering Part B: Reviews, 2009. **15**(3): p. 353-370.

94. Rouwkema, J., N.C. Rivron, and C.A. Van Blitterswijk, *Vascularization in tissue engineering.* Trends in Biotechnology, 2008. **26**(8): p. 434-441.
95. Butt, O.I., et al., *Stimulation of Peri-Implant Vascularization with Bone Marrow-Derived Progenitor Cells: Monitoring by In Vivo EPR Oximetry.* 2007. **13**(8): p. 2053-2061.
96. Frueh, F.S., et al., *Current and emerging vascularization strategies in skin tissue engineering.* Critical Reviews in Biotechnology, 2017. **37**(5): p. 613-625.
97. Zhang, W., et al., *Vascularization of hollow channel-modified porous silk scaffolds with endothelial cells for tissue regeneration.* 2015. **56**: p. 68-77.
98. Shah, S. and K.-T. Kang, *Two-Cell Spheroid Angiogenesis Assay System Using Both Endothelial Colony Forming Cells and Mesenchymal Stem Cells.* Biomolecules and Therapeutics, 2018. **26**(5): p. 474-480.
99. Patel, M., et al., *Mouse Metanephric Mesenchymal Cell–Derived Angioblasts Undergo Vasculogenesis in Three-Dimensional Culture.* The American Journal of Pathology, 2018. **188**(3): p. 768-784.
100. Wang, X., Q. Sun, and J. Pei, *Microfluidic-Based 3D Engineered Microvascular Networks and Their Applications in Vascularized Microtumor Models.* Micromachines, 2018. **9**(10): p. 493.
101. Lee, S., et al., *Microfluidic-based vascularized microphysiological systems.* Lab on a Chip, 2018. **18**(18): p. 2686-2709.
102. Soojung Oh, H.R., Dongha Tahk, Jihoon Ko, Yoojin Chung, Hae Kwang Lee, Tae Ryong Lee and Noo Li Jeon, *"Open-top" microfluidic device for in vitro three-dimensional capillary beds.* Lab Chip, 2017. **17**: p. 3405-3414.
103. Abe, Y., et al., *Balance of interstitial flow magnitude and vascular endothelial growth factor concentration modulates three-dimensional microvascular network formation.* APL Bioengineering, 2019. **3**(3): p. 036102.
104. Piel, F.B., et al., *Global Burden of Sickle Cell Anaemia in Children under Five, 2010–2050: Modelling Based on Demographics, Excess Mortality, and Interventions.* PLoS Medicine, 2013. **10**(7): p. e1001484.
105. Kauf, T.L., et al., *The cost of health care for children and adults with sickle cell disease.* American Journal of Hematology, 2009. **84**(6): p. 323-327.
106. Kato, G.J., et al., *Sickle cell disease.* Nature Reviews Disease Primers, 2018. **4**(1): p. 18010.
107. Ashley-Koch, A., Q. Yang, and R.S. Olney, *Sickle Hemoglobin (Hb S) Allele and Sickle Cell Disease: A HuGE Review.* American Journal of Epidemiology, 2000. **151**(9): p. 839-845.
108. Ferrone, F., J. Hofrichter, and W. Eaton, *Kinetics of sickle hemoglobin polymerization. II. A double nucleation mechanism.* Journal of Molecular Biology, 1985. **183**(4): p. 611-631.
109. Makis, A.C., E.C. Hatzimichael, and K.L. Bourantas, *The role of cytokines in sickle cell disease.* 2000. **79**(8): p. 407-413.
110. Belcher, J., et al., *Activated monocytes in sickle cell disease: potential role in the activation of vascular endothelium and vaso-occlusion.* Blood, 2000. **96**(7): p. 2451-2459.
111. Shah, N., et al., *Characterization of the hypercoagulable state in patients with sickle cell disease.* Thrombosis Research, 2012. **130**(5): p. e241-e245.

112. Platt, O.S., *Sickle cell anemia as an inflammatory disease.* 2000. **106**(3): p. 337-338.
113. Trinh-Trang-Tan, M.M., et al., *Intercellular adhesion molecule-4 and CD36 are implicated in the abnormal adhesiveness of sickle cell SAD mouse erythrocytes to endothelium.* 2010. **95**(5): p. 730-737.
114. Barabino, G.A., M.O. Platt, and D.K. Kaul, *Sickle Cell Biomechanics.* 2010. **12**(1): p. 345-367.
115. Kaul, D., *The pathophysiology of vascular obstruction in the sickle syndromes.* 1996. **10**(1): p. 29-44.
116. Sparkenbaugh, E. and R. Pawlinski, *Prothrombotic aspects of sickle cell disease.* Journal of Thrombosis and Haemostasis, 2017. **15**(7): p. 1307-1316.
117. Faes, C., E.M. Sparkenbaugh, and R. Pawlinski, *Hypercoagulable state in sickle cell disease.* Clinical Hemorheology and Microcirculation, 2018. **68**: p. 301-318.
118. Al Dieri, R., et al., *Thrombin generation, a function test of the haemostaticthrombotic system.* Thrombosis and Haemostasis, 2006. **96**(11): p. 553-561.
119. Whelihan, M.F., M.Y. Lim, and N.S. Key, *Red blood cells and thrombin generation in sickle cell disease.* 2014. **133**: p. S52-S53.
120. Whelihan, M.F., et al., *The contribution of red blood cells to thrombin generation in sickle cell disease: meizothrombin generation on sickled red blood cells.* 2013. **11**(12): p. 2187-2189.
121. Hemker, H.C., et al., *Calibrated Automated Thrombin Generation Measurement in Clotting Plasma.* Pathophysiology of Haemostasis and Thrombosis, 2003. **33**(1): p. 4-15.
122. DL, Y., et al., *Thromboelastographic and hemostatic characteristics in pediatric patients with sickle cell disease.* Arch Pathol Lab Med, 2005. **129**(6): p. 760-765.
123. Ataga, K.I., et al., *Coagulation activation and inflammation in sickle cell disease-associated pulmonary hypertension.* 2008. **93**(1): p. 20-26.
124. Noubouossie, D., et al., *Thrombin generation reveals high procoagulant potential in the plasma of sickle cell disease children.* American Journal of Hematology, 2012. **87**(2): p. 145-149.
125. Amin, C., et al., *Coagulation activation in sickle cell trait: an exploratory study.* British journal of haematology, 2015. **171**(4): p. 638-646.
126. Gerotziafas, G.T., et al., *The acceleration of the propagation phase of thrombin generation in patients with steady-state sickle cell disease is associated with circulating erythrocyte-derived microparticles.* Thromb Haemost, 2012. **107**(06): p. 1044-1052.
127. Chantarangkul, V., et al., *Standardization of the endogenous thrombin potential measurement: how to minimize the effect of residual platelets in stored plasma.* 2004. **124**(3): p. 355-357.
128. Betal, S.G., et al., *Thrombin Generation in Sickle Cell Disease: Insights From Computerized Automated Thrombography.* Blood, 2009. **114**(22): p. 2587-2587.
129. Charneski, L. and H.B. Congdon, *Effects of antiplatelet and anticoagulant medications on the vasoocclusive and thrombotic complications of sickle cell disease: A review of the literature.* American Journal of Health-System Pharmacy, 2010. **67**(11): p. 895-900.

130. Nardo-Marino, A., V. Brousse, and D. Rees, *Emerging therapies in sickle cell disease.* British Journal of Haematology, 2020.
131. Roberts, M.Z., et al., *Effectiveness and safety of oral anticoagulants in patients with sickle cell disease and venous thromboembolism: a retrospective cohort study.* Journal of Thrombosis and Thrombolysis, 2018. **45**(4): p. 512-515.
132. Telen, M.J., et al., *Sevuparin binds to multiple adhesive ligands and reduces sickle red blood cell-induced vaso-occlusion.* 2016.
133. Biemond, B.J., et al., *Efficacy and Safety of Sevuparin, a Novel Non-Anti-Coagulant Heparinoid, in Patients with Acute Painful Vaso-Occlusive Crisis; A Global, Multicenter Double-Blind, Randomized, Placebo-Controlled Phase 2 Trial (TVOC01)*. 2019, American Society of Hematology Washington, DC.
134. Trudel, M., et al., *Sickle cell disease of transgenic SAD mice.* Blood, 1994. **84**(9): p. 3189-3197.
135. Roszell, N.J., et al., *Fibrinogen deficiency, but not plasminogen deficiency, increases mortality synergistically in combination with sickle hemoglobin SAD in transgenic mice.* 2007. **82**(12): p. 1044-1048.
136. Chantrathammachart, P., et al., *Tissue factor promotes activation of coagulation and inflammation in a mouse model of sickle cell disease.* 2012. **120**(3): p. 636-646.
137. Manci, E.A., et al., *Pathology of Berkeley sickle cell mice: similarities and differences with human sickle cell disease.* Blood, 2006. **107**(4): p. 1651-1658.
138. Sparkenbaugh, E.M., et al., *Differential contribution of FXa and thrombin to vascular inflammation in a mouse model of sickle cell disease.* 2014. **123**(11): p. 1747-1756.
139. Arumugam, P.I., et al., *Genetic diminution of circulating prothrombin ameliorates multiorgan pathologies in sickle cell disease mice.* 2015. **126**(15): p. 1844-1855.
140. Flick, M.J., et al., *Leukocyte engagement of fibrin(ogen) via the integrin receptor αMβ2/Mac-1 is critical for host inflammatory response in vivo.* The Journal of Clinical Investigation, 2004. **113**(11): p. 1596-1606.
141. Nasimuzzaman, M., et al., *Elimination of the fibrinogen integrin aMb2-binding motif improves renal pathology in mice with sickle cell anemia.* Blood Advances, 2019. **3**(9).
142. Irigoyen, J.P., et al., *The plasminogen activator system: biology and regulation.* 1999. **56**(1): p. 104-132.
143. Lutgens, E., *Disruption of the Cathepsin K Gene Reduces Atherosclerosis Progression and Induces Plaque Fibrosis but Accelerates Macrophage Foam Cell Formation.* 2005. **113**(1): p. 98-107.
144. Caroline Cvetkovic, M.C.F.-F., Eunkyung K, Lauren Grant, Hyunjoon Kong, Manu O. Platt, and Rashid Bashir, *Investigating the Life Expectancy and Proteolytic Degradation of Engineered Skeletal Muscle Biological Machines.* Scientific Reports, 2017. **7**.
145. An, S.S.A. and Rajangam, *Fibrinogen and fibrin based micro and nano scaffolds incorporated with drugs, proteins, cells and genes for therapeutic biomedical applications.* International Journal of Nanomedicine, 2013: p. 3641.
146. Wilder, C.L., et al., *Manipulating substrate and pH in zymography protocols selectively distinguishes cathepsins K, L, S, and V activity in cells and tissues.* Archives of Biochemistry and Biophysics, 2011. **516**(1): p. 52-57.

147. Barry, Z.T. and M.O. Platt, *Cathepsin S Cannibalism of Cathepsin K as a Mechanism to Reduce Type I Collagen Degradation.* Journal of Biological Chemistry, 2012. **287**(33): p. 27723-27730.
148. Wilder, C.L., et al., *Manipulating substrate and pH in zymography protocols selectively distinguishes cathepsins K, L, S, and V activity in cells and tissues.* 2011. **516**(1): p. 52-57.
149. Park, K.-Y., W.A. Li, and M.O. Platt, *Patient specific proteolytic activity of monocyte-derived macrophages and osteoclasts predicted with temporal kinase activation states during differentiation.* 2012. **4**(12): p. 1459.
150. Mebius, M.M., et al., *Fibrinogen and fibrin are novel substrates for Fasciola hepatica cathepsin L peptidases.* Molecular and Biochemical Parasitology, 2018. **221**: p. 10-13.
151. Wu, H., et al., *Cathepsin S Activity Controls Injury-Related Vascular Repair in Mice via the TLR2-Mediated p38MAPK and PI3K−Akt/p-HDAC6 Signaling PathwayHighlights.* 2016. **36**(8): p. 1549-1557.
152. Platt, M.O., R.F. Ankeny, and H. Jo, *Laminar Shear Stress Inhibits Cathepsin L Activity in Endothelial Cells.* Arteriosclerosis, Thrombosis, and Vascular Biology, 2006. **26**(8): p. 1784-1790.
153. J. Liu, G.K.S., J. T. Yang et al., *Cathepsin L expression and regulation in human abdominal aortic aneurysm, athero- sclerosis, and vascular cells.* Atherosclerosis, 2006. **184**(2): p. 302-311.
154. Kimura, Y. and K. Yokoi-Hayashi, *Polymorphonuclear leukocyte lysosomal proteases, cathepsins B and D affect the fibrinolytic system in human umbilical vein endothelial cells.* 1996. **1310**(1): p. 1-4.
155. Whelihan, M.F., et al., *Thrombin generation and cell-dependent hypercoagulability in sickle cell disease.* 2016. **14**(10): p. 1941-1952.
156. Oliveira, M., et al., *Cysteine cathepsin S processes leptin, inactivating its biological activity.* 2012. **214**(2): p. 217-224.
157. Lafarge, J.-C., et al., *Cathepsin S inhibition lowers blood glucose levels in mice.* 2014. **57**(8): p. 1674-1683.
158. Sharma, V., et al., *Structural requirements for the collagenase and elastase activity of cathepsin K and its selective inhibition by an exosite inhibitor.* 2015. **465**(1): p. 163-173.
159. Liu, Y., et al., *Usefulness of Serum Cathepsin L as an Independent Biomarker in Patients With Coronary Heart Disease.* 2009. **103**(4): p. 476-481.
160. Van Hinsbergh, V.W.M., A. Collen, and P. Koolwijk, *Role of fibrin matrix in angiogenesis*, in *Annals of the New York Academy of Sciences*. 2001. p. 426-437.
161. Uibo, R., et al., *Soft materials to treat central nervous system injuries: Evaluation of the suitability of non-mammalian fibrin gels.* 2009. **1793**(5): p. 924-930.
162. Vedakumari, W.S., et al., *Fibrin nanoparticles as Possible vehicles for drug delivery.* 2013. **1830**(8): p. 4244-4253.
163. Witjas, F.M.R., et al., *Concise Review: The Endothelial Cell Extracellular Matrix Regulates Tissue Homeostasis and Repair.* STEM CELLS Translational Medicine, 2019. **8**(4): p. 375-382.
164. Sherbet, G., *Vascular Endothelial Growth Factor.* Growth Factors and Their Receptors in Cell Differentiation, Cancer and Cancer Therapy, 2011: p. 55-64.

165. Fitzgerald, K.A., et al., *FGF*, in *The Cytokine FactsBook and Webfacts (Second Edition)*, K.A. Fitzgerald, et al., Editors. 2001, Academic Press: London. p. 230-243.
166. Wang, H. and J.A. Keiser, *Vascular Endothelial Growth Factor Upregulates the Expression of Matrix Metalloproteinases in Vascular Smooth Muscle Cells : Role of flt-1*. 1998. **83**(8): p. 832-840.
167. Ghajar, C.M., et al., *Mesenchymal cells stimulate capillary morphogenesis via distinct proteolytic mechanisms.* 2010. **316**(5): p. 813-825.
168. Lv, B.-J., et al., *Plasma levels of cathepsins L, K, and V and risks of abdominal aortic aneurysms: A randomized population-based study.* 2013. **230**(1): p. 100-105.
169. Madfis, N., et al., *Co-emergence of Specialized Endothelial Cells from Embryonic Stem Cells.* Stem Cells and Development, 2018.
170. Haase, K., et al., *Pericytes Contribute to Dysfunction in a Human 3D Model of Placental Microvasculature through VEGF-Ang-Tie2 Signaling.* Advanced Science, 2019. **6**(23): p. 1900878.
171. Whisler, J.A., *Engineered, functional, human microvasculature in a perfusable fluidic device (PhD Thesis).* Available from DSpace@MIT, 2017.
172. Offeddu, G.S., et al., *An on-chip model of protein paracellular and transcellular permeability in the microcirculation.* Biomaterials, 2019. **212**: p. 115-125.
173. Buchanan, C.F., et al., *Flow shear stress regulates endothelial barrier function and expression of angiogenic factors in a 3D microfluidic tumor vascular model.* 2014. **8**(5): p. 517-524.
174. Li, X., et al., *In Vitro Recapitulation of Functional Microvessels for the Study of Endothelial Shear Response, Nitric Oxide and [Ca2+]i.* 2015. **10**(5): p. e0126797.
175. Galie, P.A., et al., *Fluid shear stress threshold regulates angiogenic sprouting.* 2014. **111**(22): p. 7968-7973.
176. Moya, M.L., et al., *In Vitro Perfused Human Capillary Networks.* Tissue Engineering Part C: Methods, 2013. **19**(9): p. 730-737.
177. Hsu, Y.-H., et al., *Full range physiological mass transport control in 3D tissue cultures.* 2013. **13**(1): p. 81-89.
178. MO, P., et al., *Oscillatory shear stress (OS) upregulates cathepsin expression while inhibiting cystatin C expression in endothelial cells (EC) - Implication in atherosclerosis.* FASEB, 2004. **18**: p. A1114–A1114.
179. James C. Powers, J.L.A., Ozlem Dogan Ekici, and Karen Ellis James, *Irreversible Inhibitors of Serine, Cysteine, and Threonine Proteases.* Chemical Reviews, 2002. **102**(12): p. 4639-4750.
180. Douglas, S.A., et al., *Human cathepsins K, L, and S: Related proteases, but unique fibrinolytic activity.* Biochimica et Biophysica Acta (BBA) - General Subjects, 2018. **1862**(9): p. 1925-1932.
181. Veillard, F., et al., *Cysteine Cathepsins S and L Modulate Anti-angiogenic Activities of Human Endostatin.* 2011. **286**(43): p. 37158-37167.
182. Troen, B.R., *The Regulation of Cathepsin K Gene Expression.* Annals of the New York Academy of Sciences, 2006. **1068**(1): p. 165-172.
183. Cheng, X.W., et al., *Localization of Cysteine Protease, Cathepsin S, to the Surface of Vascular Smooth Muscle Cells by Association with Integrin αvβ3.* 2006. **168**(2): p. 685-694.

184. Bezenah, J.R., Y.P. Kong, and A.J. Putnam, *Evaluating the potential of endothelial cells derived from human induced pluripotent stem cells to form microvascular networks in 3D cultures.* Scientific Reports, 2018. **8**(1).
185. Ghajar, C.M., S.C. George, and A.J. Putnam, *Matrix metalloproteinase control of capillary morphogenesis.* Critical reviews in eukaryotic gene expression, 2008. **18**(3): p. 251-278.
186. Helske, S., *Increased Expression of Elastolytic Cathepsins S, K, and V and Their Inhibitor Cystatin C in Stenotic Aortic Valves.* 2006. **26**(8): p. 1791-1798.
187. Mason, S.D. and J.A. Joyce, *Proteolytic networks in cancer.* Trends in Cell Biology, 2011. **21**(4): p. 228-237.
188. Haase, K. and R.D. Kamm, *Advances in on-chip vascularization.* Regenerative Medicine, 2017. **12**(3): p. 285-302.
189. Shockey, W.A., et al., *Dynamic Model of Protease State and Inhibitor Trafficking to Predict Protease Activity in Breast Cancer Cells.* Cellular and Molecular Bioengineering, 2019.
190. Grant, L., et al., *Long-Term Cryopreservation and Revival of Tissue-Engineered Skeletal Muscle.* Tissue Engineering Part A, 2019. **25**(13-14): p. 1023-1036.
191. Lee, H., et al., *A bioengineered array of 3D microvessels for vascular permeability assay.* Microvascular Research, 2014. **91**: p. 90-98.
192. Zhu, W.-H., et al., *Regulation of Vascular Growth and Regression by Matrix Metalloproteinases in the Rat Aorta Model of Angiogenesis.* 2000. **80**(4): p. 545-555.
193. Ataga, K.I. and N.S. Key, *Hypercoagulability in Sickle Cell Disease: New Approaches to an Old Problem.* Hematology, 2007. **2007**(1): p. 91-96.
194. Choe, Y., et al., *Substrate Profiling of Cysteine Proteases Using a Combinatorial Peptide Library Identifies Functionally Unique Specificities.* Journal of Biological Chemistry, 2006. **281**(18): p. 12824-12832.
195. Doolittle, R.F., *Clotting of Mammalian Fibrinogens by Papain: A Re-examination.* 2014. **53**(42): p. 6687-6694.
196. Keegan, P.M., C.L. Wilder, and M.O. Platt, *Tumor necrosis factor alpha stimulates cathepsin K and V activity via juxtacrine monocyte–endothelial cell signaling and JNK activation.* 2012. **367**(1-2): p. 65-72.
197. Pawlinski, R., *It's "PT" for SCD!* 2015. **126**(15): p. 1739-1740.
198. Ceglie, G., et al., *Gender-Related Differences in Sickle Cell Disease in a Pediatric Cohort: A Single-Center Retrospective Study.* Frontiers in Molecular Biosciences, 2019. **6**(140).
199. Rawlings, N.D. and A.J. Barrett, *Families of cysteine peptidases.* Methods In Enzymology, 1994. **244**: p. 461-486.
200. Antalis, T.M., T.H. Bugge, and Q. Wuz, *Membrane-Anchored Serine Proteases in Health and Disease.* Progress in Molecular Biology and Translational Science, 2011. **99**.
201. Pechik, I., et al., *Structural Basis for Sequential Cleavage of Fibrinopeptides upon Fibrin Assembly † , ‡.* 2006. **45**(11): p. 3588-3597.
202. Bandeira, I.C.J., et al., *Chronic inflammatory state in sickle cell anemia patients is associated with HBB*S haplotype.* Cytokine, 2014. **65**(2): p. 217-221.

203. Sparkenbaugh, E. and R. Pawlinski, *Interplay between coagulation and vascular inflammation in sickle cell disease.* British journal of haematology, 2013. **162**(1): p. 3-14.
204. Qari, M.H., U. Dier, and S.A. Mousa, *Biomarkers of Inflammation, Growth Factor, and Coagulation Activation in Patients With Sickle Cell Disease.* Clinical and Applied Thrombosis/Hemostasis, 2011. **18**(2): p. 195-200.
205. Pathare, A., et al., *Cytokine profile of sickle cell disease in Oman.* American Journal of Hematology, 2004. **77**(4): p. 323-328.
206. Yun, J.K., J.M. Anderson, and N.P. Ziats, *Cyclic-strain-induced endothelial cell expression of adhesion molecules and their roles in monocyte-endothelial interaction.* J Biomed Mater Res, 1999. **44**(1): p. 87-97.
207. Proença-Ferreira, R., et al., *Endothelial activation by platelets from sickle cell anemia patients.* PloS one, 2014. **9**(2): p. e89012-e89012.
208. Naik, R.P., et al., *Venous thromboembolism in adults with sickle cell disease: a serious and under-recognized complication.* The American journal of medicine, 2013. **126**(5): p. 443-449.
209. Jackson, S.P., R. Darbousset, and S.M. Schoenwaelder, *Thromboinflammation: challenges of therapeutically targeting coagulation and other host defense mechanisms.* Blood, 2019. **133**(9): p. 906-918.
210. Guo, L. and M.T. Rondina, *The Era of Thromboinflammation: Platelets Are Dynamic Sensors and Effector Cells During Infectious Diseases.* Frontiers in immunology, 2019. **10**: p. 2204-2204.
211. Francis, R.B., Jr. and C.S. Johnson, *Vascular occlusion in sickle cell disease: current concepts and unanswered questions.* Blood, 1991. **77**(7): p. 1405-14.
212. Manwani, D. and P.S. Frenette, *Vaso-occlusion in sickle cell disease: pathophysiology and novel targeted therapies.* Blood, 2013. **122**(24): p. 3892-3898.
213. Gersh, K., C. Nagaswami, and J. Weisel, *Fibrin network structure and clot mechanical properties are altered by incorporation of erythrocytes.* Thrombosis and Haemostasis, 2009. **102**(12): p. 1169-1175.
214. Banerjee, R., K. Nageshwari, and R.R. Puniyani, *The diagnostic relevance of red cell rigidity.* Clinical Hemorheology and Microcirculation, 1998. **19**: p. 21-24.
215. Dobbe, J.G.G., et al., *Analyzing Red Blood Cell-Deformability Distributions.* 2002. **28**(3): p. 373-384.
216. Messmann, R., et al., *Mechanical properties of sickle cell membranes.* Blood, 1990. **75**: p. 1711-7.
217. Maciaszek, J.L. and G. Lykotrafitis, *Sickle cell trait human erythrocytes are significantly stiffer than normal.* Journal of Biomechanics, 2011. **44**(4): p. 657-661.
218. Bornstein, P., *Matricellular proteins: an overview.* Journal of cell communication and signaling, 2009. **3**(3-4): p. 163-165.
219. Chen, C.-C. and L.F. Lau, *Functions and mechanisms of action of CCN matricellular proteins.* The International Journal of Biochemistry & Cell Biology, 2009. **41**(4): p. 771-783.
220. Apte, S.S., *A disintegrin-like and metalloprotease (reprolysin type) with thrombospondin type 1 motifs: the ADAMTS family.* The International Journal of Biochemistry & Cell Biology, 2004. **36**(6): p. 981-985.
221. Allison, A.C., *Properties of sickle-cell haemoglobin.* 1957. **65**(2): p. 212-219.

222. Dunn, E.J., et al., *Molecular mechanisms involved in the resistance of fibrin to clot lysis by plasmin in subjects with type 2 diabetes mellitus.* 2006. **49**(5): p. 1071-1080.
223. Fan, N.K., et al., *Experimental and Imaging Techniques for Examining Fibrin Clot Structures in Normal and Diseased States.* Journal of Visualized Experiments, 2015(98).
224. Deanfield, J.E., J.P. Halcox, and T.J. Rabelink, *Endothelial Function and Dysfunction.* Circulation, 2007. **115**(10): p. 1285-1295.
225. Aird, W.C., *Endothelial cell heterogeneity.* Cold Spring Harbor perspectives in medicine, 2012. **2**(1): p. a006429-a006429.
226. Aird, W.C., *Phenotypic Heterogeneity of the Endothelium.* Circulation Research, 2007. **100**(2): p. 158-173.
227. De Smet, F., et al., *Mechanisms of Vessel Branching.* Arteriosclerosis, Thrombosis, and Vascular Biology, 2009. **29**(5): p. 639-649.
228. Carmeliet, P., et al., *Branching morphogenesis and antiangiogenesis candidates: tip cells lead the way.* Nature Reviews Clinical Oncology, 2009. **6**(6): p. 315-326.
229. Gerhardt, H., et al., *VEGF guides angiogenic sprouting utilizing endothelial tip cell filopodia.* Journal of Cell Biology, 2003. **161**(6): p. 1163-1177.
230. Hellström, M., et al., *Dll4 signalling through Notch1 regulates formation of tip cells during angiogenesis.* Nature, 2007. **445**(7129): p. 776-780.
231. Blancas, A.A., et al., *Specialized Tip/Stalk-Like and Phalanx-Like Endothelial Cells from Embryonic Stem Cells.* 2013. **22**(9): p. 1398-1407.
232. Kapoor, C., et al., *Seesaw of matrix metalloproteinases (MMPs).* Journal of Cancer Research and Therapeutics. **12**(1): p. 28-35.
233. Li, W.A., et al., *Detection of femtomole quantities of mature cathepsin K with zymography.* 2010. **401**(1): p. 91-98.
234. Göőz, P., et al., *ADAM-17 regulates endothelial cell morphology, proliferation, and in vitro angiogenesis.* 2009. **380**(1): p. 33-38.
235. Caolo, V., et al., *ADAM10 and ADAM17 have opposite roles during sprouting angiogenesis.* 2015. **18**(1): p. 13-22.
236. Weskamp, G., et al., *Pathological Neovascularization Is Reduced by Inactivation of ADAM17 in Endothelial Cells but Not in Pericytes.* 2010. **106**(5): p. 932-940.
237. Guenzi, E., *The guanylate binding protein-1 GTPase controls the invasive and angiogenic capability of endothelial cells through inhibition of MMP-1 expression.* 2003. **22**(15): p. 3772-3782.
238. Lee, C.H., et al., *Engineering of a human kringle domain into agonistic and antagonistic binding proteins functioning in vitro and in vivo.* 2010. **107**(21): p. 9567-9571.
239. Rios-Steiner, J.L., et al., *Structure and binding determinants of the recombinant kringle-2 domain of human plasminogen to an internal peptide from a group A Streptococcal surface protein.* 2001. **308**(4): p. 705-719.
240. Cao, Y., R. Cao, and N. Veitonmaki, *Kringle Structures and Antiangiogenesis.* Current Medicinal Chemistry - Anti-Cancer Agents, 2002. **2**(6): p. 667-681.
241. Ruby, et al., *The X-ray Crystal Structure of Full-Length Human Plasminogen.* Cell Reports, 2012. **1**(3): p. 185-190.

242. Fredenburgh, J.C. and J.I. Weitz, *Chapter 122 - Overview of Hemostasis and Thrombosis*, in *Hematology (Seventh Edition)*, R. Hoffman, et al., Editors. 2018, Elsevier. p. 1831-1842.
243. Soff, G.A., *Angiostatin and Angiostatin-related Proteins.* Cancer and Metastasis Reviews, 2000. **19**(1): p. 97-107.
244. Luciano, P., et al., *Cathepsin V, but not cathepsins L, B and K, may release angiostatin-like fragments from plasminogen.* Biological Chemistry, 2008. **389**(2): p. 195-200.
245. Coppini, L.P., et al., *Plasminogen hydrolysis by cathepsin S and identification of derived peptides as selective substrate for cathepsin V and cathepsin L inhibitor.* Biol Chem, 2010. **391**(5): p. 561-70.
246. Ferrall-Fairbanks, M.C., et al., *PACMANS: A bioinformatically informed algorithm to predict, design, and disrupt protease-on-protease hydrolysis.* Protein Science, 2017. **26**(4): p. 880-890.
247. Aĭsina, R. and L. Mukhametova, *Structure and functions of plasminogen/plasmin system.* Bioorganicheskaia khimiia, 2015. **40**: p. 642-57.
248. Barrett, C.D., et al., *Human neutrophil elastase mediates fibrinolysis shutdown through competitive degradation of plasminogen and generation of angiostatin.* J Trauma Acute Care Surg, 2017. **83**(6): p. 1053-1061.
249. Machovich, R. and W.G. Owen, *An elastase-dependent pathway of plasminogen activation.* 1989. **28**(10): p. 4517-4522.
250. Kafienah, W.E., et al., *Human cathepsin K cleaves native type I and II collagens at the N-terminal end of the triple helix.* 1998. **331**(3): p. 727-732.
251. Lanzkron, S., C.P. Carroll, and C. Haywood, Jr., *Mortality rates and age at death from sickle cell disease: U.S., 1979-2005.* Public health reports (Washington, D.C. : 1974), 2013. **128**(2): p. 110-116.
252. Jiang, H., et al., *Cathepsin K-mediated notch1 activation contributes to neovascularization in response to hypoxia.* 2014. **5**.
253. Lutgens, S.P.M., et al., *Cathepsin cysteine proteases in cardiovascular disease.* FASEB Journal, 2007(21): p. 3029-3041.
254. Wang, B., *Cathepsin S Controls Angiogenesis and Tumor Growth via Matrix-derived Angiogenic Factors.* 2005. **281**(9): p. 6020-6029.
255. Perrin, J., et al., *In vitro effects of human neutrophil cathepsin G on thrombin generation: Both acceleration and decreased potential.* 2010. **104**(3): p. 514-522.
256. Raffini, L.J., et al., *Prolongation of the prothrombin time and activated partial thromboplastin time in children with sickle cell disease.* 2006. **47**(5): p. 589-593.
257. Ferrall-Fairbanks, M.C., C.A. Kieslich, and M.O. Platt, *Reassessing enzyme kinetics: Considering protease-as-substrate interactions in proteolytic networks.* Proceedings of the National Academy of Sciences, 2020. **117**(6): p. 3307-3318.
258. Smith, E.B., et al., *Fate of fibrinogen in human arterial intima.* 1990. **10**(2): p. 263-275.
259. Thompson, W.D., et al., *Angiogenic activity of fibrin degradation products is located in fibrin fragment E.* The Journal of Pathology, 1992. **168**(1): p. 47-53.
260. Bootle-Wilbraham, C.A., et al., *Fibrin fragment E stimulates the proliferation, migration and differentiation of human microvascular endothelial cells in vitro.* Angiogenesis, 2001. **4**(4): p. 269-275.

261. Piccin, A., et al., *Circulating microparticles, protein C, free protein S and endothelial vascular markers in children with sickle cell anaemia.* 2015. **4**(0).
262. Wright, J.G., et al., *Protein C and protein S in homozygous sickle cell disease: does hepatic dysfunction contribute to low levels?* 1997. **98**(3): p. 627-631.
263. Panepinto, J.A., et al., *Matched-related donor transplantation for sickle cell disease: report from the Center for International Blood and Transplant Research.* 2007. **137**(5): p. 479-485.
264. Bolaños-Meade, J. and R.A. Brodsky, *Blood and marrow transplantation for sickle cell disease: overcoming barriers to success.* 2009. **21**(2): p. 158-161.
265. Dunlay, S.M. and V.L. Roger, *Gender Differences in the Pathophysiology, Clinical Presentation, and Outcomes of Ischemic Heart Failure.* 2012. **9**(4): p. 267-276.
266. Vaccarino, V., et al., *Sex-Based Differences in Early Mortality after Myocardial Infarction.* New England Journal of Medicine, 1999. **341**(4): p. 217-225.
267. Lorenz, M., et al., *Does cellular sex matter? Dimorphic transcriptional differences between female and male endothelial cells.* 2015. **240**(1): p. 61-72.